AN EFFECTIVE CONTROL TECHNIQUE FOR AUTOMATIC SOLAR TRACKING

By

Motlatsi Cletus Lehloka

Dissertation submitted in fulfilment of the requirements for the degree:

Master of Engineering

In

Electrical Engineering

Department of Electrical, Electronic and Computer Engineering

Faculty of Engineering, Build Environment and Information Technology

Central University of Technology, Free State

Supervisor: Prof. A.J. Swart

Co-Supervisor: P.E. Hertzog

November 2021

Declaration

I, MOTLATSI CLETUS LEHLOKA, student number _____, declare that this work has not been previously accepted in substance for any degree and is not being concurrently submitted for any degree. This dissertation is being submitted in fulfilment of the requirements for the degree Master of Engineering in Electrical Engineering at the Department of Electrical Engineering, Central University of Technology, Bloemfontein campus. This dissertation is the result of my own work, except where otherwise stated. Other sources are acknowledged by giving explicit references. A reference list is appended.

MC Lehloka

18 November 2021

Acknowledgement

Thanks to the almighty God for providing me with life and strength to keep on trying, even under unbearable situations.

To my main supervisor, Prof A.J. Swart, I will not forget the phrase you used whenever the going got tough: “Don’t give up!” – I now know its real meaning. My sincere gratitude for all the vigorous efforts to guide me.

To Prof P. Hertzog and Prof N. Luwes, thank you also for the enthusiasm with which you offered direction.

To the University of South Africa, Department of Electrical and Mining Engineering (power group), thank you very much, team, for all your advice.

Lastly, to my better half (Matebello Lerato Lehloka), thanks a lot team member, had it not been for you it would have been more difficulty to complete the degree.

Dedication

I dedicate this work to my lovely little daughter, Kamohelo Precious Lehloka.

You mean the world to daddy, my girl.

Abstract

Due to global climate change as a result of pollution caused by the burning of fossil fuels, the world has changed its view when it comes to power generation. The focus is now more on natural and clean energy, such as solar photovoltaic (PV) systems. An effective solar PV system is not a simple system, as the sun is not a stationery object. The sun moves from east to west daily, which makes the design and installation of an effective solar PV system challenging for optimal power harvesting.

Harvesting of solar energy from a PV module efficiently is affected not only by varying environmental conditions, but also by the installation angles, load profile, latitude of the location of interest and energy management system. An energy management system may include a maximum power point tracker (MPPT) that is required to adjust a PV module's output voltage to a value, which enables the maximum energy to be transferred to a given load. PV module energy conversion can further be increased by using solar tracking technologies. Tracking the sun to enable maximum output power from a PV module varies in complexity. However, it is essential to deliver the highest possible power to the load continuously when variations in the insolation and temperature occur, to maintain a high overall system efficiency.

The purpose of this research study was to develop an effective control technique for an automatic solar tracking system in order to maximise the output power yield that may be obtained from a dual-axes tracking-type system. Three fixed-type PV modules (installed at tilt angles of latitude plus 10° (36°), latitude (26°) and latitude minus 10° (16°)) and the direct-tracking system (controlled by Boolean algorithm) served as the baseline for analysing the simulated power results of two selected algorithms (linear regression and fuzzy logic). These tilt angles are utilised based on the recommendations by Heywood and Chinnery in 1971. The Boolean algorithm is developed and programmed in a National Instruments (NI) LabVIEW user interface software to control three linear actuators to meet the requirements for a dual-axes tracker. The two algorithms (fuzzy logic and linear regression) are developed and simulated using Microsoft Excel.

It took 41 functional blocks and four comparison calculations to develop and execute the direct-tracking system. For the direct-tracking system, two comparison calculations per axis of previous and current voltage readings were done to detect if the PV module should move forward or backwards. The direct-tracking system could move the PV module either forward or backward in both axes (X and Y).

The LabVIEW user interface was also used to visualise the measured data. It was designed and developed for this research study pertaining to the operating parameters of PV modules and linear actuators. The system was installed on the top of the Euclid building at the University of South Africa (UNISA), Science Campus, Florida, Johannesburg. The global positioning system (GPS) coordinates of the building are 26, 1586° S, 27, 9033° E.

It was discovered that the daily performance of the fixed system power (16° PV module) was better than the 26° and 36° fixed systems power by 3.49% and 10.69%, respectively. The direct-tracking system power showed 32% improvement over the fixed system power (16°) due to the fact that it was always aligned to the movement of the sun. The daily simulated power for fuzzy logic was 5.31% better than the direct-tracking system power. The direct- tracking system power was better than the simulated power for linear regression by 2.24%. A key recommendation is to align a PV module perpendicular to the sun from sunrise to sunset, using an effective control technique based on fuzzy logic principles, in order to extract the maximum amount of available energy.

Table of contents

List of figures

List of tables

List of abbreviations

DAQ	Data acquisition
NI	National instruments
PV	Photovoltaic
UN	United Nations
SDG	Sustainable development goals
MPPT	Maximum power point tracker
MPP	Maximum power point
PC	Programmable controller
PWM	Pulse width modulation

Chapter 1 – Introduction

1.1 Background

With the rapid increase in population and economic development, the problem of energy shortages and global warming continues to be a cause for increasing concern globally (Wang and Lu, 2013). South Africa is not immune to energy shortages; predictions are that these energy shortages will increase, thereby necessitating the implementation of alternative energy sources, such as photovoltaic (PV) energy systems (Hertzog and Swart, 2015). As a clean and renewable energy source, solar energy has been drawing more and more attention, especially in the field of electrical energy generation (Yao *et al.*, 2014). PV energy systems provide an attractive method of power generation and meet the criteria of clean and sustainable energy (Ozemoya *et al.,* 2012). Global partnerships to meet the sustainable development goals (SDG) of the United Nations (UN) exist, which include supporting the initiative of ensuring access to affordable, reliable, sustainable and modern energy for all (SDG No. 7) (United Nations, 2015).

The power from the sun intercepted by the Earth is approximately 1.8 x 10^{11} MW, which is larger than the present consumption rate on earth of all commercial energy sources. The problem associated with the use of solar energy is that its availability varies widely with time due to the day night cycle and also seasonally due to the earth's orbit around the sun (Vijayalakshmi, 2016). To extract the maximum output power from a PV energy system requires a solar tracker that can be used to track the sun's direction so that the sun's rays may always be perpendicular to the face of the PV module (Fathabadi, 2016). The performance of a PV module is primarily affected by its orientation and tilt angles with the horizontal plane (Kacira *et al,* 2004). Optimising the output power of any PV array or module requires a number of factors to be considered, including the tilt angle, orientation angle and environmental conditions (Hertzog and Swart, 2015). Some PV installation designs do not take into account the effect that varying atmospheric conditions have on the sustainability of a designed system (Hertzog and Swart, 2015).

South Africa has some of the highest solar irradiance in the world and experiences some of the highest levels of yearly horizontal solar irradiation globally (see Figure 1.1). The average daily solar radiation in South Africa is between 4.5 and 6.5 kWh / m^2 / day (Scholtz *et al.*, 2017). When compared to industrialised countries that are using solar thermal technology on a much larger scale, many of South Africa's provinces have higher levels of solar irradiation than many of these countries, including the United States of America and the United Kingdom.

Yet, South Africa lags behind countries with a lesser solar resource, such as Spain and Germany (Scholtz *et al.*, 2017). Though the country has a higher irradiance, the optimum angles at which a solar collector should be fixed are often debated (Le Roux, 2016).

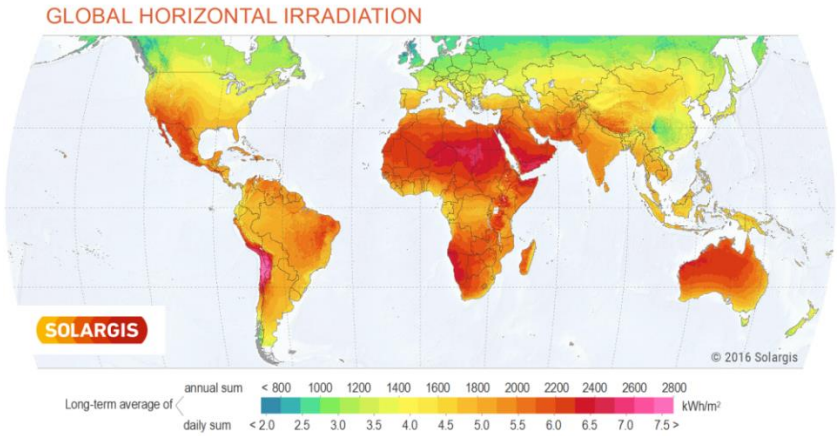

Figure 1.1. Global horizontal irradiation (Le Roux, 2016).

As solar energy is abundantly available in nature, increasing the effectiveness of harnessing solar energy should be one of the foremost research endeavours. The challenge in tapping this energy relates to increasing system efficiency. Therefore, an attempt should be made to use various control mechanisms to improve efficiency, including maximum power point tracking (MPPT) and solar trackers. Various algorithms are used in these control mechanisms, including fuzzy logic and linear regression.

A key deficiency of PV modules is their low efficiencies, where the solar-to-electricity conversion efficiency can be less than 20% for commercial PV products. That means that 80% of the absorbed solar energy is actually dumped by the PV modules as waste heat. These low efficiencies necessitate the optimum installation of PV modules according to the relevant environmental conditions and site coordinates (Hertzog and Swart, 2015). Solar systems, like any other system, need to be operated with the maximum possible performance. This can be achieved by proper design, construction and orientation (Shariah, 2002).

The maximum solar energy available to an Earth-surface collector was examined as a function of latitude, tilt and whether the collector is an ideal tracker or a fixed type (Neville, 1977). The output of a PV module is highest when the incident ray is perpendicular to the plane of the PV module. Due to variations in the locus of the sun over the year, the alignment of the module should be changed according to the sun's position for maximum generation (Khan *et al.,* 2015). Results revealed that for the single as well as for the two-axis system, there is an additional gain of energy of about 33% and 37% respectively compared to the static (fixed) system (Vermaak, 2014). The best method to optimise the tilt and the orientation of a PV

module is by applying an active sun tracker. Active sun trackers are electromechanical or pure mechanical devices that keep changing the tilt and the orientation of a PV module periodically during the day (Khatib *et al.,* 2012). Figure 1.2 illustrates the position of the sun and the PV module. It is evident from the figure that the maximal energy yield could only be achieved at 12 noon for a fixed-type system.

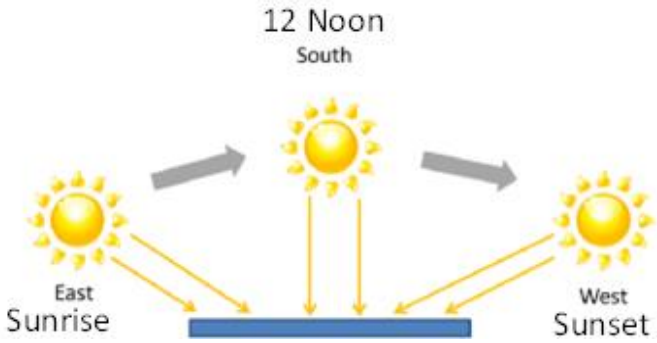

Figure 1.2. Fixed system showing the sun's position to the PV module throughout the day (Solargis, 2010).

However, the maximal energy yield could be enhanced through the day for a tracking-type system where the module is constantly perpendicularly aligned to the sun (see Figure 1.3).

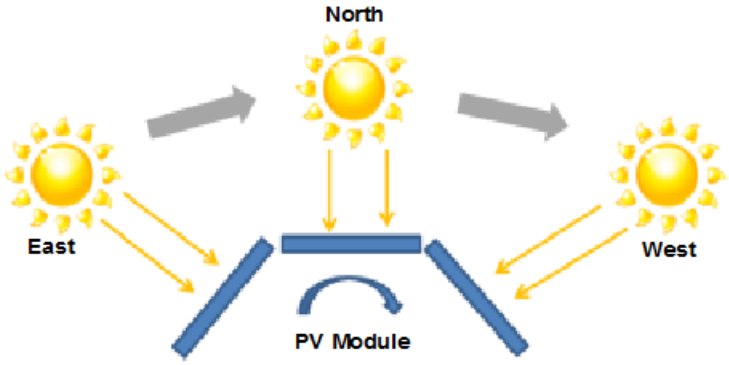

Figure 1.3. Tracking system showing the sun's position to the PV module throughout the day (Solargis, 2010).

1.2 Problem statement

PV modules may be either fixed in position to a roof or mounted directly onto a frame, resulting in a stationary fixed-type system. The sun, however, is not a stationery object, as it is constantly changing its position in the sky relative to a fixed position on Earth during daytime. As a result, the conversion efficiency between solar energy and electrical energy is not always at an optimum level, as the PV module is not always perpendicularly aligned to the direct beam radiation of the sun. One way to increase the conversion efficiency is to vary the tilt and orientation angle of an adjustable PV module automatically, constantly aligning it to the direct

beam radiation of the sun, making the choice between various control techniques for a solar tracking-type system challenging.

1.3 Objectives of the study

The aim of this study was to optimise the available output power from a PV module by constantly aligning it to the direct beam radiation of the sun. This alignment improved the efficiency of the PV system, as it was exposed to the direct beam radiation of the sun for longer periods of time, resulting in higher amounts of energy generated from the system. For the practical set-up, three fixed-type systems were used as the reference or control setup, so as to compare the results to the direct-tracking system, which then served as an experimental setup baseline to the simulated results. Two different algorithms were applied for simulation purposes in order to compare the empirical results of the direct-tracking system with the simulated results. The direct-tracking system made use of a Boolean algorithm to track the movement of the sun across the sky from sunrise to sunset, creating optimum output for a longer period. The optimum tilt angle for fixed-type systems involved placing the PV module at an orientation angle of 0˚ and changing the tilt angle to 16°, 26° and 36°, respectively, depending on the season of the year (Asowata *et al.*, 2012). The three fixed-type systems were placed at 16°, 26° and 36° respectively.

The research objectives are to:

- Clarify a simple calibration method for the systems to ensure data validity;
- Substantiate which tilt angle enables the highest energy yield from a fixed-type system where a singular PV module is located on the Highveld of South Africa;
- Implement a direct-tracking system where a Boolean algorithm is used to obtain empirical results; and
- Determine which algorithm (fuzzy logic or linear regression) will enable the highest output power from a proposed PV module, using simulation.

1.4 Methodology

This section describes the research procedures and methodology engaged in for the empirical study. Identical PV modules, with the same load profile, were used in the practical setup. A reference tilt angle of 26° was used in this research, corresponding to the latitude value of the installation site at the University of South Africa (UNISA), Science Campus, Florida, Johannesburg. Three PV modules were fixed at tilt angles of 16°, 26° and 36° (fixed orientation angle of 0° N), while one PV module (representing the direct-tracking system) was moving between 90° in the morning, 0° at 12 noon and 90° in the afternoon (this is for the tilt angle).

The orientation angle was limited to +180° at 06:00 am and -180° at 06:00 pm. Figure 1.4 illustrates the proposed practical setup. It is essential to state that both these angles (tilt and orientation) were dependent on the proposed lookout angles that were used in the development of the fuzzy logic rule set, in the linear regression algorithm and the simulated results. Both tilt and orientation angles were varied throughout the day.

The direct-tracking system used a basic Boolean algorithm as a controller to align a PV module with the movement of the sun in the sky. The voltage and current were measured from this PV module, with the measurements relayed via an interface to a computer software program, where the power was calculated and used to activate control signals. These signals were then relayed back to the direct-tracking system where actuators were used to adjust the tilt and orientation of the PV module. Microsoft excel was used to simulate the output power of the system by applying a linear regression algorithm and a fuzzy logic algorithm.

LabVIEW was used to house the basic Boolean algorithm from which the control signals emanated. LabVIEW's features include simple network communication, turnkey implementation of common communication protocols (RS232, GPIB, etc.), powerful toolsets for process control and data fitting, fast and easy user interface construction and an efficient code execution environment (Hertzog and Swart, 2015).

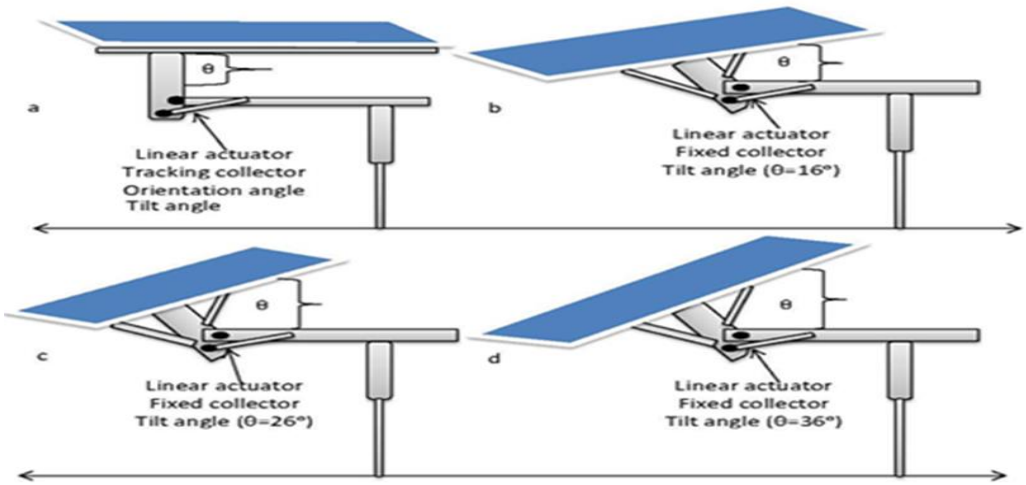

Figure 1.4. The proposed practical setup.

For logging interface, the system used five resistors connected in series and they were also used as a system's load. Logging interface circuit may be used for power conditioning (Hertzog and Swart, 2018). Logging interface circuit has also been reported on by a number of researchers and provides power conditioning between PV modules and Arduino board, which is connected to a personal computer and interfaced with LabVIEW software (Hertzog and Swart, 2015).

1.5 Definition of terms

- **Fuzzy logic controller:** Fuzzy Logic is a problem-solving control methodology that lends itself to implementation in systems ranging from simple, small, embedded micro-controllers to large, networked, multi-channel programmable controllers (PC) or workstation-based data acquisition and control systems. It provides a simple way to arrive at a definite conclusion based upon vague, ambiguous, imprecise, noisy, or missing input information (Kaehler, 2013).
- **Linear regression controller:** This is designed to study the relationship between a pair of variables that appear in a data set. It is designed to study the relationship between one variable and several other variables. In both cases, the sample is considered a random sample from some population. The two variables, X and Y, are measured outcomes for each observation in the data set (Campbell and Campbell, 2008)
- **Orientation angle:** This is defined as the angle between true South (or true North) and the projection of the normal of the PV module to the horizontal plane (Swart and Hertzog, 2016). It is described as a PV module installation angle relative to the Earth's surface (Asowata *et al.,* 2012). Many PV modules should be installed at the suggested orientation angle of 0° N in South Africa (Swart and Hertzog, 2016).
- **Tilt angle:** This is defined as the angle between the PV module surface and the horizontal plane (Swart and Hertzog, 2016).
- **LabVIEW:** National Instruments LabVIEW is a graphical programming language that has its roots in automation control and data acquisition. Its graphical representation, similar to a process flow diagram, was created to provide an intuitive programming environment for scientists and engineers. The language has matured over the past 20 years to become a general-purpose programming environment. LabVIEW has several key features, which make it a good choice in an automation environment (Hertzog and Swart, 2016a).
- **Look (or lookout) angles:** These are most commonly expressed as azimuth and elevation angles of satellites communication. Antenna look angles of a geostationary communications satellite provide the information required to ensure that the control station antenna is directed towards the satellite; more specifically to ensure that the main lobe of the antenna is aligned with the main lobe of the satellite's antenna and to ensure that the largest amount of energy is captured from the satellite (Ayansola and Yinusa, 2012).
- **Azimuth angle:** This is the angular displacement from the south of the beam radiation projection on the horizontal (Seyed *et al.,* 2017).
- **Elevation angle:** The angle of the sun, which is numerically equal to the angle between the direction of the sun and the idealised horizon (Wang, 2017).

In this current study, the azimuth angle relates to the orientation angle, while the elevation angle relates to the tilt angle. Just as an Earth station can track a satellite in outer space using the lookout angles, so a PV module can track the movement of the sun using similar proposed lookout angles, which can translate to appropriate tile and orientation angles.

1.6 Importance of the research

The output power produced by high-concentration solar thermal and PV systems is related directly to the amount of solar energy acquired by the system, which is enhanced by tracking the sun's position with a high degree of accuracy (Lee *et al.*, 2009). Available output power from a PV module should be optimised to enable a higher yield of solar energy and reduce dependence on traditional energy sources such as fossil fuels (Asowata *et al.*, 2013). Tracking the position of the sun in order to expose a PV module to maximum radiation at any given time will enable the highest yield of energy. Aligning the PV module constantly with the sun (90°) can increase the conversion efficiency and reduce the number of PV modules required.

Tracking the sun for the maximum power point (MPP) of a PV module varies in complexity. However, it is essential to continuously deliver the highest possible power to the load when variations in the insolation and temperature occur, to maintain a high overall system efficiency. It therefore becomes necessary to use a control mechanism (Boolean algorithm) in order to ensure the efficient operation of the solar collector. It is essential to validate or compare the empirical results with a simulation model, as this can solve real world challenges safely and efficiently. The simulation model can provide analysis, which is easily verified and understood.

A PV module's performance depends on the location and position of the module, with the solar energy conversion becoming more popular in power generation; more research still needs to be done in order to understand the basic operation of the sun tracking system. The method of control and basic algorithms are aspects to get optimal power output from the system, which will ensure that as much clean energy as possible is harvested from this technology.

1.7 Delimitation

It is important to state that the physical construction of the practical setup was done by a private service provider. The effects of relative humidity and temperature on the PV module's performance was ignored as all the PV modules were exposed to the same environmental conditions, where only the output power was considered. The design and construction of a data acquisition system also did not form part of this research. The study was limited to the summer period of the Highveld of South Africa, as the winter period has lower solar radiation

values. The empirical results from a direct-tracking system were used to obtain simulated results for the fuzzy logic algorithm and linear regression algorithm.

1.8 Overview of the chapters

Chapter 1 outlines the background and overview of the study. The problem statement, engaged methodology, definition of the used terminologies and the importance of the study are incorporated.

Chapter 2 discusses the literature review on the algorithms of the study. The software and technique to be used to control the direct-tracking PV module are also discussed.

Chapter 3 presents the design and the depiction of the practical setup. The fixed and direct- tracking systems are sketched and described.

Chapter 4 analyses and discusses the results of the study. The analysis is based on the results obtained from the fixed system, the direct-tracking system and the simulation. The algorithm that yields the maximum power output compared to the direct-tracking system will be established.

Chapter 5 presents the conclusions and recommendations based on the results obtained from comparison of the fixed-type systems at different tilt angles, the direct-tracking system using the Boolean algorithm and the simulation using different algorithms (linear regression and fuzzy logic).

1.9 Summary

There are times of the day, like early morning and late afternoon, when a fixed-type system will collect very little energy when the available amount of solar energy is quite high. This has led to the introduction of a solar tracker. The presence of a solar tracker is not essential for the operation of a PV module, but without it, performance is reduced. An ideal tracking-type system will allow a PV module's surface to always be pointing towards the sun, compensating for both changes in the altitude angle of the sun (through the day), latitudinal offset of the sun (during seasonal changes) and changes in azimuth angle.

Chapter 1 dwelled on a brief comparison between a tracking-type system and a fixed-type system. A brief methodology was also presented in this chapter. Different terminologies used in the study were explained. Chapter 2 will provide further details on the three control algorithms.

Chapter 2 – Literature review on algorithms and the system requirements

2.1 Introduction

The previous chapter (Chapter 1) introduced various algorithms that are applicable to the study. The research procedure and methodology were briefly discussed in that chapter. Different terminologies used in the study were explained.

The aim of this chapter is to provide a contextual overview of three algorithms that were used in this study, along with the control software and hardware for the direct-tracking system.

2.2 Overview of algorithms

There are different algorithms to consider for the solar tracking approach. Some of the algorithms are robust and simple, whereas others require very sophisticated logic devices, such as microcontrollers. The Boolean algorithm (true or false) could be considered the basic algorithm to consider for a solar tracking system. The Boolean algorithm was used for implementation for experimental sun follower platforms at the Polytechnic University of Bucharest. It was discovered that with the aid of the algorithm, the efficiency of the PV module was increased (Stamatescu *et al.*, 2014). However, fuzzy logic and linear regression algorithms (that will be detailed in 2.3 and 2.4) can also be considered for solar tracking systems, even though they require a more sophisticated design. Fuzzy logic algorithm was utilised in a dual-axis solar tracking system at the Universiti Teknologi Malaysia (Zakariah *et al.*, 2015). Linear regression algorithm was also used for a solar automatic tracking system that generates power for lighting greenhouses at the Jilin University China (Zhang *et al.*, 2015).

2.3 Boolean algorithm

The Boolean algorithm is the basic algorithm for computer science and applications, including digital circuit design, law, reasoning about any subject and any kind of specifications, as well as providing a foundation for all mathematics (Hehner, 2012). The Boolean algorithm is an algorithm structure defined on a set of elements (0 and 1), two binary operators ("+" and " . "), with operation rules equivalent to the AND and OR operations and a complement operator equivalent to the NOT operator (Hussein, 2020). According to Millan *et al.* (2014), hill climbing offers a fast way to obtain Boolean functions, which are widely used in solar tracking applications (Adarsh *et al.*, 2015). Hill and climb algorithms are broadly applied in solar tracking controllers because of their ease and simplicity of execution (Hichamia *et al*, 2021).

In this current study, hill and climb will be used to execute the Boolean algorithm due to their similarities.

Hill climbing is an optimisation technique that is used to find an optimum solution to a computational problem. It starts off with a solution that is normally very poor compared to the optimal solution and then iteratively improves from there. It does this by generating other solutions, which are better than the current solution. It repeats the process until it finds the most optimal solution where it can no longer find any better improvements (Rohan *et al.*, 2019). Figure 2.1 depicts the hill climbing block diagram that was applied to the direct-tracking solar system in this study and from which empirical results were obtained. The hill climbing algorithm started with sending signals to the actuators to move the PV module to the initiating position. Simultaneously, it kept reading the voltage and current from the PV module and compared them with the previous measurements. The value change in readings was stored to establish any increase or decrease, from which the required movements were determined. This process kept on repeating from sunrise to sunset (06:00 am to 06:00 pm).

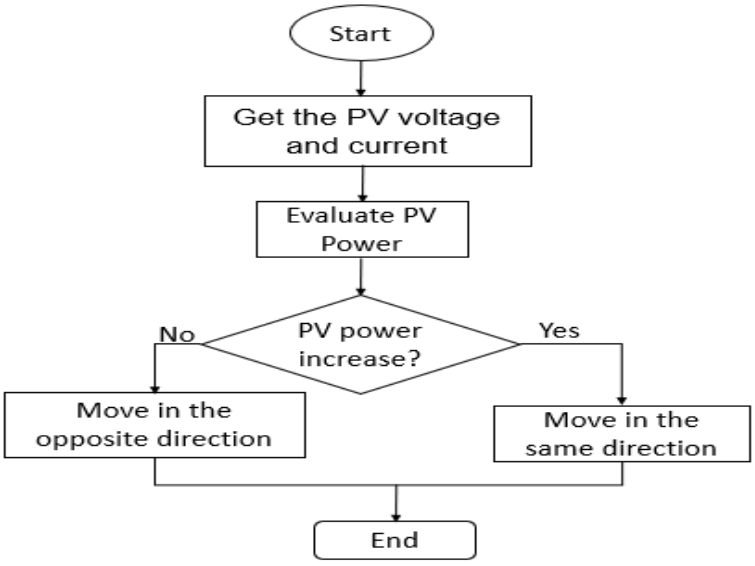

Figure 2.1. The hill climbing algorithm block diagram (Zulfikri and Ulinuha, 2020).

Table 2.1 lists the advantages and disadvantages of the Boolean algorithm. The Boolean algorithm was used in the design and testing of a parallel kinematic solar tracker at the Department of Mechanical and Aerospace Engineering, Politecnico di Torino, Torino, Italy. Even though the design used voltage signals coming from the PV module, as in the current study, the system produced energy only if the PV modules were oriented with misalignment errors lower than 0.4°. The results showed a satisfactory behaviour, as the orientation of the PV modules alignment error was always maintained under 0.4° (Hehner, 2012). The current study uses a Boolean algorithm, since it is easier to implement.

Table 2.1. Advantages and disadvantages of the Boolean algorithm.

Advantages	**Disadvantages**
• Boolean algorithm is very easy to explain and to understand (Zohuri, 2017). • Boolean algorithm is useful in conditional systems (true or false), as well as strings (Stamatescu, 2014). • Boolean algorithm enables many logical functions to be manipulated simultaneously. (Edwards, 1971).	• Boolean algorithm is both time-consuming and unstable (Lu *et al.*, 2014). • Boolean algorithm makes it difficult to rank output (Lashkari *et al.*, 2009). • It is easier for information loss (Ristevski, 2013).

2.4 Linear regression algorithm

Linear regression analysis is defined as a statistical technique for investigating and modelling the relationship between variables (Jiang, 2008; Kaehler, 2013). According to Ibrahim *et al.* (2012), regression analysis is modelling the relationship between a scalar variable Y and one or more variables denoted as X. The polynomial regression is a form of linear regression in which the relationship between an independent variable X and a dependent variable Y is modelled. According to Montgomery *et al.* (1981) a simple linear regression algorithm is given by:

$$Y = \beta_o + \beta_1 x + \varepsilon \qquad \text{equation 2.1}$$

The magnitude and direction of that relation are given by the slope parameter (β_1) and the status of the dependent variable, when the independent variable is absent, is given by the intercept parameter (β_o). An error term (ε) captures the amount of variation not predicted by the slope and intercept terms. For example, a regression with time as an independent variable and increasing voltage as a dependent variable would show a very high regression coefficient. The regression coefficient (R^2) shows how well the values fit the data (Campbell and Campbell, 2008).

Figure 2.2 presents a block diagram for a model with the linear regression algorithm (Chong *et al.*, 2009). The collected data from a PV module are used to estimate the unknown parameters (β_0 and β_1) in order to satisfy equation 2.1. Linear regression is proposed as a way of modelling solar tracking systems, due to its efficiency (Clack, 2017). However, the algorithm may introduce significant errors due to its limitation of working better only with linear correlated

values (Zárate *et al.*, 2004). Table 2.2 presents the advantages and disadvantages of linear regression algorithm.

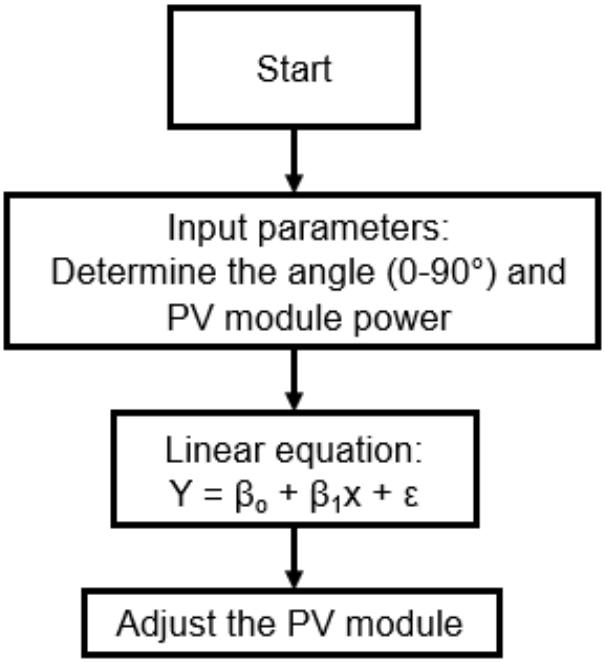

Figure 2.2. Open loop sun tracking system with linear regression controller (Chong et al., 2009).

Table 2.2. Advantages and disadvantages of the linear regression algorithm.

Advantages	**Disadvantages**
• Almorox and Hontoria (2004b) discovered that the linear regression is the most simple and accurate algorithm. • In the linear regression analysis, dependent variable is regressed in a single analysis on all independent variables (Jeon, 2015). • The linear regression prediction can capture the trend of a time series accurately (Wu *et al.,* 2009).	• The algorithm may introduce significant errors due to its limitation of working better only with linear correlated values (Zárate *et al.*, 2004). • This algorithm is probabilistic because the uncontrolled factors are modelled by ε. The error term ε is a random variable and it is assumed to be uncorrelated and distributed with mean 0 (constant variance) (Kwon, 2012). • One of the limitations imposed by linear regression models is that they will underperform when used to model nonlinear systems (Jiang, 2008). • Linear regression will fail to give good results when any of the variables is not valid (Campbell and Campbell, 2008).

Linear regression algorithm was applied on a generic sun-tracking algorithm for an on-axis solar collector in mobile platforms at the Universiti Tunku Abdul Rahman, Kuala Lumpur, Malaysia. The algorithm produced a better outcome as compared to the other algorithms (Lai *et al.*, 2014). However, the filtering algorithm was applied on the data to remove noises in the raw data before being substituted into the general formula and computation. It is essential to state that data filtration might result in elimination of a true reflection of the results. The main reason for using this algorithm in this current study is because of its simplicity and accuracy in analysing data.

2.5 Fuzzy logic algorithm

Fuzzy logic is defined as a form of many-value logic, which deals with reasoning that is approximate, rather than fixed and exact (Robert *et al.*, 2014). Fuzzy logic incorporates a simple, rule-based approach, “if x and y then z”, to solve a control problem rather than attempting to model a system mathematically (Allman *et al.*, 2013). The fuzzy logic is set up by means of a triangle consisting of the ownership function values between zero and one, corresponding to each input variable value, in which the horizontal coordinates for the input variable value are the degree of ownership (Huang, *et al.*, 2016).

The optimisation of the conversion efficiency of a solar tracking system, regardless of climatic factors and the associated load, can be achieved by using a fuzzy logic algorithm (Algarín *et al.*, 2017). An intelligent algorithm is needed in order to rotate the PV module according to its voltage output in a solar tracking system. Hence, in solar tracking, an intelligent algorithm like fuzzy logic can be used (Zakariah *et al.*, 2015). Fuzzy logic is one of the most preferred control algorithms compared to other methods, such as neural networks and genetic algorithms (Ouali and Salah, 2010). A fuzzy logic algorithm is adaptive and nonlinear in nature, which provides robust performance under load, supply voltage disturbances and parameter variation (Kiyak and Gol, 2016a). Fuzzy logic algorithm seems to be appropriate when working with a certain level of imprecision, uncertainty and partial knowledge. It is also appropriate in cases where the knowledge of operating with the process can be translated into a control state that improves the results reached by other classical strategies (Stamatescu, *et al.*, 2014).

A fuzzy logic algorithm was used for the design and implementation of a fuzzy decision support system for the control of PV module movements in order to improve the availability of solar energy at the University Politehnica of Bucharest, Romania (Stamatescu, *et al.*, 2014). The system used measured values of radiation from appropriate sensors and provided commands for two positioning motors. This is different in the present study, where measured voltages are used to make a decision with commands relayed to linear actuators. Compared to traditional

sensor solar tracking algorithms, fuzzy logic algorithm is more accurate in controlling the various angles and the circuit design is simpler, without considering the error caused by external environment changes (Huang *et al.*, 2016). These were the main reasons for selecting this algorithm for the present study.

The knowledge base of a fuzzy logic algorithm consists of a data base and a rule base. The fuzzy control rules are based on a fuzzy model of the process. This means that fuzzy control rules (IF-THEN) are generated in order to track the maximum intensity of voltage that is directly related to the amount of direct beam radiation from the sun. This method is somewhat more complicated than other approaches, but it yields better performance and reliability for dealing with nonlinearities of the sun movement (Zakariah *et al.*, 2015). For rule-based fuzzy logic algorithms, the degree of fulfilment of the THEN part is formed from the degree of fulfilment of the IF part by a certain method. The degree of fulfilment of the THEN part is equivalent to the degree of fulfilment of the rule. All these individual rule evaluations put together result in one membership function for the output signal. The resulting membership function describes a fuzzy control command. When the IF part contains a combined statement IF-AND-THEN, the fuzzy logic AND operation is executed first and the degree of fulfilment is used in the overall rule evaluation (Stamatescu, *et al.*, 2014).

Fuzzy logic has been applied to track the position of the sun, where the logic controller's output is connected to the driver of the linear actuator to rotate the module until it faces the sun (Huang *et al.*, 2016). The voltage and current readings are passed to a fuzzy logic controller for aligning the module in the direction of the sun. The block diagram in Figure 2.3 represents an algorithm used for fuzzy-based control for a solar tracking system. The value of the PV module's voltage and current is read, the use of fuzzy sets is defined, the membership functions are quantified and continuous use of the triangular membership functions is made to reduce errors (Huang *et al.*,2016). The results obtained as a result of the rules are sent to the defuzzification unit and then converted into real numbers according to a scale (Kiyak and Gol, 2016b). Defuzzification is the conversion of a fuzzy quantity to a precise quantity, just as fuzzification is the conversion of a precise quantity to a fuzzy quantity (Ross, 2010).

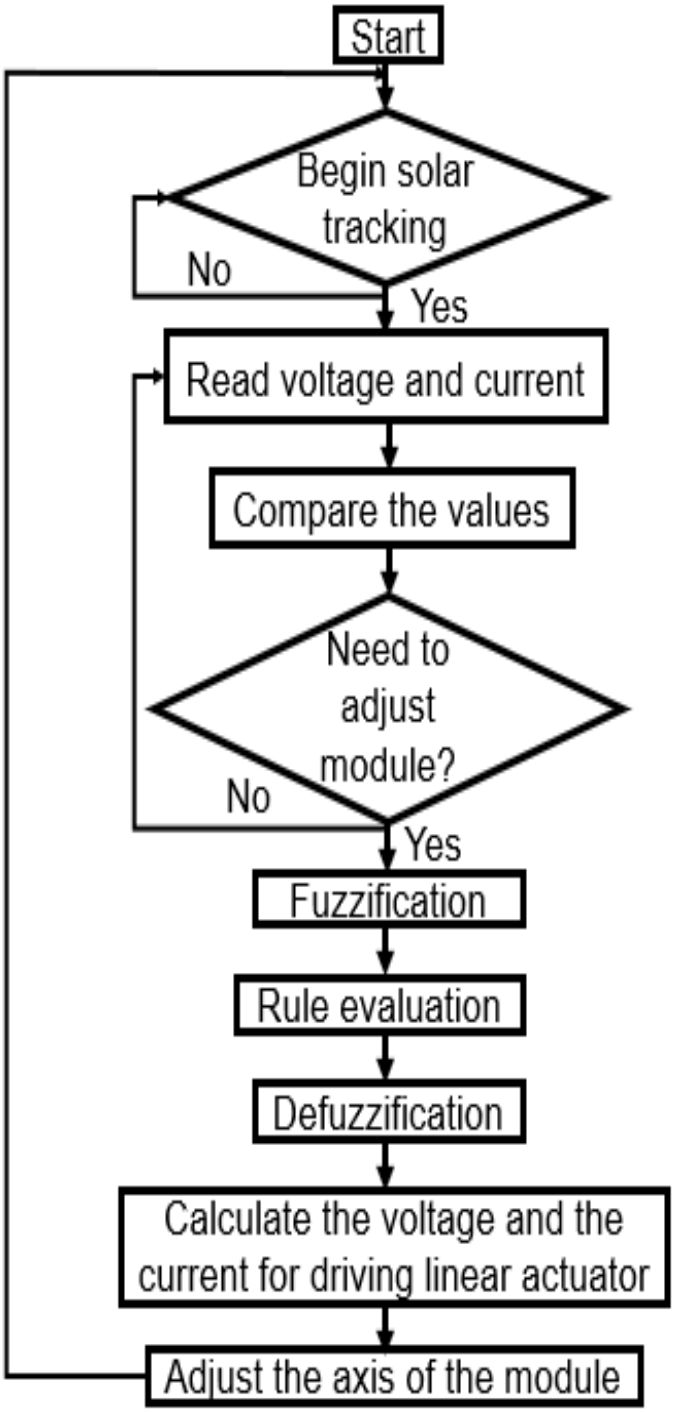

Figure 2.3. The block diagram using fuzzy logic algorithm (Kiyak and Gol, 2016b).

The membership functions of a fuzzy logic algorithm can be tuned for achieving better performances in terms of initial tracking time and transition responses according to practical characteristics of PV modules (Na *et al.*, 2017). However, the algorithm has some disadvantages, such as high cost and complexity (Bounechba *et al.*, 2014). The advantages and disadvantages of a fuzzy logic algorithm are listed in Table 2.3.

Table 2.3. The advantages and disadvantages of fuzzy logic algorithm.

Advantages	**Disadvantages**
• A fuzzy logic controller has the advantages of working with imprecise inputs, not needing an accurate mathematical model and handling nonlinearly (Kumari, 2013). • Fuzzy logic provides a simple way to arrive at a definite conclusion based upon vague, ambiguous, imprecise, noisy, or missing input information. A fuzzy logic approach to control problems mimics how a person would make decisions, only much faster (Kaehler, 2013). • The good thing about fuzzy logic control is that the linguistic system definition becomes the control algorithm (Hamed and El-Moghany, 2012). • Compared to traditional sensor sun tracking systems, the fuzzy logic system is more accurate as it is easier to control the angle and the circuit design is simpler, without considering the error caused by external environment changes (Huang *et al.*,2016).	• The algorithm has high cost and complexity (Bounechba *et al.*, 2014). • Even though fuzzy logic has more promising advantages it does not fit to every problem. In areas that have good mathematical descriptions and solutions, the use of fuzzy logic is often sensible when computing power restrictions are too severe for a complete mathematical implementation (Reus, 1994). • Task definitions with insufficient knowledge of the system and little or very imprecise knowledge of the system behaviour results in bad, possibly unusable fuzzy solutions (Stamatescu, *et al.*, 2014). • Designing of the fuzzy logic rules to track the maximum power point is one of the difficult part of the algorithm (Garg *et al.*, 2015). • Usually no adaptability and learning capability if the system behaviour changes (Stamatescu *et al.*, 2014).

Prediction of electricity demand was done in India using a fuzzy logic algorithm. The study showed that this approach did not only give a better forecasting performance but it also has a simple procedure in handling forecasting problems. However, the study made use of simplified fuzzy inference in which the consequence of the fuzzy rule was expressed in crisp numbers only (Saravanan *et al.*, 2014). The weather and climate conditions of the Highveld of South Africa are often associated with extreme events such as flash floods and severe droughts (Mambo and Faccer, 2017). Due to the extreme weather and climate events, which are experienced in the Highveld of South Africa, it is important to take weather conditions'

uncertainty into consideration by applying fuzzy logic. This research study aims to make use of a fuzzy logic algorithm due to its ability to deal with nonlinearities of the system and to convert linguistic system definitions into a control rule base or control algorithm.

2.6 LabVIEW

National Instruments LabVIEW is a graphical programming language that has its roots in automation control and data acquisition. Its graphical representation, similar to a process flow diagram, was created to provide an intuitive programming environment for scientists and engineers. LabVIEW has several key features, which make it a good choice in an automation environment. These include simple network communication, turnkey implementation of common communication protocols (RS232, GPIB, etc.), powerful toolsets for process control and data fitting, fast and easy user interface construction and an efficient code execution environment (Hertzog, 2015). The LabVIEW user interface is shown in Figure 2.4. A user interface gives users a way to interact with the source code. It allows the user to change the values passed to the source code and see the data that the source code computes. In LabVIEW, the user interface is the front panel. It is important to identify the inputs and outputs of a software development problem during the design phase of the development method. This identification leads directly to the design of the front panel window (Instruments, 2015). National Instruments embedded control and monitoring tools are the core component of the graphical system design approach. LabVIEW system design software and reconfigurable hardware provide a superior method for design teams to complete demanding embedded control and monitoring tasks faster without requiring custom design (Instruments, 2012). According to Stamatescu *et al.* (2014), LabVIEW software is easier to interface with real-world signals, enabling the analysis of data for meaningful information and sharing. Table 2.4 lists some of the advantages and the disadvantages of using LabVIEW.

While LabVIEW provides a variety of features and tools, ranging from interactive assistants to configurable user interfaces, it is differentiated by its graphical, general-purpose programming language along with an associated integrated compiler, a linker and debugging tools. It is imperative to understand its language so as to correctly use the software (Instruments, 2013).

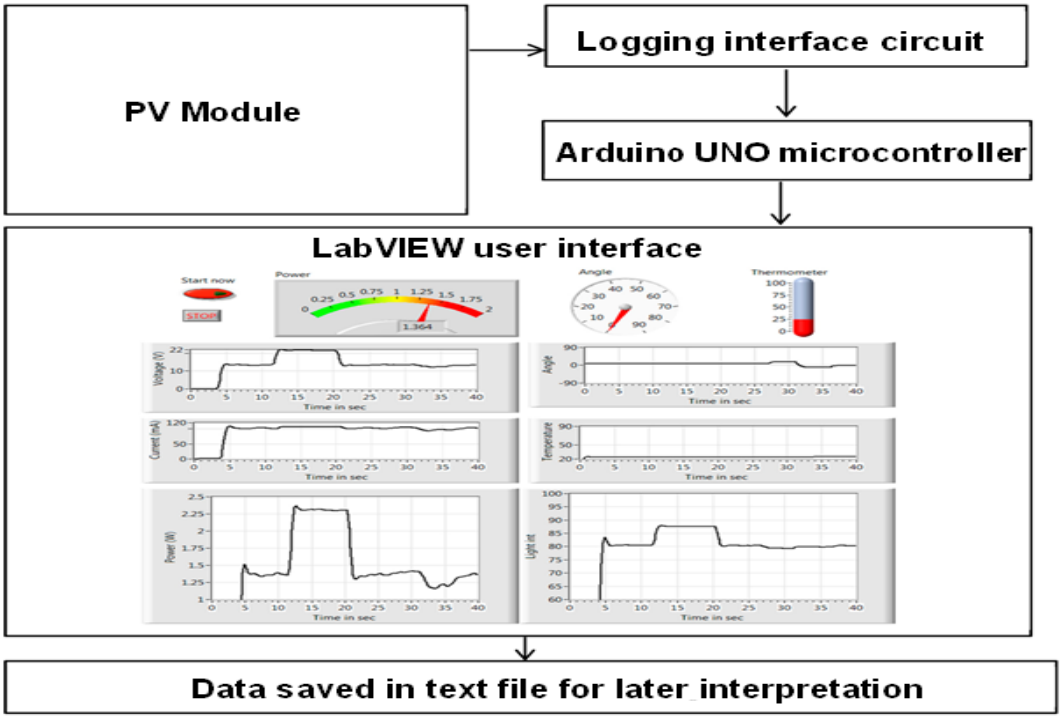

Figure 2.4. The LabVIEW interface (Hertzog and Swart, 2015).

Table 2.4 The advantages and disadvantages of using LabVIEW.

Advantages	**Disadvantages**
• LabVIEW is precise and accurate (Instruments, 2012). • LabVIEW is easier to interface with real-world signals, analyse data for meaningful information and share results (Stamatescu *et al.*, 2014). • One tool for design, prototyping and deployment (Labview, 2012).	• In LabVIEW it is always important to specify data type for all the input pins even if the data type is of no significance (Mackin, 1998). • An issue, which has been reported by many LabVIEW Web Services users, concerns the stability of this technology. For the presented distance laboratory, failure to run of the services without any information has been noted (Bauer and Ionel, 2013). • Failure to deploy with no apparent cause has been an issue (Bauer and Ionel, 2013).

LabVIEW software was used to record data to validate the optimum tilt angle for PV module in the central region of South Africa for the winter season. It was discovered that PV modules installed at the tilt angle of latitude plus 10° produced the highest output power for the months of May to July 2015 (Hertzog, 2015). However, optimising the output power of any PV module

involves a number of factors, including the orientation angle (Swart, 2015). The results obtained for the months of May to July 2015 were in contrast to PV modules installations for pollution-intensive areas. Only one research installation site was used for a three-month period, resulting in a time-lag study. The software was also used for data collection for a fixed PV module (Hertzog, 2015).

LabVIEW was also used in a study to track the sun and maintain maximum efficiency of a PV module (Jamal *et al.*, 2016). In another study, a sun tracker was effectively controlled using LabVIEW (Kaur *et al.*, 2016). According to Pradeep *et al.* (2014), a high quality solar tracker consists of three main sections, which are the inputs (e.g. PV module), controller (e.g. Arduino) and the outputs (e.g. LabVIEW).

Because of its simplicity in network communication, LabVIEW software was used to control the linear actuator in this research study. With power measured from the PV modules used as an input parameter, the software was used not only to control the tilt angle, but also the orientation angle. The data were collected for a longer period of six months, accommodating the other seasons of the year in a highly polluted environment, being the Highveld region of the Gauteng province. The linear actuator is discussed next.

2.7 Linear actuators and stepper motors

Linear actuators and stepper motors are devices that may be used to direct PV modules in a desired direction. Figure 2.5 illustrates a single PV module with a linear actuator controller that controls the tilt angle. The linear actuator consists of a built-in direct current (dc) motor with dc worm gear that allows a smooth and precise extension of the arm (Chai *et al.*, 2011). Linear actuators are widely used in home solar tracking applications as compared to the stepper motors since they are easy to control, relatively inexpensive and require less current as they do not resonate (Dante *et al.*, 2013).

Linear actuators are very attractive components to use for compressor applications, where they provide better efficiency, better dynamic performance and smoother operation (Birbilen and Lazoglu, 2018). However, some of the central control problems, such as robust stabilisation in the presence of matched nonlinear uncertainties, remain challenging (Saberi *et al.,* 1996). The advantages and disadvantages of the linear actuator are listed in Table 2.5.

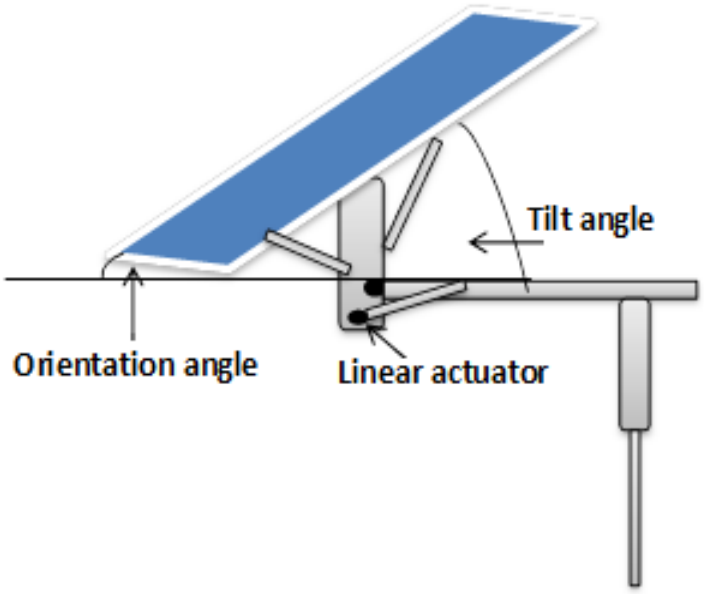

Figure 2.5. Linear actuator controlling the PV modules.

Table 2.5. The advantages and disadvantages of linear actuator.

Advantages	**Disadvantages**
• Linear actuators are widely used in home solar tracking application as compared to the stepper motors since they are easy to control, relatively inexpensive and require less current as they do not resonate (Dante *et al.*, 2013). • An actuator is capable of producing a positive thrusting or pulling force acting in a straight line, which may be accurately controlled (Schrader and Mex, 1958). • Linear actuators do not require any kind of gearbox (Martins *et al.*, 2006).	• The linear actuator is a stage proportional magnet because its driving current changes for a number of cycles and a series of reset points will occur as the current undergoes cyclic changes. A large number of reset points across the full stroke of the platform results in significant reduction in the linear behaviour (Ulbrich, 1994). • It's also difficult for linear actuators to provide the slow, controlled speeds that are needed in certain applications (Sotoodeh, 2019). • Requires additional power and not safe in explosive atmospheres (Sotoodeh, 2019).

A solar tracking system was designed using linear actuators at the University of Engineering and Technology, Lahore, Pakistan. The results pointed to the simplicity, accuracy and applicability of the design in meeting different operational conditions. However, the controlling device to the linear actuator only operated by reading the time from a real-time clock and the

PV module was set according to that time (Vijayalakshmi, 2016). According to Gordo *et al.* (2015), time alone cannot be used to control the position of a PV module, as sun intensity, cloud cover, relative humidity and heat build-up affect the module as well.

Because they can be controlled easily, are relatively inexpensive and require less current, this research study used linear actuators to move the PV modules to the desired positions to align it with the direct beam radiation of the sun. With control signals from the LabVIEW software, the discretion to move the modules was not based on a real-time clock. All varying environmental factors affecting a PV module influence its output power (voltage and current output), which was used as the input data to the LabVIEW software where the two previously explained algorithms were housed.

2.8 Application to solar tracker

It is predicted that as the sun rises in the early hours, the amount of power from the module is minimum and then rises to its maximum around 12 noon, when the module's glass surface is perpendicular to the sun. After 12 noon, the amount of power starts decreasing until the sun sets. Figure 2.6 shows direct beam radiation received by a specific PV module from sunrise to sunset. Direct beam radiation directly from the sun is extremely important for concentrated PV systems and has a direct bearing on the tilt angle of installation (Swart and Hertzog, 2016).

On a clear sunny day, the direct beam radiation contributes about 90% to the total available solar radiation (Hertzog, 2015). In order to produce energy from the sun's radiation, the PV modules surface must be aligned with the sun at an angle of 90° (Gabler *et al.*, 2008). The output of a PV module is highest when the incident ray is perpendicular to the plane of the module (Khan *et al.*, 2015), while an incident angle of 44° can produce 15% of a PV module's peak output power (Swart and Hertzog, 2016).

From Figure 2.6, it is evident that the angle of incidence is indirectly proportional to the amount of energy produced by the PV module at 12:00. As the incident angle narrows, at around 11 am, the module starts picking up in energy production and produces maximum at 12 am, when the incident ray is perpendicular to module. However, as the incident angle widens after 12 am, the module starts losing energy gradually until sunset. Due to variations in the locus of the sun over the year, the alignment of the module should be changed according to the sun's position for maximum generation (Khan *et al.*, 2015).

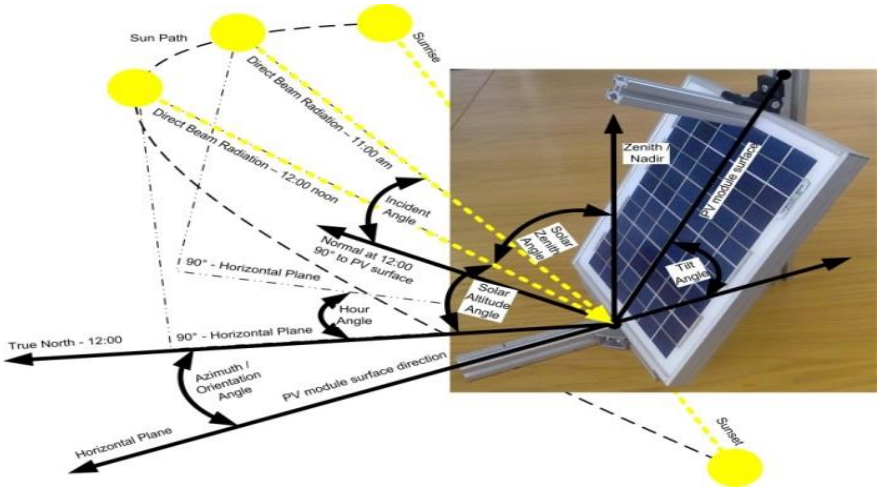

Figure 2.6. PV module geometry showing different angles (Hertzog and Swart, 2016a).

It is essential to state that the azimuth angle of the sun correlates to the orientation angle of the PV module. Similarly, the altitude angle of the sun correlates to the tilt angle of the PV module. This correlation is presented in Annexure C, where a lookout angle is used to represent both values (tilt and orientation or azimuth and altitude).

PV modules are most efficient when oriented perpendicular to the sun's rays, that is, $\theta = 0$. The orientation of a PV module can be specified by two angles, the tilt angle β and the azimuth angle γ, as demonstrated in Figure 2.7. These two angles can be changed during each day with the sun position to minimise the angle of incidence θ of the beam radiation on PV surface and thus maximise the incident beam radiation by sun tracking (Al-najjar, 2013).

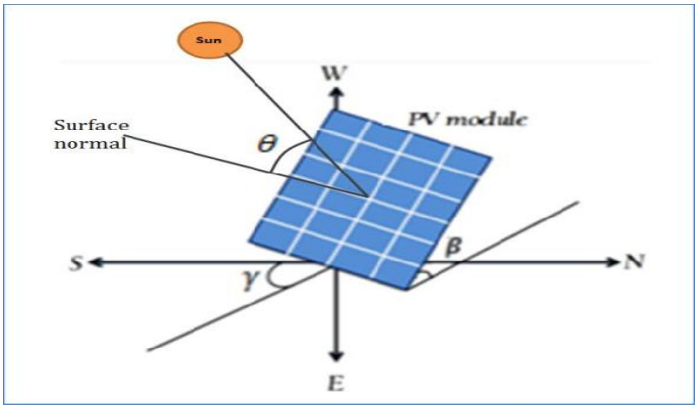

Figure 2.7. Tilt, azimuth and incidence angles for PV module (Al-najjar, 2013).

The sun's position is predicted to be different at different times of the day. Solar radiation is obtained on various inclined planes with different orientations (Guo *et al.*, 2017). Varying the tilt and orientation angles to obtain optimum power output from a PV module system for a specific location of interest at different times is vital. The sun's paths are different due to factors such as the:

- Location (local latitude)
- Rising and setting position of the sun (based on the time of the year)
- Duration of the day and night (based on the time of the year).

In the Northern Hemisphere, the summer season days are longer and the sun is higher in the sky (June 21) while in the winter season, days are shorter and the sun is lower in the sky (December 21) (Chang, 2009). During the fall and spring equinoxes, the sun passes directly over the equator (Seyed *et al.*, 2017). Figure 2.8 illustrates the path of the sun through the sky in summer, spring/autumn and winter. From Figure 2.8, it is evident that the maximum harvesting of the sun occurs at 12 noon in all the seasons. As schematically illustrated in Figure 2.8, the maximum and minimum declination angle values of the Earth's orbit produce seasons (Seyed *et al.*, 2017) and need to be accounted for to enable the optimum output power yield from a PV module throughout the day and year.

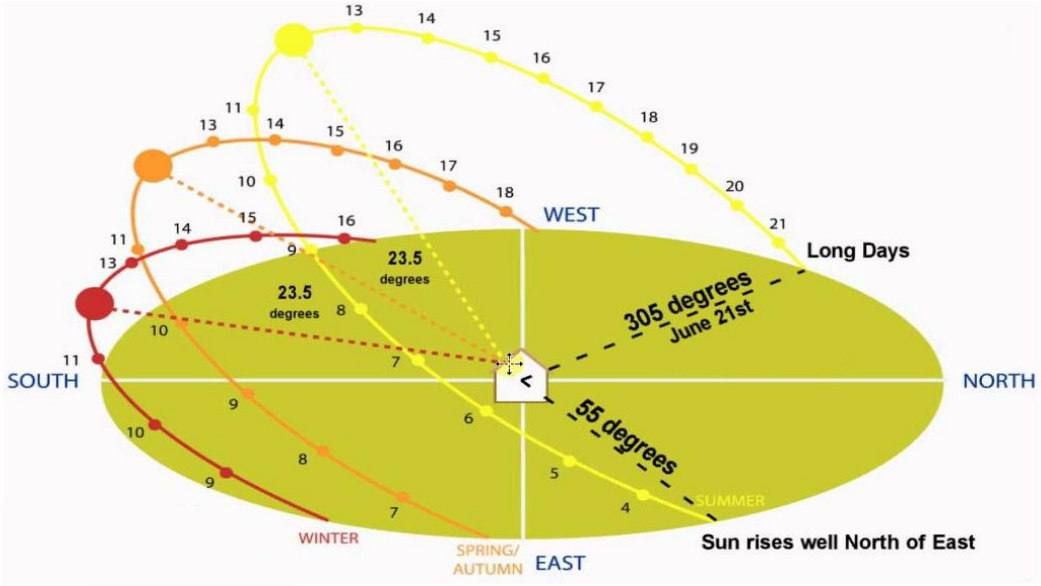

Figure 2.8. The daily sun's behaviour in the sky in summer, winter and spring/autumn in the Northern Hemisphere (Vishal, 2018).

At 15:00, the PV module would have to be turned right and away from due South (0° orientation angle), which occurs at 12 noon. This would equate to a positive orientation angle change, which would occur throughout the day. Sunlight incidence angles vary throughout the year due to the rotation of the Earth around its own axis and its elliptical orbit. This would result in a higher solar altitude angle (dotted yellow line; also see Figure 2.7) for the month of June, in the Northern Hemisphere, at 12 noon and a lower angle for the month of December (dotted red line). Sunlight should fall perpendicular to a PV module to enable maximum power yield (Karafil *et al.*, 2015). In the Southern Hemisphere, the tilt angles of PV modules would be

lower in summer and higher in winter months, as the tilt angle is inversely proportional to the solar altitude angle.

The maximum output power of a PV module depends on atmospheric conditions, load profile and the tilt and orientation angles (Asowata *et al.*, 2012). The variation of tilt and orientation angles changes the amount of solar radiation reaching the collector surface (Skeiker, 2009). According to Belay *et al.* (2015), maximum solar power output is obtained when PV modules orientation and tilt angles vary with the movement of the sun. Figure 2.9 represents a PV module with fixed orientation and tilt angles for the Southern Hemisphere. These angles have to be varied to make sure that the module is perpendicular to the suns' rays throughout the day.

Figure 2.9. PV module showing orientation (Y) and tilt (α) angles (Asowata *et al.*, 2012).

2.9 Conclusion

The algorithms that are to be used in this research study were discussed in detail in this chapter. The chapter also elaborated on what parameters are required for the control process that may be facilitated using LabVIEW software. Furthermore, the chapter clarified why the linear actuator is preferred for this study over the stepper motor, especially due to its lower current consumption.

The design of the practical setup for the fixed systems (16°, 26°, 36°) that serve as baseline to the direct-tracking system used in this research study will be discussed in the next chapter (Chapter 3). The design will include the components that are used and experimental pictures will be provided and explained.

Chapter 3 – The practical setup

3.1 Introduction

The previous chapter (Chapter 2) contextualised the three algorithms (direct-tracking algorithm, linear regression and fuzzy logic) that may be used in an automatic solar tracking-type system and the controlling software and hardware (linear actuator with Laboratory Virtual Instrument Engineering Workbench (LabVIEW)). The aim of this chapter is to provide an overview of the direct-tracking algorithm as a whole by listing and explaining all the components that are used in the practical setup. The development of linear regression and fuzzy logic algorithms will also be outlined in this chapter.

3.2 An overview of the practical system

The system consists of five identical photovoltaic (PV) modules. The first three modules are fixed at tilt angles of latitude, latitude +10°, latitude -10° and an orientation angle of 0° North. According to Asowata *et al.* (2012), the optimum tilt angle for a 26° angle of latitude involves placing the PV panel at an orientation angle of 0° and setting the angle of tilt to 16°, 26° or 36° respectively. These angles are derived from the Heywood and Chinnery equations of latitude for calculating tilt angles of PV panels in South Africa. The fixed modules serve as baselines to the two direct-tracking modules. The two direct-tracking modules use the Boolean algorithm in order to establish consistency for the direct power measurement. The Boolean algorithm is programmed in a National Instruments (NI) LabVIEW user interface software so as to control three linear actuators to meet the requirements for the direct-tracking. Each PV system consists of a load of five resistors connected in series that also serves as the logging interface. The system's block diagram is shown in Figure 3.1. All the individual components of the system are discussed in the subsequent sections.

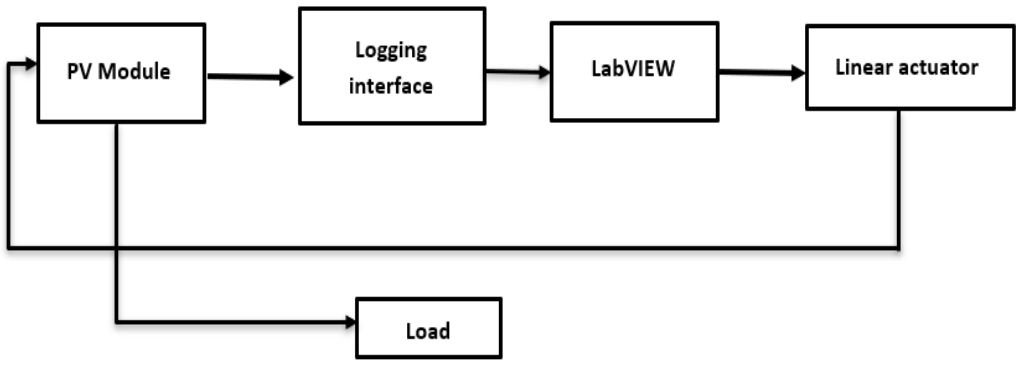

Figure 3.1. The system's block diagram.

3.2.1 The PV modules

There are a wide range of PV modules available worldwide today. PV modules are normally classified into three generations (first, second and third) (Ranabhat *et al.*, 2016). First generation includes silicon solar cells. They are made from a single silicon crystal (mono-crystalline or polycrystalline). Second generation are thin-film solar cells, which are less expensive to produce than traditional silicon solar cells as they require less material to manufacture. As the name implies, a physically thin technology has been applied to the manufacturing process of these cells. They are only slightly less efficient in power generation compared to other cells. The third generation includes several thin-film technologies often described as emerging PV's. Most of them have not yet been commercially applied and are still in the research or development phase (Bagher *et al.*, 2016). Figure 3.2 shows six 310 W YL310P-35b polycrystalline PV modules that are used in this study with the NI data acquisition (DAQ) hardware installed inside the control boxes. They are used because they are low in cost and have better performance in areas of direct solar radiation (Asowata *et al.*, 2012). The PV modules are rated at 36.3 V (voltage at maximum power), 45.6 V (open circuit voltage), 8.53 A (current at maximum power) and 8.99 A (short circuit current). They are installed on the top of the Euclid building at the University of South Africa (UNISA), Science Campus, Florida, Johannesburg. The global positioning system (GPS) coordinates of the building are 26.1586° S, 27.9033° E. It must be noted that there is one PV module that is not part of this study, as it provides redundancy in the event of a failure of the other system. The direct-tracking system ensures redundancy and consistency of the direct power measurements.

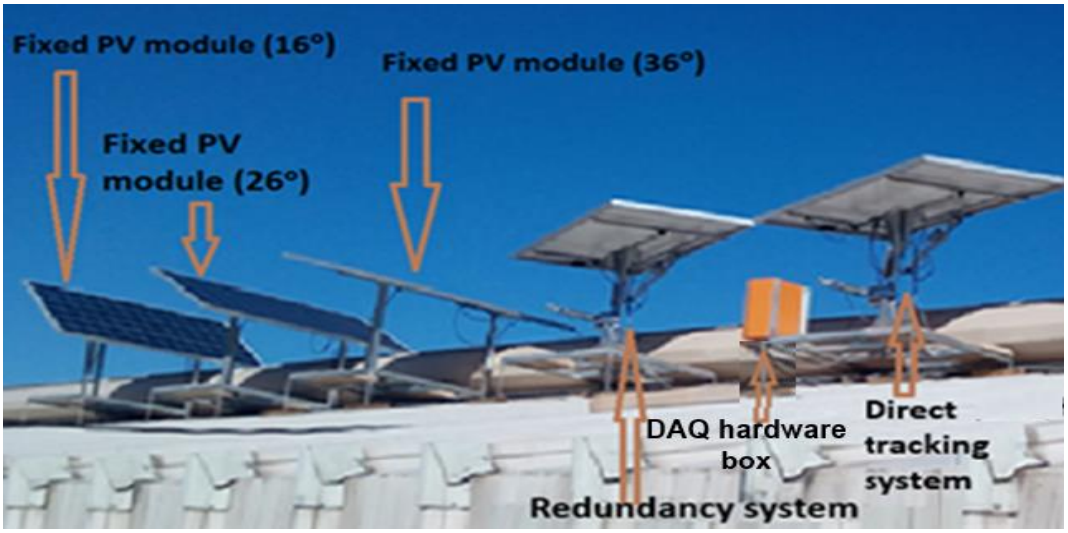

Figure 3.2. The three fixed PV modules and the tracking module.

Table 3.1 lists key parameters of the PV module made in China. It is a 72-cell series 2 module with a standard test condition (STC) power per unit area of 158.9 W/m^2 and a utility scale

application test condition (PTC) power of 280 W. The basic operating principle of the system is to measure the output voltage of the modules and use the measurements to command the controlling devices to align the PV modules perpendicular to the sun. One way to increase the efficiency of PV modules and to produce the maximum amount of energy, is to align it perpendicular to the light source (Allamehzadeh, 2016). A PV module tracking system using input voltages from a PV module was developed at the Islamic University of Science and Technology, India. The PV modules rotate to the position where the maximum power is absorbed (Zahoor and Sharief, 2017).

Table 3.1. 310 W YL310P-35b polycrystalline module characteristics.

Characteristics	**Value**
Rated power	310 W
Peak efficiency	15.89%
Tight positive power tolerance	0 W to +5 W
Rated voltage	36.3 V
Open circuit voltage	45.6 V
Rated current	8.53 A
Short circuit current	8.99 A
Maximum series fuse	15 A
Maximum system voltage	1000 V
NOCT	46°C
Length	1.970 mm
Depth	50 mm
Width	990 mm
Weight	26.8 kg

3.2.2 Logging interface

Figure 3.3 shows the data logging interface circuit that is also used as the system load, which will be outlined in Section 3.2.5. A solar tracking system, using a data logging interface, was developed at the SEGi University, Malaysia, to record different variables that were present in a system to enable the user to make further improvements to the system (Chow and Abiera, 2013). A logging interface circuit was also developed and used for power conditioning for optimum tilt angles for PV modules in a semi-arid region of the Southern Hemisphere (Hertzog and Swart, 2018). Voltage, current and temperature readings were limited to below 5 V in order to protect the analogue to digital converters on the Arduino Mega microcontroller. Voltage reduction was achieved by using a voltage divider circuit with resistors having a 1%

tolerance value. Current readings from that study were obtained by measuring the voltage across one of the resistors and then by applying Ohm's law.

A data logging interface circuit, using a voltage divider, was used in another study at the Central University of Technology (CUT), Bloemfontein, South Africa. This was done in order to validate the optimum tilt angle for PV modules in a semi-arid region of South Africa for the winter season (Hertzog and Swart, 2016b).

A typical voltage divider consists of two or more resistors connected in series across a source voltage. As the source voltage is dropped in successive steps through the series resistors, any desired portion of the source voltage may be "tapped off" to supply individual voltage requirements (Kuphaldt, 2014).

The voltage divider circuit provides signal conditioning, as the output voltage of the PV module (open circuit voltage = 45.6 V) is much higher than the allowed input voltage to the DAQ unit (this is limited to 10 V). Using the voltage divider rule in the data logging interface circuit enables the input voltage to the NI DAQ to be less than 10 V. Equation 3.1 shows how the voltage (10 V) limitation is achieved when considering an input voltage of 36.3 V:

$$V_{out} = V_{in}\left(\frac{R1}{RT}\right) \qquad \text{equation 3.1}$$

$$= 36.3\left(\frac{1}{4.28}\right)$$

$$= 8.48\ V$$

Where: V_{out} = Voltage divider output to the DAQ system

V_{in} = PV module output voltage

R_1 = System 1 Ω resistor where the voltmeter is connected across

R_T = Total resistance of the circuit in series ($R_1 + R_2 + R_3 + R_4 + R_5 = 4.28\ \Omega$)

This DAQ is connected directly to a personal computer running the LABVIEW software where measurements are recorded and the control algorithms are implemented.

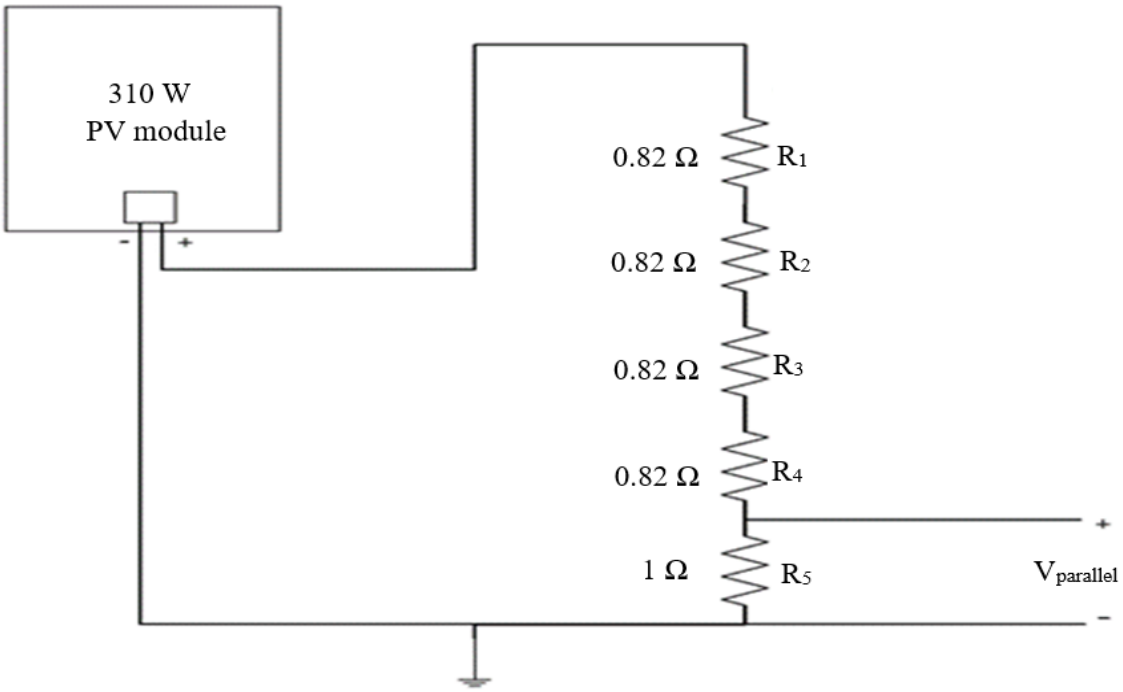

Figure 3.3. The data logging interface circuit.

3.2.3 LabVIEW

A PV module tracking system rotates automatically based on the sun's irradiance during the day while remaining in sleep mode at night. This can be achieved by modelling the system utilising a software program such as MATLAB-Simulink (Chin *et al.*,2011). Siemens also developed a solar software library around a solution for a movable tracking system that precisely follows the course of the sun. However, the library and control solution are only for the Simatic S7-1200 programmable logic controller (PLC) processors that computes the alignment of the tracker on the basis of its exact location in the world, for any given time and date (Prinsloo, 2015).

Data can also be measured and displayed simultaneously using the LabVIEW visual programming software. All values stored in a matrix can eventually be written to a text file for further analysis in MS Excel (Hertzog and Swart, 2018). LabVIEW has several key features, which make it a good choice in an automation environment (Hertzog and Swart, 2015b). It is easier to interface LabVIEW with real-world signals, analyse data for meaningful information and share results (Stamatescu, *et al.*, 2014a) while also providing for accuracy (Instruments, 2012). A number of research studies have been conducted on the operating parameters of PV modules under various environmental conditions, using computer-controlled energy monitoring systems built on the LabVIEW software (Swart, 2018).

LabVIEW is a graphical control, test and measurement environment development package. The programs created in LabVIEW have three basic components: the front panel, the block diagram and the icon connector. The front panel is the user interface and the code is inside the block diagram that contains the graphical code (Stamatescu *et al.*, 2014). A graphic interface made with LabVIEW software allows the user to monitor and save the data in a file (Liu *et al.*, 2018). Figure 3.4 shows the LabVIEW user interface that is used to display voltage and current readings from the PV modules. NI LabVIEW DAQ hardware and software modules have become the most widely used tools to capture, view and process controls, instrumentation and power system data, both in academia and the industry (Pecen *et al.*, 2004).

LabVIEW software may also be used to control linear actuators that adjust PV modules to different angles (Jovanovic *et al.*, 2016). DAQ hardware is required for this, which is located at the PV modules (see Figure 3.2), with a network cable linking it to a personal computer in a research laboratory. LabVIEW connects to this DAQ hardware for the reception of electronic measurements and for the transmission of commands from the two control strategies, or algorithms. The two algorithms are housed in the LabVIEW software that has its roots in automation control and data acquisition. Its graphical representation, like a process flow diagram, was created to provide an intuitive programming environment for scientists and engineers (Hertzog and Swart, 2015).

The LabVIEW user interface provides the following information:

- Analog instantaneous value of voltage for each PV module (point A);
- Digital instantaneous value of voltage for each PV module (point B);
- Analog instantaneous value of current for each PV module (point C);
- Digital instantaneous value of current for each PV module (point D);
- Instantaneous value of voltage for each PV module in graph form (point E);
- Instantaneous value of current for each PV module in graph form (point F);
- Manual start of the measuring system ignoring the set system's start time (G);
- Manual stop button function to control the while loop execution (point H);
- Indicator outputs showing the system start time and PV module repositioning (06:00 am) and system stop time (06:00 pm) (I);
- Time and date strings showing the current system's time and date (J); and
- PV module movement direction indicators and over right controls, for example, vertical or horizontal (point K-L).

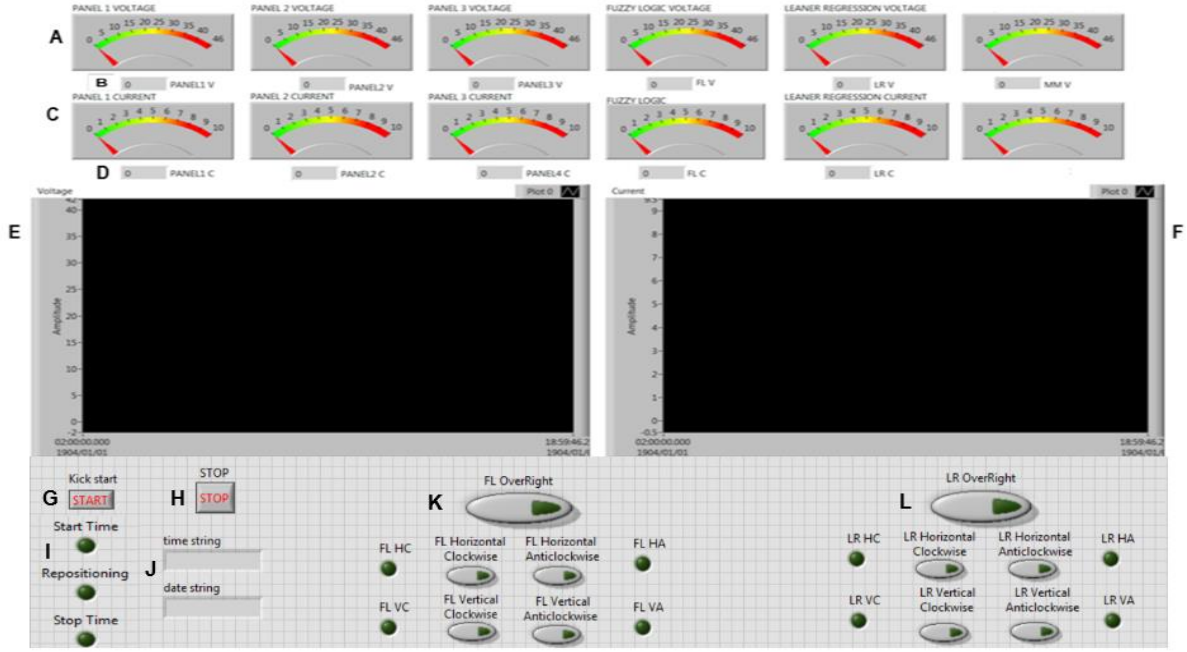

Figure 3.4. The LabVIEW user interface front panel.

3.3 Direct-tracking system

Figure 3.5 illustrates the direct-tracking system controller block diagram in the LabVIEW user interface programme. The programme is a single input (voltage) and single output (voltage) system. The system makes use of its measured voltage as feedback for the direct-tracking controller. According to Salas *et al.,* (2006), direct solar tracking methods include methods that use PV module voltage and/or current measurements. The methods consider the variations of the PV module operating points and the optimum operating point obtained. The methods belonging to this group include the differentiation, feedback voltage, auto-oscillation, among others.

At 06:00 am, when the programme executes, the PV module is moved to its start position (lookout angle of 110° – this translates to an orientation angle of 110° and to a tilt angle of 90° (Annexure C)). The date-time string function (point F) in the block diagram instructs the system to iterate from 06:00 am to 06:00 pm every day. The system measures the instantaneous voltage from the PV module and then compares it to the previous voltage readings read from the shift register (point I). If the latest readings are greater or equal to the previous value, then the PV module tilts forward to check if the readings improve. If the latest voltage reading is less than the previous reading, then the PV module tilts backward, monitoring the change in voltage readings. The PV module movements happen once every four seconds, preventing oscillation. The following can be observed from Figure 3.5:

- The analogue signal (voltage from PV modules) is acquired from the DAQ system (point A);
- The reading from each individual PV module is obtained by splitting the signal (point B);
- The numeric indicators indicating the analogue and digital voltage from PV modules (point C);
- The X-axis and Y-axis motion commands based on the fuzzy based rules (point H); the PV modules should not move concurrently to prevent oscillation (point G);
- The signal is merged again (point D) after the set conditions are met in order to be conveyed to the DAQ system (point E) to drive the PV modules accordingly;
- The date-time string function to start and stop the programme's execution (point F); and
- The shift register presents the previous voltage sample that is used in comparison with the current voltage sample to indicate an increase or decrease, which then determines the direction in which the PV module is shifted (point I).

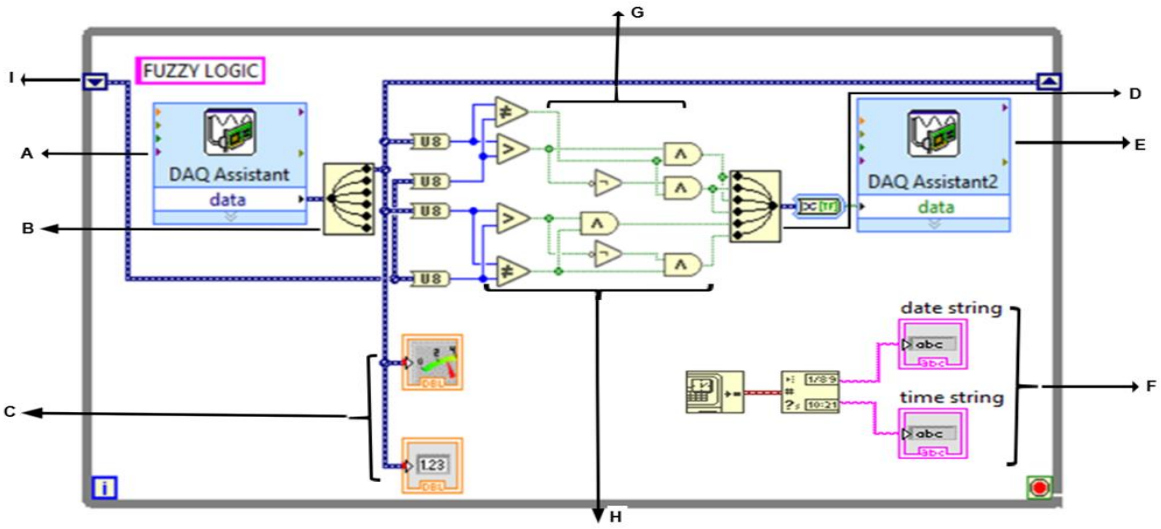

Figure 3.5. The direct-tracking algorithm block diagram in LabVIEW.

3.4 The linear actuator

Stepper motors are commonly used in precision positioning control applications. For PV module solar tracking systems, stepper motors have been considered because they are brushless, load independent, have open loop positioning capability, good holding torque and excellent response characteristics (Anuraj and Gandhi, 2014). The biggest drawback with stepper motors that are relevant for PV module solar tracking systems is that they have a low efficiency since they draw a lot of current when they operate (Lawless and Kärrfelt, 2018).

For optimisation of a PV module solar tracking system, servomotors can be used as they are able to receive pulse width modulation (PWM) signals from controllers. The selection of a standard servomotor is not fit for movement along horizontal axis, which needs to cover 360° of motion. The solution is to use a continuous servomotor that is modified to control continuous rotation in two directions. However, the drawback of the continuous servomotor is that it does not provide feedback on the shaft position (Chow and Abiera, 2013).

One of the key components of a solar tracker is the motion mechanism that can include a linear actuator (Jovanovic *et al.*, 2016), which does not suffer from the aforementioned two drawbacks. Linear actuators can provide better efficiency, better dynamic performance and smoother operation (Birbilen and Lazoglu, 2018). A 'tilt-roll' tracker for a PV module employs a linear actuator (Christian *et al.*, 2015). Two linear actuators can be used to move PV modules horizontally (Aksoy *et al.*, 2015). The key advantage of using two linear actuators is that the rotating head can be rotated more than 180 degrees to around 240 degrees. Another advantage is that two shorter linear actuators can be used instead of a single long actuator. By rotating 240 degrees, the area of the world between two tropic zones can benefit without physically moving the actuators whenever the sun orbit is crossing the zenith point. These tropical zones of the world enjoy the most sunshine days throughout the year (Liao, 2013). Horizontal rotation is achieved by anchoring the bases of two linear actuators on a tracker frame and connecting the stroke to the PV module. In the present study, two linear actuators are used for x-axis rotation, as illustrated in Figure 3.6.

Linear actuators create motion in a straight line, providing stable, quiet and good movement, in contrast to the circular motion of a conventional electric motor (Ceyda *et al.*, 2015). The ability to create motion in a straight line (Ferdaus *et al.*, 2015) makes the linear actuators ideal to adjust the tilt angle of a PV module. This subsequently gives linear motion by varying the tilt angle of a PV module between the horizon (0°) and the sky (90°). The linear actuator shown in Figure 3.7 controls the tilt angle of the PV module. The vertical motion is achieved by anchoring the linear actuator base on a tracker frame and connecting the stroke to the PV module. Three linear SKF actuators with the characteristics of 4 A (rated current) and 25% (duty cycle), were thus used for this present study; two for the orientation angle and one for the tilt angle, as shown in Figure 3.8.

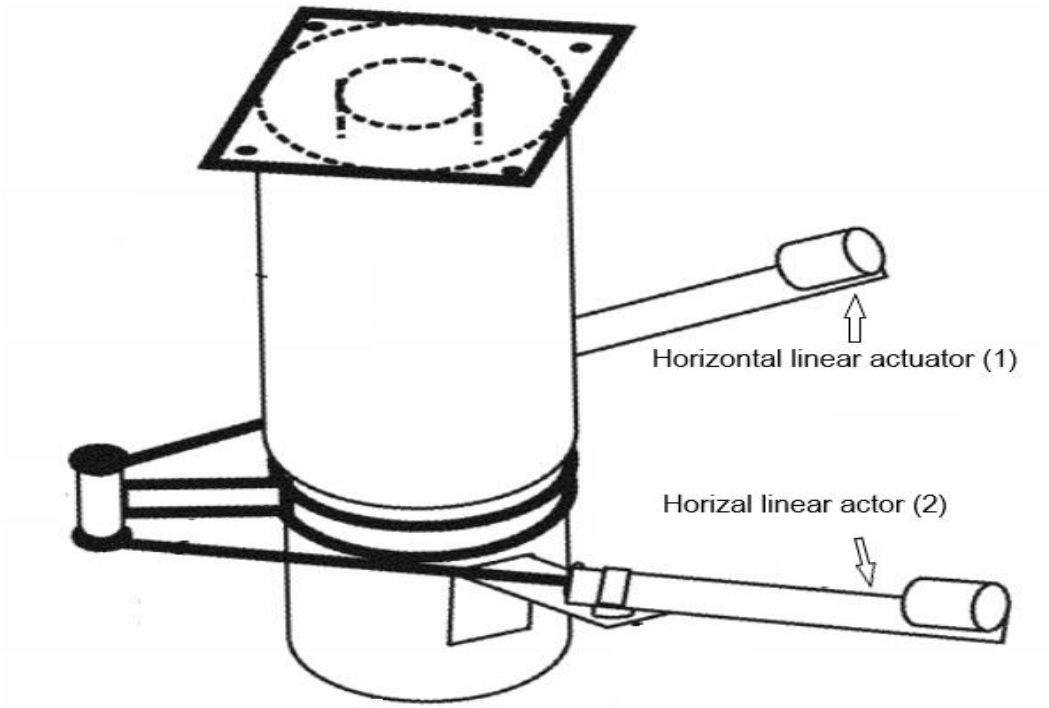

Figure 3.6. The dual linear actuators (Liao, 2013).

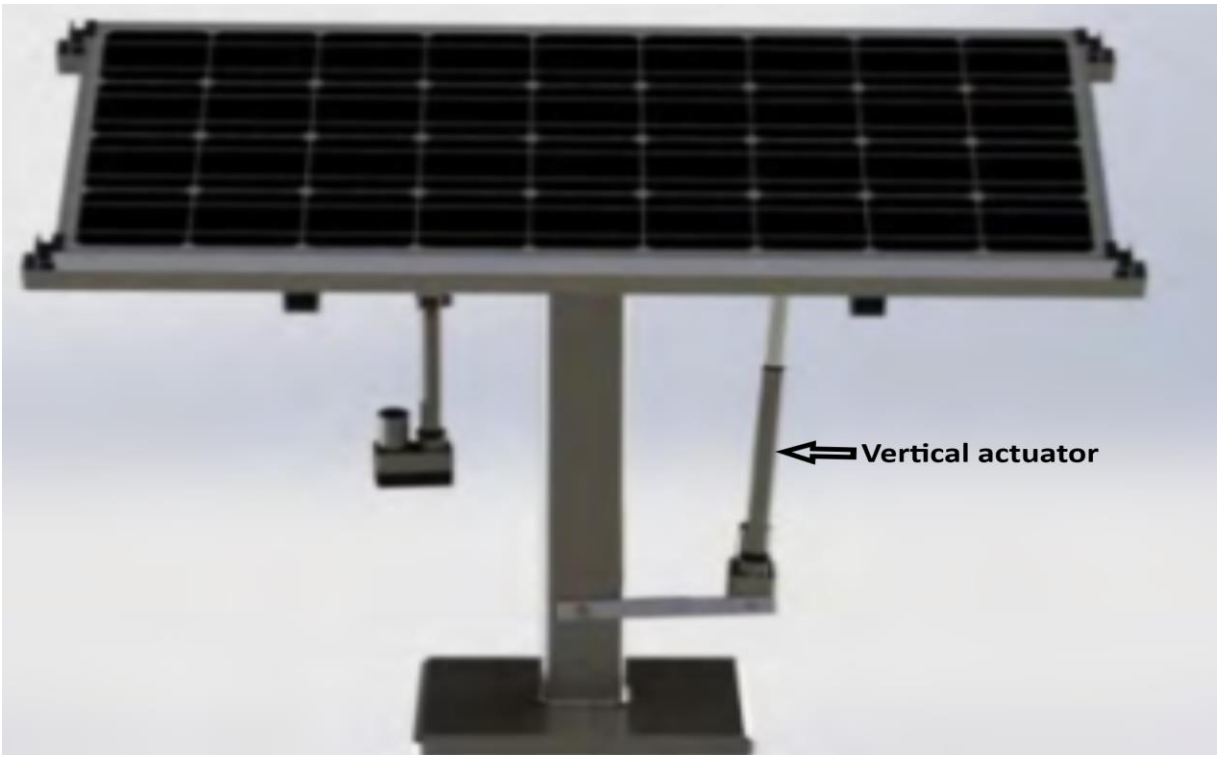

Figure 3.7. The vertical linear actuator (Ceyda et al., 2015).

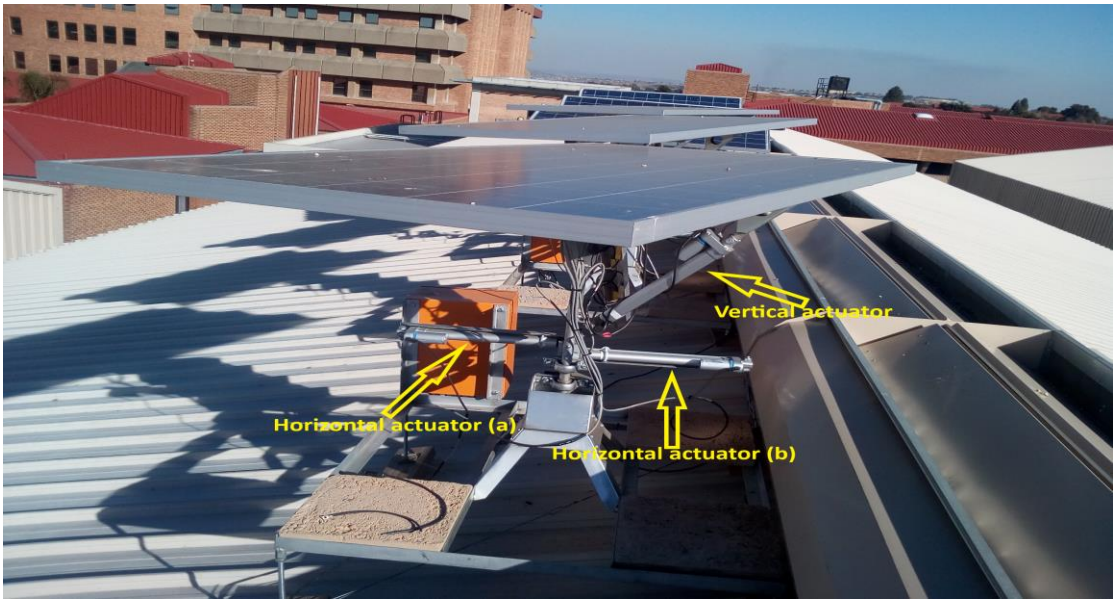

Figure 3.8. The linear actuators.

Table 3.2 lists the characteristics of the SKF linear actuators. The SKF linear actuators operate with an input voltage of 24 V and can handle a maximum load of 500 N (490 kg), which is much higher than each individual PV module's weight (26.8 kg). They have five wires; the first two are for powering the linear actuator (positive and ground), while the other three are for a built-in potentiometer that operates with a 5 V input voltage. The purpose of the built-in potentiometer is for position feedback and to determine the extended length so that the actuators are not pressed beyond their limits (Juang and Radharamanan, 2014). Two horizontal actuators vary the orientation angle by moving the PV module either to the right or the left of 0° North. The vertical actuator varies the tilt angle by moving the module upwards or downwards (between the horizon (0°) and the sky (90°)). The following aspects were observed when choosing the linear actuators: the full actuators length at the two extreme inclinations, actuators force to hold the PV module against the wind, actuators power to move the PV module against the wind and actuators linear extension (or contraction) for rotation at different tracker angles.

Table 3.2. The SKF linear actuator characteristic.

Characteristics	**Value**
Input voltage	24 V dc
Rated current	4 A
Duty cycle	25%
Maximum speed	16 mm/s
Maximum load	500 N

3.5 The load

To establish an economically viable load when considering similar output power results from a PV module, various loads including batteries, solar controllers or maximum power point trackers(MPPTs), regulated and non-regulated light emitting diode (LED) lamps and fixed load resistors can be used (Swart and Hertzog, 2016). LED lamps, instead of a MPPT or a solar controller with a given load, have been used before as an economically viable load in determining the acceptance zone and switch-on times of specific PV modules (Swart and Hertzog, 2016). However, using a fixed load resistance was an effective and easy method to start loading PV modules located outdoors for measurement purposes (Swart and Hertzog, 2016). Fixed resistive loads are also a more viable option for monitoring long-term PV module performance (Osterwald *et al.*, 2006).

Figure 3.9 shows the system load featuring five fixed high power (100 W, 0.82 Ω, 1 Ω) resistors connected in series across a source voltage. The 1 Ω resistor is used because measuring the voltage drop across it allows easy computation of circuit current (V = IR), which translates the measured current to be the measured voltage. The rated PV module open circuit voltage is given as 45.6 V and the measuring equipment (DAQ) can only accept analogue input from 0 – 10 V. To achieve this, a voltage divider circuit is used, with the voltage measured across the 1 Ω resistor. A resistor network of 3.28 Ω and 1 Ω helps to scale down the PV module output voltage to within 0 – 10 V required by the DAQ as shown on Figure 3.3. The 3.28 Ω resistor is realised by using four 0.82 Ω resistors in series. The rated power that the resistors should have is given by equation 3.2. Table 3.3 lists the corresponding values of the resistors used in the system and their possible voltage drops when considering the PV module rated voltage. The rated voltages are determined by equation 3.3.

$$P_{rated} = (V_{rated})\ (I_{rated}) \qquad \text{equation 3.2}$$

$$= (36.3)\ (8.53)$$

= 309.639 W (which is almost the given rated power from the PV module nameplate, 310 W).

$$V_{out} = (I_{rated})\ (R) \qquad \text{equation 3.3}$$

$$= (8.53)\ (0.82 + 0.82 + 0.82 + 0.82 + 1)$$

= 36.5 V (which is the given rated voltage from the PV module nameplate, 36.5 V).

Table 3.3. The load resistors and their voltage drops for a PV module voltage of 36.5 V.

Resistor	Resistance (Ω)	Possible voltage drops across individual resistors (V)
R_1	0.82	6.99
R_2	0.82	6.99
R_3	0.82	6.99
R_4	0.82	6.99
R_5	1	8.53

Figure 3.9. The system's load.

3.6 Fuzzy logic development

A computer simulation model can be an effective tool for validating theory. Simulation models are increasingly being used to solve problems and to aid in decision making. The decision makers using information obtained from the empirical results and the individuals affected by decisions based on such models are all rightly concerned with whether a model and its results are correct. This concern is addressed through model verification and validation (simulation). Model verification is often defined as ensuring that the computer program of the computerised model and its implementation are correct. Model validation is usually defined to mean substantiation that a computerised model within its domain of applicability possesses a satisfactory range of accuracy consistent with the intended application of the model (Stamatescu, 2014).

The lookout angles for the summer season were obtained from the solar elevation angle calculator, which is an online application that is used to calculate the solar angles (Keisan, 2019) . It is essential to state that the current study only focused on the summer season of the

Highveld of South Africa. In this current study, linear equation was used to manipulate the lookout angles of the sun for the day from which the fuzzy logic rule set was derived. Table 3.4 lists the methods that were engaged to develop the fuzzy set rules together with the relevant annexures (please see annexure A and B in this regard). The output power profile of both fixed and tracking systems was used to determine the amount of power reduction due to cloud movement.

Table 3.4. The development of the fuzzy rules.

Step	Description	Reason
1	Obtain the look-out angles for the summer solstice for the research site. These are derived from the azimuth and elevation angles obtained from Keisan.com website.	Used to determine the amount of change required for the orientation and tilt angle for various seasons so as to account for different solar radiation values. A translation table can be used to calculate the tilt and orientation angles using the look-out angles.
2	Obtain an output profile of a fixed solar module for the research site	Used to determine the amount of power reduction for cloud movement to be used as one of the Fuzzy rule inputs derived from historical values
3	Obtain an output profile of a direct-tracking system for the research site	Used to determine the rate of change required for the orientation and tilt angle over a 12-hour day so as to prevent oscillations and reduce power consumption (value per movement)
4	Sketch an anticipated output profile of a solar-tracking system for the research site and indicate the various times of importance	Used to determine the amount of change and rate of change for the solar module
5	Develop a concise generic rule set based on the information of the preceding steps	To be used in the programming of the algorithm in LabView

Figure 3.10 illustrates the flowchart on how the fuzzy decisions were made. At 6:00 am, the system moves to the starting point and checks the season of the year (only the summer season being considered for the current study) and then stipulates a lookout angle of 110° (see Annexure C for the translation table to obtain the actual tilt and orientation angles). It is

essential to state that the tilt angle of the PV module is limited to maximum of 90°. During a sunny day, the motion is kept according to the sun's angles for the day with intervals of 15 minutes while recording and saving the readings. The same condition is maintained even when there is a single cloud based on the condition that the cloud does not last for more than 15 minutes.

Since the sun behaves differently in different seasons, it is essential to state that there should be a slight deviation on the fuzzy rules depending on the season of the year. Figures 3.10, 3.11 and 3.12 depict the fuzzy logic flowchart rules for the summer season and for different times of the day (1A, 1B-1E 1F-1I). At the beginning, the system determines the season of the year (summer), then the time of the day and applies the relevant rule set. The flowchart shows 1A, which represents 6:15 am -9 am, 1B (9 am -10 am), 1C (10 am -11 am), 1D (11 am -12 pm), 1E (12 pm -13 pm), 1F (13 pm -14 pm), 1G (14 pm -15 pm), 1H (15 pm -16 pm) and 1I representing 16 am -18 pm. The system also makes use of the power history values for decision-making purposes. If the output power falls by more than 80% over two consecutive readings, then a subroutine is called (see Table 3.6) as it is assumed that multiple clouds are present. According to Linares *et al.,* (2012), a threshold dip range is considered to be 80% of full load.

The system proposes lookout angles as outputs with necessary adjustments (increments of 2.5° at 3 pm and 1.7° at 4 pm). The adjustments are determined by the difference between four consecutive lookout angles in an interval of 15 minutes, then the difference is utilised to determine the hourly average change (increase). That means the system will assume a lookout angle of 110° at 6 am and automatically adjusts (increases) the lookout angle by 1.9° between 6:15 am and 9 am and by 3° between 9 am and 10 am (please refer to Annexure B and figures 3.10-3.12 for the whole day sequence). Table 3.5 lists the daily lookout angles from the website and the daily average lookout angles increase calculated for the fuzzy logic algorithm.

For any given location on Earth, the sun is observed to trace a higher path above the horizon in the summer and a lower path in the winter (Figure 2.7 from Chapter 2). During autumn/spring it traces an intermediate path. This means that the sun takes a greater amount of time across the sky in the summer and a shorter amount of time in the winter. For the summer season the PV module starts at an angle of 110°, while in the winter season it would start at an angle of 90° (orientation).

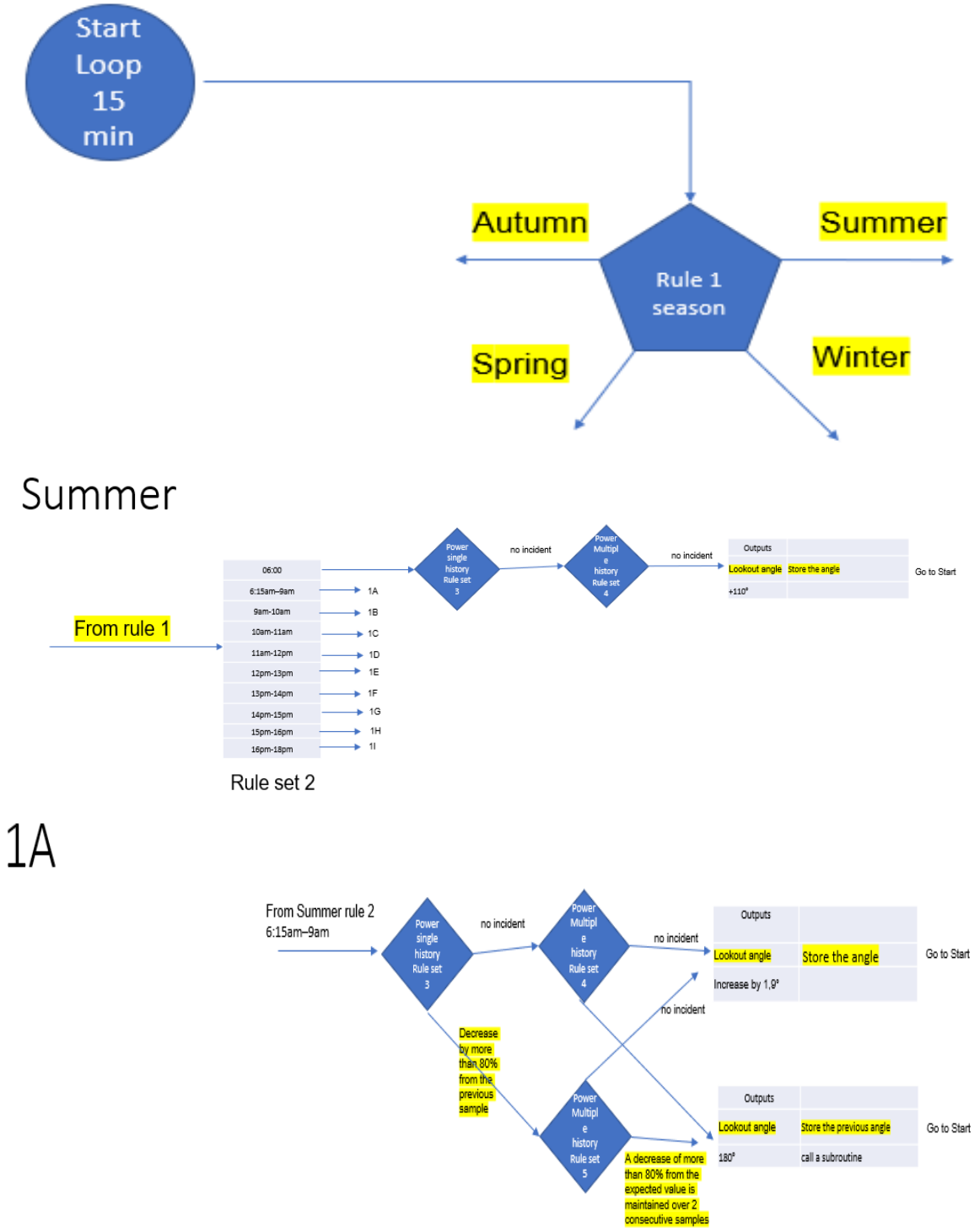

Figure 3.10. The fuzzy logic flowchart showing start loop, season of the year and time of the day (1A).

1B

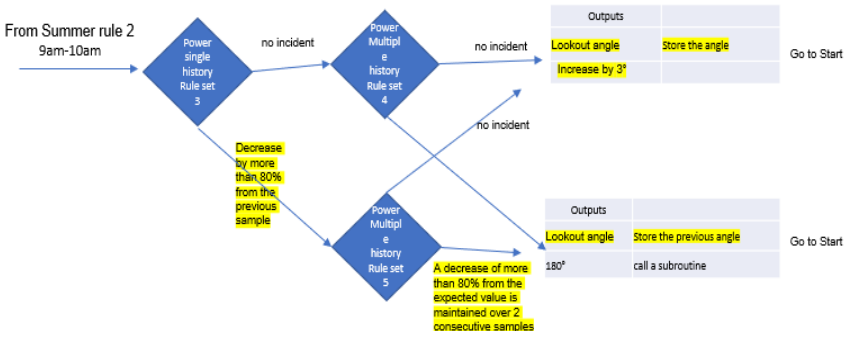

1C

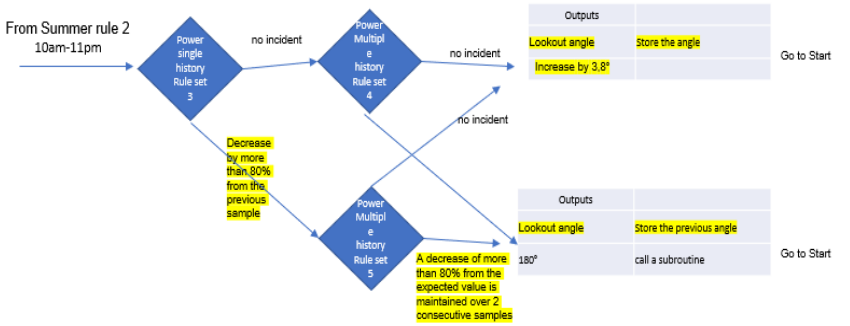

1D

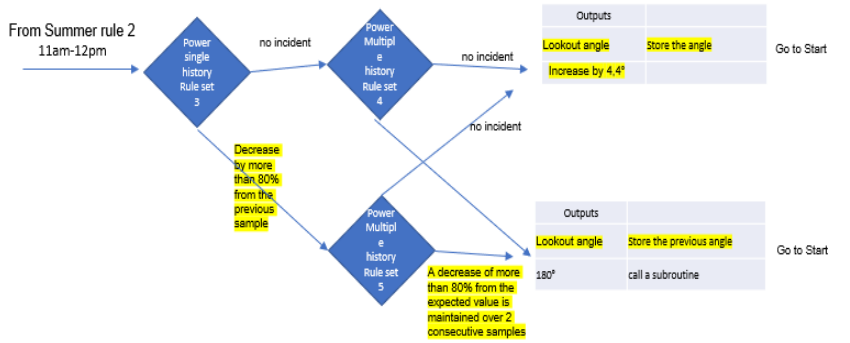

1E

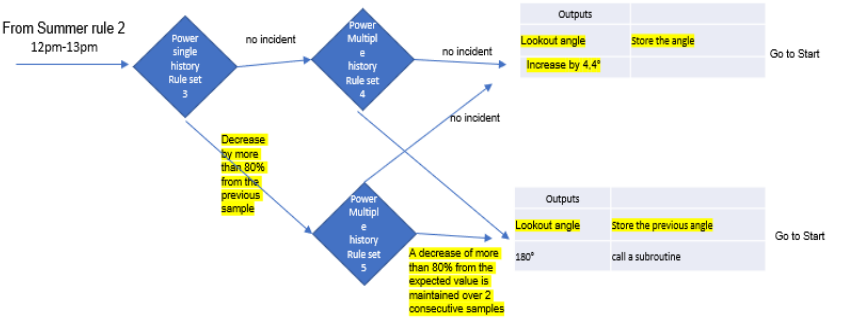

Figure 3.11. The fuzzy logic flowchart showing season of the year and time of the day (1B-1E).

1F

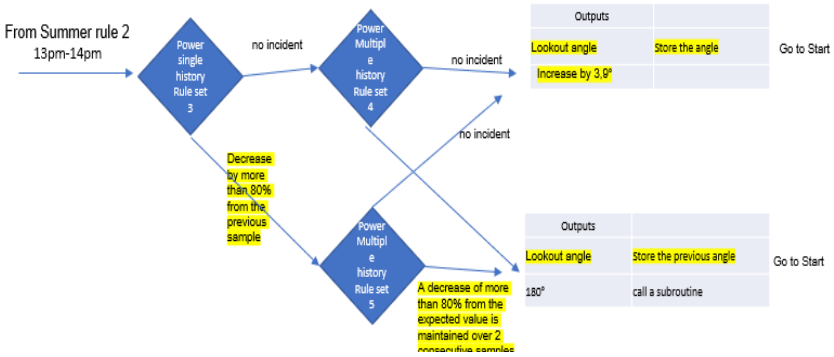

1G

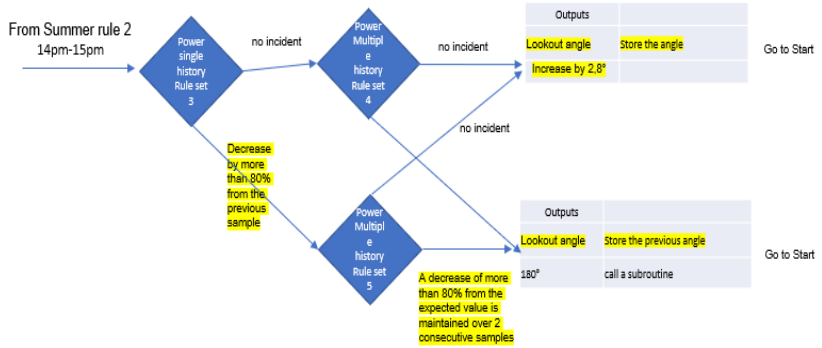

1H

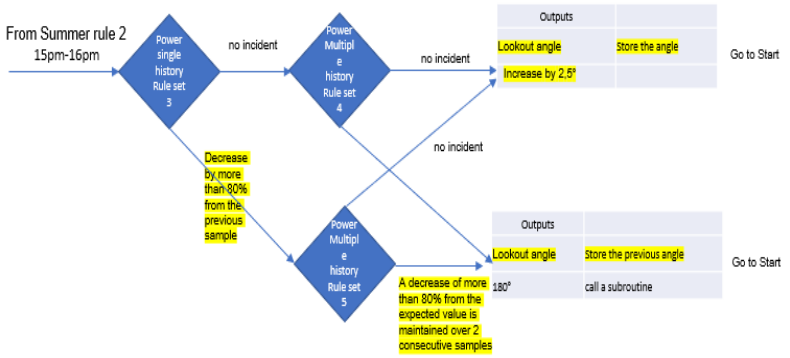

1I

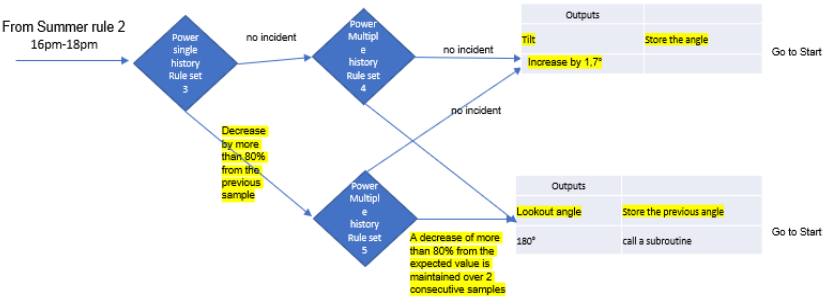

Figure 3.12. The fuzzy logic flowchart showing season of the year and time of the day (1F-11).

Table 3.5. The daily lookout angles from the website and the daily average lookout angles increase calculated for the fuzzy logic algorithm.

Time of the day (hours)	**Lookout angles from the Keisan website (°)**	**Average increase calculated (°)**
06:15 am	112,1	1,9
07:00 am	116,8	
08:00 am	124,3	
09:00 am	133,6	
10:00 am	149,1	3
11:00 am	160,7	3.8
12:00 pm	178,1	4,4
13:00 pm	195,9	4,4
14:00 pm	211,5	3,9
15:00 pm	222,6	2,8
16:00 pm	232,7	2,5
17:00 pm	240,0	1,8
18:00 pm	246,6	1,7

On the condition whereby there are multiple clouds, the direct-tracking PV module should be flat (adjusted to lookout angle of 180°, which correlates to 0° tilt angle and 0° orientation angle). This is to avoid damage to the system due to stormy weather. The system remains flat as long as there is no power increase of more than 80% over two consecutive samples. However, if there is 80% power increase, the system moves back to the stored output and goes back to the main loop, as listed on the subroutine rules in Table 3.6.

Table 3.6. Subroutine rules.

Input					**Action**
ID	**Season**	**Time of the day**	**Power history value (single cloud)**	**Power history value (multiple clouds)**	**Action**
1	Summer	6:15am–9am	NA	No increase by more than 80% over the previous sample	Stay at 180° and increase the stored angle value from the main loop by 1.9°
2	Summer	6:15am–9am	NA	Increase by more than 80% over previous samples	Go back to the main loop and increase by 1.9°
3	Summer	9am-10am	NA	No increase by more than 80% over the previous sample	Stay at 180° and increase the stored angle value from the main loop by 3°

4	Summer	9am-10am	NA	Increase by more than 80% over previous samples	Go back to the main loop and increase by 3°
5	Summer	10am-11am	NA	No increase by more than 80% over the previous sample	Stay at 180° and increase the stored angle value from the main loop by 3.8°
6	Summer	10am-11am	NA	Increase by more than 80% over previous samples	Go back to the main loop and increase by 3.8°
7	Summer	11am-12pm	NA	No increase by more than 80% over the previous sample	Stay at 180° and increase the stored angle value from the main loop by 4.4°
8	Summer	11am-12pm	NA	Increase by more than 80% over previous samples	Go back to the main loop and increase by 4.4°
9	Summer	12pm-13pm	NA	No increase by more than 80% over the previous sample	Stay at 180° and increase the stored angle value from the main loop by 4.4°
10	Summer	12pm-13pm	NA	Increase by more than 80% over previous samples	Go back to the main loop and increase by 4.4°
11	Summer	13pm-14pm	NA	No increase by more than 80% over the previous sample	Stay at 180° and increase the stored angle value from the main loop by 3.9°
12	Summer	13pm-14pm	NA	Increase by more than 80% over previous samples	Go back to the main loop and increase by 3.9°
13	Summer	14pm-15pm	NA	No increase by more than 80% over the previous sample	Stay at 180° and increase the stored angle value from the main loop by 2.8°
14	Summer	14pm-15pm	NA	Increase by more than 80% over previous samples	Go back to the main loop and increase by 2.8°
15	Summer	15pm-16pm	NA	No increase by more than 80% over the previous sample	Stay at 180° and increase the stored angle value from the main loop by 2.5°
16	Summer	15pm-16pm	NA	Increase by more than 80% over previous samples	Go back to the main loop and increase by 2.5°
17	Summer	16pm-18pm	NA	No increase by more than 80% over the previous sample	Stay at 180° and increase the stored angle value from the main loop by 1.7°
18	Summer	16pm-18pm	NA	Increase by more than 80% over previous samples	Go back to the main loop and increase by 1.7°

It is essential to state that the fuzzy set for the other three seasons would still need to be determined. However, the current study only focused on the summer season, as noted under the delimitations in Chapter 1.

3.7 The linear regression development

In this current study, a linear regression equation (equation 3.4) was used to determine proposed lookout angles for the solar-tracking system for 21 December (solstice day). The system executes at 6 am, assuming the lookout angle of 103.81°, which was determined by

using equation 3.4 (Annexure C), keeping the motion with intervals of 15 minutes. According to Keisan (2019), the lookout angle of the sun at 6 am is 110,7°. However, based on the calculations using the linear regression equation the angle is calculated to be 103,8° (Table 3.7). Table 3.7 lists the hourly changes of lookout angles from the website and the calculations using equation 3.4 followed by the demonstration on how the equation was utilised to come up with the lookout angle (Y) of 103,7°. The other variables used are listed and explained under equation 3.4 while the rest of the calculations can be found on Annexure C. It must be stated that the lookout angles can be translated into tilt and orientation angles (Annexure C). The output power profile of both fixed and direct-tracking systems was used to predict the power profile during the day. It is essential to state that the linear regression equation assumes the straight-line motion (no backwards motion) and is not influenced by the weather conditions. That means whether there is a single cloud or multiple clouds, it keeps on moving froward from 6 am to 6 pm.

$$Y = a + bx \qquad \text{equation 3.4}$$

Where:

Y = Linear regression function (dependent variable)

a = Y-intercept

b = Slope

x = X-axis value (independent variable)

In this current study the equation will be used as follows:

Y = Simulated lookout angles

a = First lookout angle of the day, which equates to 103.65°

b = Multiplying constant (0.0039)

x = Accumulated power total from direct-tracking system

The application of equation 3.4 yields the following lookout angle for a given direct power measurement:

$$Y = 103{,}648 + (3.993 \times 10^{-3})\ (41{,}42)$$

$$= 103{,}8^{\circ}$$

Table 3.7. The daily lookout angles from the website and calculated lookout angles using the linear regression equation.

Time of the day (hours)	Lookout angle from the website (°)	Calculated lookout angles (°)
06:00 am	110,7	103,8
07:00 am	116,8	113,0
08:00 am	124,3	125,9
09:00 am	133,6	138,5
10:00 am	145,6	151,2
11:00 pm	160,7	164,5
12:00 pm	178,1	178,2
13:00 pm	195,9	192,2
14:00 pm	211,5	260,6
15:00 pm	222,6	219,4
16:00 pm	232,7	231,8
17:00 pm	240,0	234,1
18:00 pm	246,6	246,6

3.8 Conclusion

The components used in the practical setup of the present study were discussed in detail in this chapter. The chapter furthermore incorporated the functional block diagrams of the software (LabVIEW user interface) that are used to house the direct-tracking algorithm. Three actuators are used to execute the movement of the system. Two horizontal actuators vary the orientation angle by moving the PV module either to the right or the left of 0° North. The vertical actuator varies the tilt angle by moving the module upwards or downwards (between the horizon (0°) and the sky (90°)). The development of fuzzy logic and linear regression algorithms were also discussed in detail. The results of the system will be discussed in detail in the next chapter (Chapter 4).

Chapter 4 – The analysis of the results of the system

4.1 Introduction

The previous chapter (Chapter 3) discussed the direct-tracking algorithm and detailed the development of the two algorithms (fuzzy logic and linear regression) that are to be used to simulate the power profile of a tracking system. The fixed photovoltaic (PV) modules, set at the same orientation angle of 0°, but at different tilt angles of 16°, 26° and 36° true North (N), were similarly discussed. The controlling software, hardware (linear actuator with Laboratory Virtual Instrument Engineering Workbench (LabVIEW)) and the system's load were also outlined. The aim of this chapter is to discuss and analyse the results of the empirical direct- tracking system, fixed PV module, simulated fuzzy logic and linear regression algorithms. The analysis will assist in establishing the algorithm that yields the maximum output power. However, to enable reliability of data obtained from the PV modules requires the system to be calibrated.

4.2 The calibration of the system

Calibration of equipment is of vital importance before measurements can be taken so as to ensure accuracy and to validate any future measurements as being reliable (Swart and Hertzog, 2019). Figure 4.1 depicts one fixed system and the direct-tracking system that were initially set at a fixed tilt (26°) and orientation angle (0°) for calibration purposes. The intention of calibrating the system was to eliminate any bias between the systems. The measurements were calibrated using a Rish Multi 16S True RMS multimeter on 09 February 2019. This was done by physically measuring the output voltage across the load resistors and the current flowing through the 1 Ω resistor.

Figure 4.1. The practical system with the PV modules used for calibration.

Figure 4.2 highlights the physically measured voltage of 34.9 V and current of 8.29 A on the digital multimeters for calibration purposes. The figure displays the measurements taken on

the fixed-system set to 26° (fixed at tilt angle of 26° and orientation angle of 0°). The other measurements for the direct-tracking system and the redundancy system fixed at 26° for calibration purposes are shown in Table 4.1. From Table 4.1, the measured values from the digital multimeter correlate well with the values obtained from the LabVIEW user interface. Before any conclusion could be reached after recording results, it was important to recheck the calibration of the system to ensure the validity and reliability of the results.

Figure 4.2. The Rish Multi 16S True RMS multimeter for the fixed 26° systems (fixed at tilt angle of 26° and orientation angle of 0°).

Table 4.1. Calibration results.

Angle	LabVIEW Current (A)	Multimeter Current (A)	Current Error Percentage (%)	LabVIEW Voltage (V)	Multimeter Voltage (V)	Voltage Error Percentage (%)
Fixed-system at (26°)	8,27	8,29	0,24	34,8	34,9	0,29
Direct-tracking system (26°)	8,27	8,29	0,24	34,3	34,5	0,58
Redundancy system (26°)	8,27	8,29	0,24	34,5	34,6	0,29

The LabVIEW user interface was used to visualise the measured data. It was designed and developed for this research study pertaining to the operating parameters of PV modules and linear actuators. The sample interval (measurements taken every 4 seconds) and cycle duration of 12 hours (6 am – 6 pm) may be adjusted after each complete cycle, as LabVIEW first needs to close an opened text file on the hard drive of the computer. This text file contains

the measurements displayed on the user interface, which are only saved at the end of the complete cycle. Figure 4.3 shows the LabVIEW user interface that was used to display voltage and current readings from the PV modules. The following information is also displayed on the LabVIEW user interface:

- Analog instantaneous value of voltage for each PV module (point A);
- Analog instantaneous value of current for each PV module (point B);
- Digital instantaneous value of voltage for each PV module (point C);
- Digital instantaneous value of current for each PV module (point D);
- Execution date and time of the system (point E and F);
- Manual start of the measuring system ignoring the set system's start time (G);
- Manual stop button function to control the while loop execution (point H);
- Instantaneous value of voltage for each PV module (point I); and
- Instantaneous value of current for each PV module (point J).

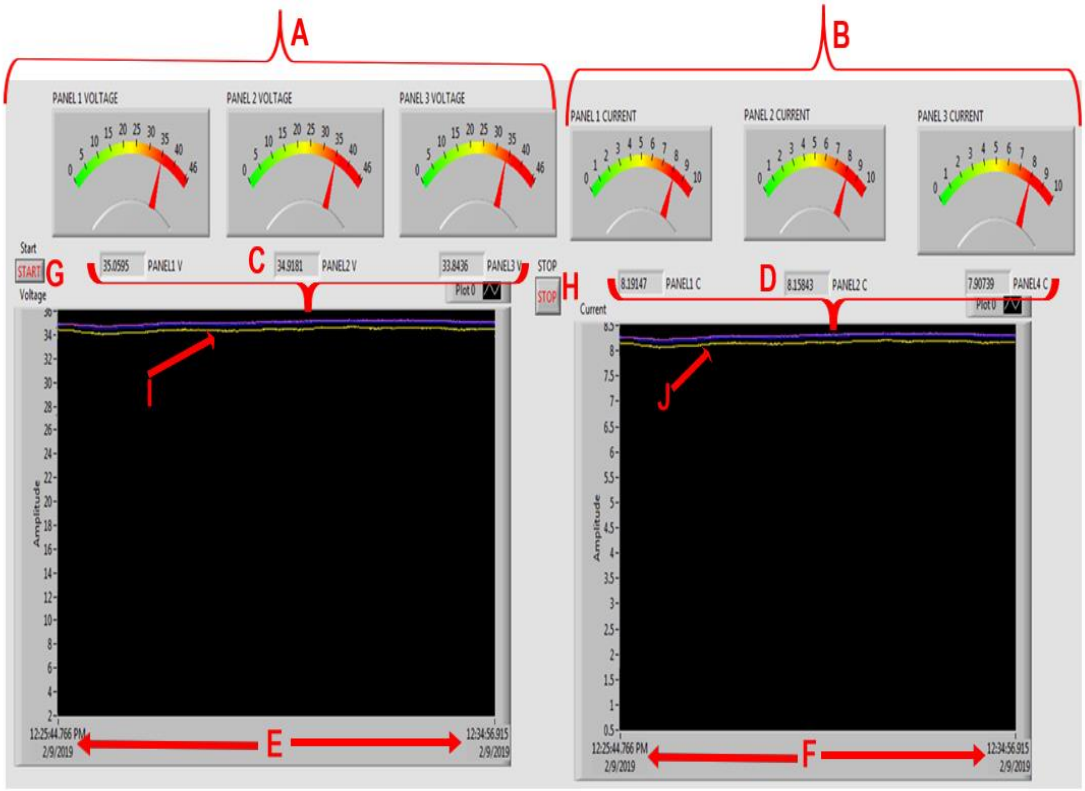

Figure 4.3. The LabVIEW front panel.

The calibration readings were compared to the available readings in the LabVIEW user interface, so that the instantaneous voltage and current values displayed on the interface equalled the values displayed on the digital multimeter. The system was calibrated between 12:30 noon and 01:00 pm when the sun was perpendicular to all the PV modules. The measurements were first done on the 26° fixed-system PV module. A current of 8,29 A from

the PV module was measured (physically) while the LabVIEW interface displayed 8,27 A. The readings (currents and voltages) measured physically and displayed by the LabVIEW interface were obtained within a 30 minutes' period. Table 4.1 further presents the percentage difference between the voltmeter and LabVIEW readings. The highest error percentage for voltage occurred for the linear regression system (being 0.58%). Results indicate that three identical PV systems can be calibrated to produce the same results, with variability of less than 1% (Swart and Hertzog, 2019). A consistent percentage (0.24%) between the multimeter and LabVIEW user interface was established for the current values. The results indicated that there was no need for adjustment to the system as all the factors were less than 1%. The voltage measured for one day was utilised to plot a graph as illustrated in Figure 4.4 where two PV modules were fixed at the same tilt and orientation angles for calibration purposes. The correlation coefficient value between the 26° fixed system and the direct-tracking system (initially placed at 26°) was found to be 0.999. A correlation coefficient of +1 indicates that the two variables are perfectly related in a positive manner (Gogtay and Thatte, 2017).

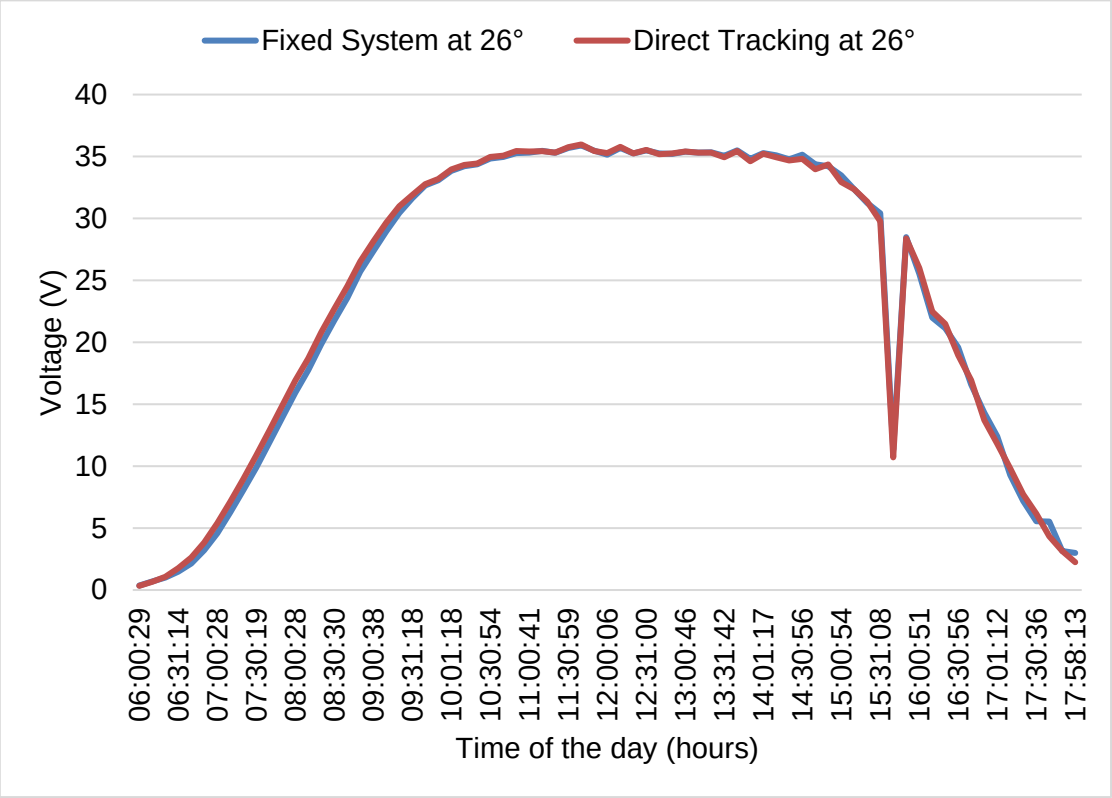

Figure 4.4. The three PV modules fixed at 0° orientation and 26° tilt angles for calibration.

From Figure 4.4, the PV modules continued to behave similarly throughout the day. From 11 am to 14:20 pm the PV modules were aligned to the larger portion of the solar radiation, which is normally maximum at 12 noon. The PV modules produced constant output voltage which was nearly the maximum rated voltage. The voltage was nearly maximum because it was

measured across a fixed load (1 Ω) resistor. Fixed load resistors limit the current drawn from the PV module and does not make use of all the available current when the resistor value is too high (Swart and Hertzog, 2016). There was a voltage dip between 15:20 pm and 16:00 pm due to cloud movement that interrupted the direct beam radiation. The purpose of the calibration was to produce the same results for all three PV modules that were orientated similarly, using the same load profile. This was achieved, which indicates that the setup is valid and that subsequent measurements would be reliable.

4.3 The fixed PV modules results

Figure 4.5 illustrates the three fixed-system PV modules that were used as the baseline for the research study. The PV modules are set at the same fixed orientation angle of 0° and fixed tilt angles of latitude minus 10° (16°), latitude (26°) and latitude plus 10° (36°). The tilt angles are derived from the Heywood and Chinnery equations of latitude for calculating tilt angles of PV modules in South Africa (SA) (Hertzog and Swart, 2015). Johannesburg lies on latitude of 26° south and longitude 27° east, giving the mathematical results for tilt angles as shown in Table 4.2 (Hertzog and Swart, 2016). A tilt angle of 26° is used in this research study, which corresponds to the latitude (θ) value of the installation site at the University of South Africa (UNISA), Science Campus, Florida, Johannesburg.

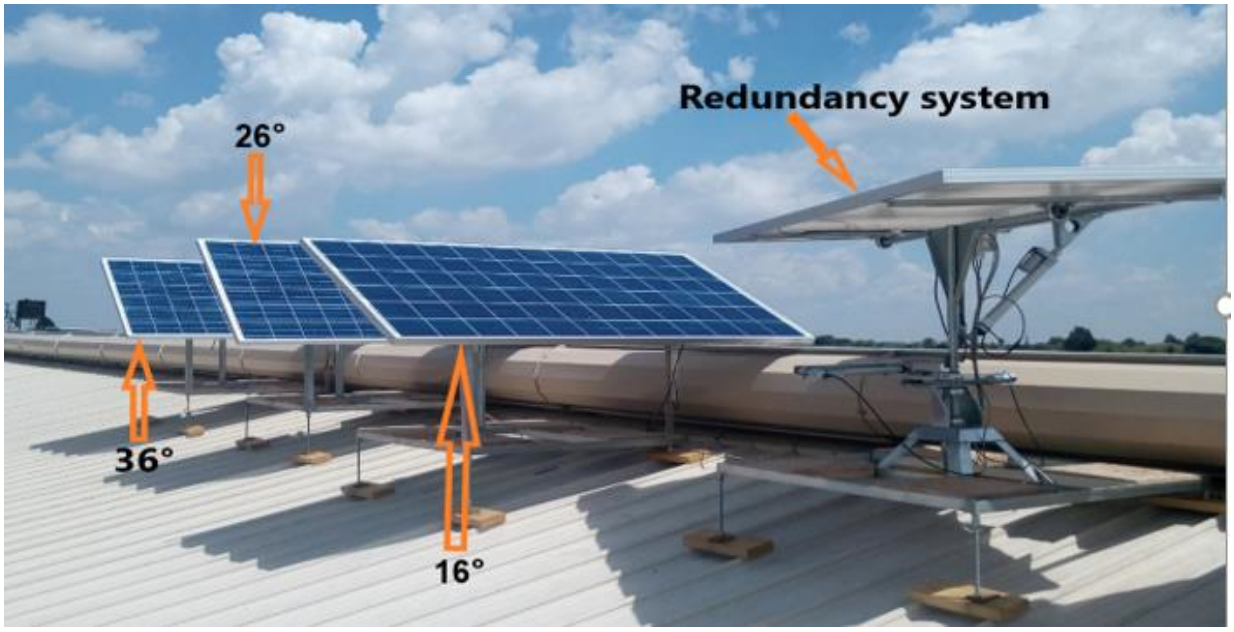

Figure 4.5. The three fixed PV modules.

Figure 4.6 illustrates one day (1 December 2018) of instantaneous power (in Watts - W) from the three PV modules fixed at the same orientation angle (0º), but set at different tilt angles

(16°, 26° and 36°). It is evident that the 16° PV module performed better than the other two PV modules from 7 am to 11:00 am and from 2:30 pm to 6:00 pm.

Table 4.2. Calculation of tilt angles.

Source	Latitude	Equation	Calculation	Tilt angle
Heywood and Chinnery (1971)	26°	θ-10°	26°-10°	16°
	26°	θ	26°	26°
	26°	θ+10°	26°+10°	36°

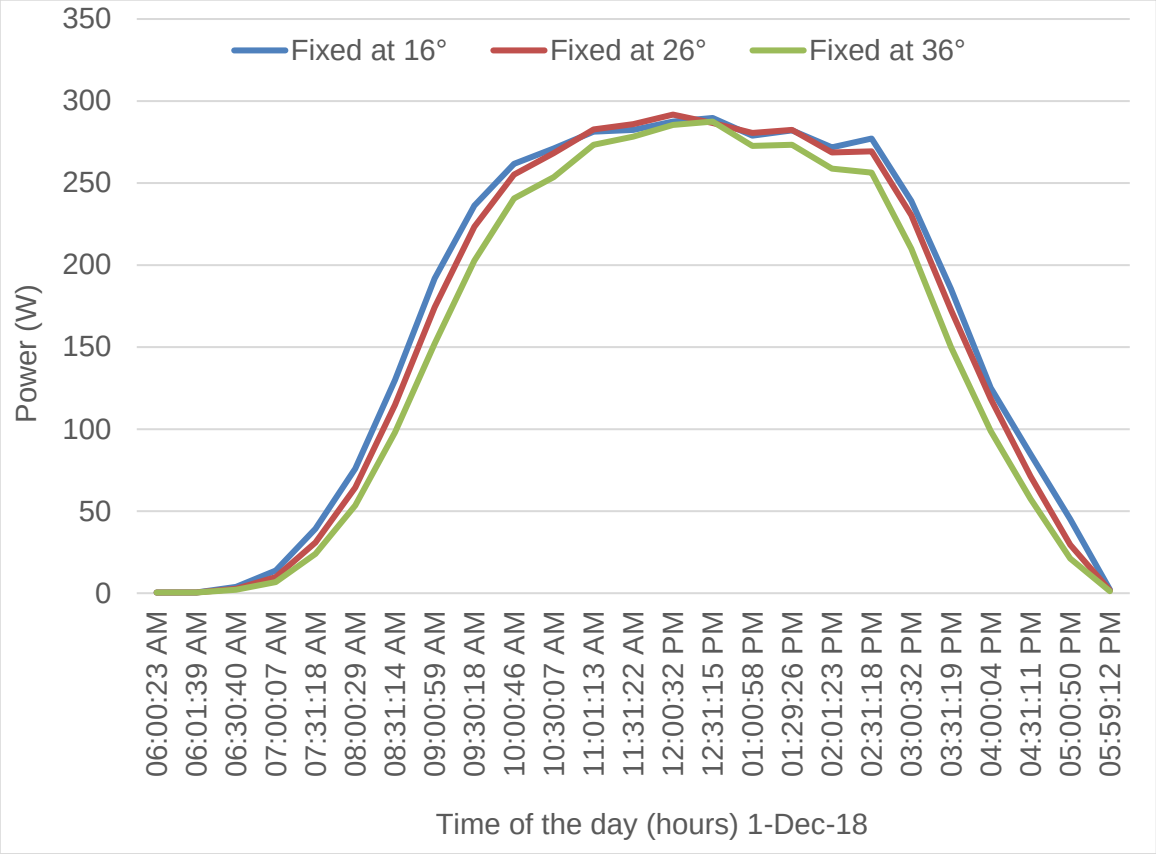

Figure 4.6. The three fixed PV modules results.

From Figure 4.6, all the PV modules produced nearly equal maximum power from 11:00 am to 2:30 pm, as their surfaces were very near to being perpendicular to the sun's rays. The three fixed-system PV modules' instantaneous power readings for each time slot are listed in Table 4.3. These instantaneous power readings were used to calculate the subsequent power over a period of time (Wh). This was done by calculating the average power per hour for the day (12 hours) and then determining the Wh readings as shown at the bottom of Table 4.3. A comparison of output power and efficiency between various continuous cooling systems of PV modules was carried out at the Universiti Malaysia Sabah, Kota Kinabalu. The measurements

were taken for a period of 10 days (13th to 22nd of March 2016) and from 06 am to 18 pm (12 hours of the day) (Sukarno *et al.*, 2017). The maximum rated power of the PV modules used in this current study is 310 W (from the nameplate). This means, if the system runs at maximum power for a period of 12 hours in a day, it can produce 3720 Wh in a day (310 W x 12 hours).

Table 4.3. The fixed PV modules average hourly power readings (W) and the total Wh for the day (1 December 2018).

Time	**16°**	**26°**	**36°**
6 am-7 am	4,78	3,40	2,55
7 am-8 am	39,80	31,85	24,96
8 am-9 am	127,04	112,76	96,79
9 am-10 am	233,28	220,09	200,82
10 am-11 am	271,23	269,06	257,48
11 am-12 pm	274,81	277,03	270,12
12 pm-13 pm	291,14	293,06	286,01
13 pm-14 pm	279,65	279,60	270,78
14 pm-15 pm	269,69	261,73	248,02
15 pm-16 pm	187,05	176,26	154,90
16 pm-17 pm	91,39	78,46	63,47
17 pm-18 pm	14,93	11,15	7,51
Total Wh for the day	2084,79	2014,44	1883,42
Percentage difference	16° > 26° = 3,49%	26° > 36°= 6,96%	16° > 36°=10,69%

The total Wh percentage difference produced per day between the 16° system and the 26° system was 3.49%, between the 16° system and 36° system was 10.69%, while between the 26° system and 36° system was 6.96%. For the 16° PV module the calculated Wh for the day was 2 084,793 Wh, which is calculated to be 55.94% of the possible maximum Wh per day (3720 Wh) if 12 hours are considered. The three fixed-system PV modules weekly average power readings for a period of six months was used to calculate the Wh for this period that is shown in Table 4.4, with the total recorded at the bottom of the table. From the PV modules' ratings, each module can produce 310 Wh every hour (310 W for an hour), for a daily duration of eight hours, the modules can produce 2 480 Wh a day. The systems run for a period of six months (181 days), which translates to a possible maximum Wh of 448 880 Wh (181 x 2 480 Wh). Using the Wh to calculate the percentage difference between the modules, the total Wh percentage difference produced for six months period between the 16° system and the 26°

system was 3.48%, between the 16° system and 36° system was 10.69%, while between the 26° system and 36° system was 6.97%. This means that the 16° tilt angle performed the best in producing more output power than the other two fixed systems.

Table 4.4. The fixed PV modules instantaneous power readings and the total Wh for six months.

Time	**16°**	**26°**	**36°**
November 2018 Week 1	1175,29	1135,42	1060,42
November 2018 Week 2	864,53	835,72	780,73
November 2018 Week 3	1238,88	1197,19	1118,05
November 2018 Week 4	1449,15	1399,89	1306,98
December 2018 Week 1	2097,34	2026,57	1894,76
December 2018 Week 2	1570,92	1517,91	1419,18
December 2018 Week 3	450,69	435,50	407,19
December 2018 Week 4	1730,19	1671,80	1563,07
January 2019 Week 1	1778,15	1718,40	1606,88
January 2019 Week 2	1138,17	1099,92	1028,54
January 2019 Week 3	930,73	899,45	841,08
January 2019 Week 4	975,33	943,61	883,33
February 2019 Week 1	1093,15	1056,41	987,85
February 2019 Week 2	822,91	795,26	743,64
February 2019 Week 3	1296,63	1253,06	1171,73
February 2019 Week 4	1067,58	1031,71	964,75
March 2019 Week 1	1264,16	1221,68	1142,39
March 2019 Week 2	623,20	602,26	563,17
March 2019 Week 3	710,54	686,66	642,10
March 2019 Week 4	424,17	409,92	383,31
April 2019 Week 1	456,66	441,32	412,68
April 2019 Week 2	280,92	271,48	253,86
April 2019 Week 3	229,72	222,00	207,59
April 2019 Week 4	189,21	182,89	171,04
Total 6 Months Ave. Wh	23858,22	23056,02	21554,31
Percentage difference	16° > 26°=3,48%	26° > 36°= 6,97%	16° > 36° = 10,69%

Table 4.5 shows the normal descriptive statistics for the fixed PV modules for a period of six months. The mean is less than the median, which translates to the data being distributed more

to the left (negatively skewed distribution). For negatively skewed distribution, the mean is less than the median (Doyle, 2009). Data is distributed normally when the kurtosis and skewness are within ±1 (Prabhakar *et al.*, 2019). In this case, the kurtosis value is -0,530 for both the 16° and the 26° fixed PV modules and -0.528 for the 36° fixed PV module and the skewness value is 0,231 for all the fixed modules, thereby suggesting a normal distribution with no unexpected or unwarranted results.

Table 4.5. The fixed PV modules approximate normal descriptive statistics for six months.

Descriptive statistics	**16°**	**26°**	**36°**
Mean	994,093	960,668	898,097
Standard Error	105,336	101,779	95,138
Median	1021,455	987,660	924,040
Standard Deviation	516,039	498,611	466,080
Sample Variance	266295,904	248612,932	217230,339
Kurtosis	-0,530	-0,530	-0,528
Skewness	0,231	0,231	0,231
Range	1908,130	1843,680	1723,720
Minimum	189,210	182,890	171,040
Maximum	2097,340	2026,570	1894,760
Sum	23858,220	23056,020	21554,310
Count	24	24	24

4.4 A comparison of the direct-tracking power with the simulated results

4.4.1 Fuzzy logic results

Figure 4.7 represents the sunny day (cloudless day) daily profile of the fixed system power (16°), the direct-tracking system power and the simulated power for fuzzy logic. The graph was drawn using data from Annexure D, which consists of the measurements for the fixed system power, the direct-tracking system power and the simulated power for the fuzzy logic. From the graph it is evident that both the empirical and simulated results behaved similarly from sunrise to sunset. However, the simulated power for fuzzy logic was better than the direct-tracking system power by 5.31%. The direct-tracking system power showed 32% improvement over the fixed system power. The fixed system power was less in the morning (06:00 am), growing gradually and becoming maximum from 10:30 am but decreasing gradually from 03:00 pm onwards.

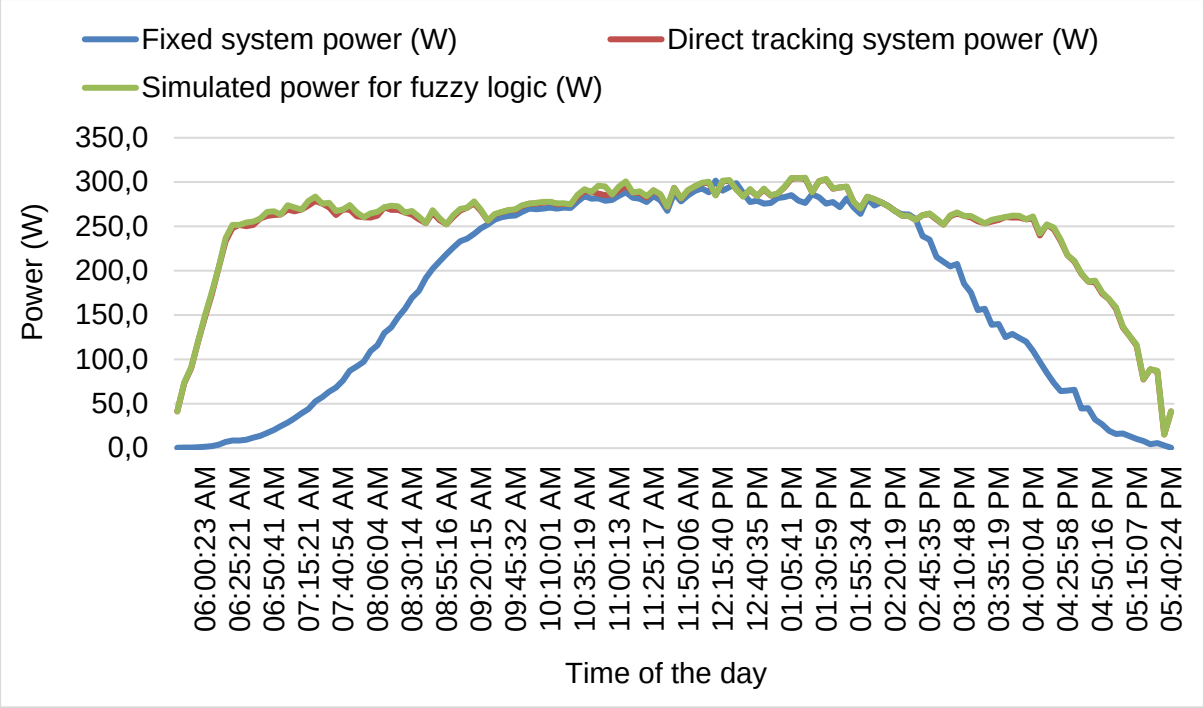

Figure 4.7. The sunny day graph for fixed system power, direct-tracking system power and simulated power for fuzzy logic.

Figure 4.8 represents the sunny day with a single cloud daily profile of the fixed system power (16°), the direct-tracking system power and the simulated power for fuzzy logic. The graph was drawn using data from Annexure E. The direct-tracking system power and the simulated power for fuzzy logic behaved similarly from sunrise to sunset. However, the simulated power for fuzzy logic was better than the direct-tracking system power by 3.7%. The direct-tracking system power showed 31% improvement over the fixed system power. It is evident from Figure 4.8 that at 02:45 pm, there was a power dip due to a single cloud in the sky. It is essential to state that the fuzzy logic algorithm will continue with the main loop during a single cloud event and will not call the subroutine, which is listed as Table 3.4 in Chapter 3.

Figure 4.9 represents the sunny day with multiple clouds (in the afternoon) daily profile of the fixed system power (16°), the direct-tracking system power and the simulated power for the fuzzy logic. The graph was drawn using data from Annexure F. Likewise, the empirical and simulated results behaved similarly from sunrise to sunset. The simulated power for fuzzy logic was better than the direct-tracking system power by 2%. The direct-tracking system power was 21.76% as compared to the fixed system power. It is essential to state that from 02:45 pm, the fuzzy logic algorithm would enter the subroutine outlined in Table 3.4. The lookout angle would be 180°, which translates to an orientation and tilt angle of 0° making the PV module flat. More translations of the lookout angles can be found in Annexure D, E and F.

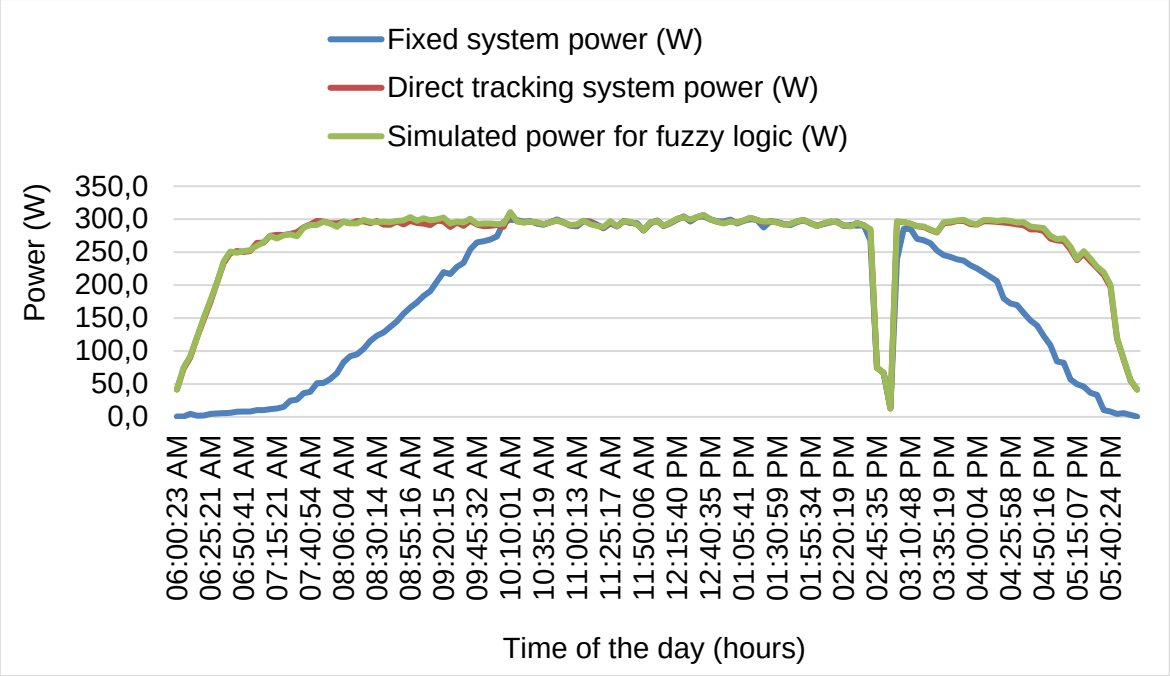

Figure 4.8. The sunny day graph with a single cloud for fixed system power, direct-tracking system power and simulated power for fuzzy logic.

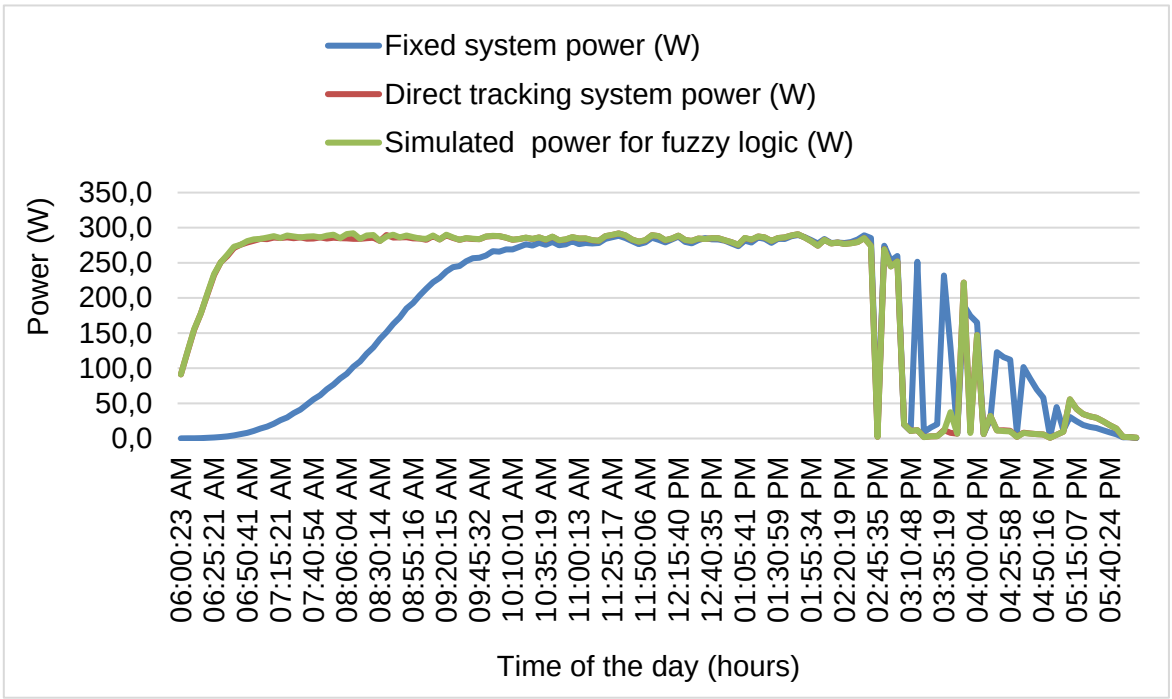

Figure 4.9. The sunny day with multiple clouds for fixed system power, direct-tracking system power and simulated power for fuzzy logic.

4.4.2 Linear regression results

Figure 4.10 represents the sunny day daily power profile of the fixed system (16°), the empirical results of the direct-tracking system and the simulated linear regression algorithm. The graph was also drawn using data from Annexure D, which consists of the measurements for the fixed system power, the direct-tracking system power and the simulated power for the linear regression algorithm. From the graph, it is evident that both the direct-tracking system power and the simulated power for linear regression behaved similarly from sunrise to sunset. Nevertheless, the direct-tracking system power was better than the simulated power for linear regression by 2.24%. This was due to the fact that the direct-tracking system had the advantage of moving forward and backwards, while the linear regression algorithm only moved forward. The simulated power for linear regression demonstrated 30.97% improvement over the fixed system power. It is essential to mention that no weather condition (single or multiple clouds) was considered because the system was designed with no extreme weather conditions in mind. This indicates a key difference between the linear regression algorithm and fuzzy logic algorithm in the sense that the fuzzy logic algorithm can respond better to changing weather conditions as compared to the linear regression algorithm.

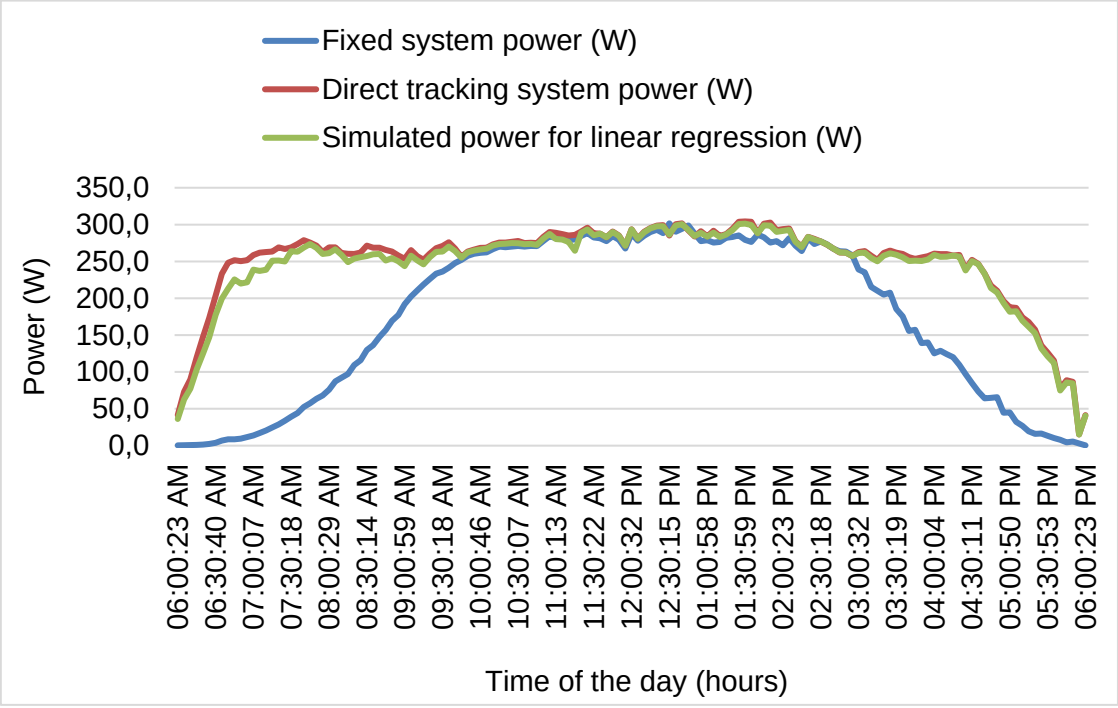

Figure 4.10. The sunny day graph for fixed system power, direct-tracking system power and simulated power for linear regression.

4.4.3 Comparison of fuzzy logic and linear regression results

Figure 4.11 depicts the daily profile for the simulated power for fuzzy logic and simulated power for linear regression. The difference in simulated power between the fuzzy logic and linear regression was 2.44%. The total power for the day produced by the best performing algorithm (fuzzy logic) was 36370.4 W, while the least performing algorithm (linear regression) produced 35484.5 W. The fuzzy logic algorithm development involved an automatic adjustment (increases) of the lookout angle by 1.9° between 6:15 am and 9 am and by 3° between 9 am and 10 am (please refer to Annexure B and Figure 3.10). The adjustments were determined by the difference between four consecutive lookout angles at intervals of 15 minutes, then the difference was utilised to determine the hourly average change (increase). The adjustments result in more power harvesting for the fuzzy logic algorithm as compared to the linear regression algorithm, which was made to directly follow the lookout angles derived from the Keisan website (Annexure C).

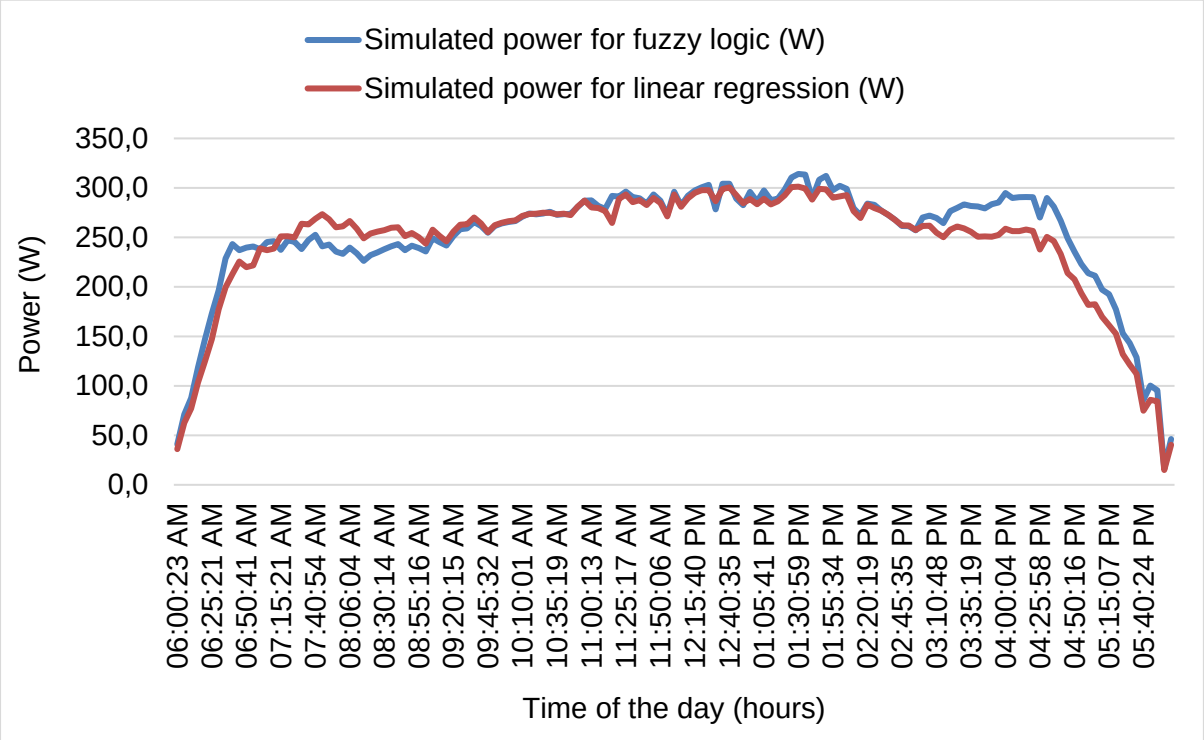

Figure 4.11. The sunny day simulated power graph (fuzzy logic and linear regression).

4.5 Conclusion

The calibration to validate the results of this research study was discussed in this chapter. The fixed-system results were also analysed. The empirical results of the direct-tracking system and simulated results for the fuzzy logic system were compared for a sunny clear day, single cloud and multiple clouds day. The direct-tracking system power and simulated power for

linear regression system were compared for a sunny clear day. It was discovered that the daily performance of the fixed system power (16° PV module) was better than the 26° and 36° fixed systems power by 3.49% and 10.69% respectively proving the study conducted by Chinnery and Heywood. The direct-tracking system power showed 32% improvement over the fixed system power (16°) due to the fact that it was always aligned to the movement of the sun. The daily simulated power for fuzzy logic was 5.31% better than the direct-tracking system power. The direct-tracking system power was better than the simulated power for linear regression by 2.24%. The simulated power result difference between fuzzy logic and linear regression was 2.44%, making fuzzy logic algorithm the better performer. The fuzzy logic algorithm performed better than the linear regression algorithm due to the fact that its development involved an average increase in the lookout angles for specific periods of a day that was based on four consecutive 15-minute changes. The adjustments result in more power harvesting for the fuzzy logic algorithm as compared to the linear regression algorithm, which was made to directly follow the lookout angles derived from the Keisan website (Annexure C).

Chapter 5 – The conclusion

5.1 Introduction

The previous chapter (Chapter 4) detailed the importance of calibration of the systems in order to validate the results of this study. The results obtained for a period of six months for the three fixed photovoltaic (PV) modules set at the same orientation angle of 0°, but at different tilt angles of 16°, 26° and 36° true North (N), were discussed and analysed. The empirical results of the direct-tracking system and simulated results for the fuzzy logic system were compared for a sunny clear day, single cloud and multiple clouds day. Furthermore, the empirical results of the direct-tracking system and simulated results of the linear regression system were compared for a sunny clear day. The simulated results for the fuzzy logic system and linear regression system were also compared and analysed. The aim of this chapter is to provide the conclusion and recommendations on the systems that yielded the maximum output power. The conclusion and recommendations will be made on both the fixed- and dual-axis solar tracking systems.

5.2 Overview of the thesis

The background to this study was detailed in Chapter 1, which stated that South Africa is not immune to energy shortages; predictions are that these energy shortages will increase, thereby necessitating the implementation of alternative energy sources, such as PV energy systems (Hertzog and Swart, 2015). The problem with PV modules is that they may be either fixed in position to a roof or mounted directly onto a frame, resulting in a stationary fixed-type system. The sun, however, is not a stationery object, resulting in the conversion efficiency between solar energy and electrical energy not always being at an optimum level. One way to increase the conversion efficiency is to vary the tilt and orientation angle of an adjustable PV module automatically, constantly aligning it to the direct beam radiation of the sun. Making an informed decision between various control techniques such as direct solar tracking system is required. The purpose of this study was to simulate two different algorithms (fuzzy logic and linear regression) in order to compare the empirical results of the direct-tracking system (using the Boolean algorithm) with the simulated results. Another aim of the study was to substantiate which tilt angle enables the highest energy yield from a PV module located on the Highveld of South Africa.

It was also emphasised in Chapter 1 that tracking the sun for the maximum power point (MPP) of a PV module varies in complexity. However, it is essential to continuously deliver the highest possible power to the load when variations in the insolation and temperature occur, to maintain

a high overall system efficiency. It therefore becomes necessary to use an algorithm (fuzzy logic or linear regression) in order to ensure the efficient operation of the solar collectors. A PV module's performance depends, to a large degree, on the location and position of the module, with solar energy conversion receiving more attention than before. Optimising the position of the module with relation to the sun can enable more clean energy to be harvested from this technology. The chapter outlined some delimitations that relate to the practical setup that was installed by a private service provider. The effects of relative humidity and temperature on the PV module's performance were also to be ignored, as all the PV modules were exposed to the same environmental conditions. The design and construction of the data acquisition system also did not form part of this research. Four objectives were listed and they are answered in the following sections of this chapter.

Chapter 2 outlined a contextual overview of the two algorithms (linear regression and fuzzy logic) that were previously applied in simulation of the output power of PV module tracking systems. Linear regression analysis is defined as a statistical technique for investigating and modelling the relationship between variables (Jiang, 2008). Regression analysis is modelling the relationship between a scalar variable Y and one or more variables denoted as X. The polynomial regression is a form of linear regression in which the relationship between an independent variable X and a dependent variable Y is modelled (Ibrahim *et al.*, 2012). In this present study, two variables, voltage (Y-axis) and time (X-axis), were used to control the movement of the PV module in relation to the position of the sun. Fuzzy logic is described as a form of many-value logic that deals with reasoning that is approximate, rather than fixed and exact (Robert *et al.*, 2014). It also incorporates a simple, rule-based approach, "if x and y then z", to solve a control problem rather than attempting to model a system mathematically. A direct-tracking system was also discussed, which features a Boolean algorithm that is similar to the hill and climb algorithm.

The control software and hardware that were used for data acquisition were also explained. National Instruments LabVIEW is described as a graphical programming language that has its roots in automation control and data acquisition (Hertzog, 2015). LabVIEW software is easier to interface with real-world signals, enabling the analysis of data for meaningful information and sharing (Stamatescu *et al.*, 2014). Linear actuators are explained as devices that may be used to direct PV modules in a desired direction. The linear actuator consists of a built-in direct current (dc) motor with a DC worm gear that allows a smooth and precise extension of the arm (Chai *et al.*, 2011). Their application to solar tracking was presented. It was stated that the direct beam radiation from the sun is extremely important for concentrated PV systems and has a direct bearing on the tilt and orientation angle of PV modules. Previous research

using the two algorithms and the control software were also discussed in Chapter 2 with their associated results. Advantages and disadvantages of the two algorithms and the control software were also highlighted.

Chapter 3 provided an overview of the tracking system as a whole by depicting, listing and explaining all the components that were used in the practical setup. Six 310 W YL310P-35b polycrystalline PV modules were used in this study with the National Instrument (NI) data acquisition (DAQ) hardware installed inside the control boxes. The PV modules are rated at 36.3 V (voltage at maximum power), 45.6 V (open circuit voltage), 8.53 A (current at maximum power) and 8.99 A (short circuit current). The key parameters of the PM modules were also listed. The basic operating principle of the system was to measure the output voltage of the modules and use the measurements to command the controlling devices to align the PV modules perpendicular to the sun. The data logging interface circuit, using a voltage divider that was also used as the system load, was outlined. The voltage divider circuit provides signal conditioning, as the output voltage of the PV module (open circuit voltage = 45.6 V) is much higher than the allowed input voltage to the DAQ unit (limited to 10 V). Using a voltage divider circuit in the data logging interface circuit enabled the input voltage to the NI DAQ to be less than 10 V. This DAQ was connected directly to a personal computer running the LABVIEW software, where measurements were recorded and the control algorithms were implemented.

Different software that can be used for solar tracking systems were also discussed. It was stated in Chapter 3 that it is easier to interface LabVIEW with real-world signals, where one can analyse data for meaningful information and share results. Data can be measured and displayed simultaneously using the LabVIEW visual programming software. All values stored in a matrix can eventually be written to a text file for further analysis in MS Excel (Hertzog and Swart, 2018). The program that was used to execute the direct-tracking system was written and presented in Chapter 3, using the LabVIEW user interface software. The fuzzy logic rules were developed in this chapter as was the linear regression algorithm.

It was stated that the linear actuator was preferred over the stepper motor because it can provide better efficiency, better dynamic performance and smoother operation (Birbilen and Lazoglu, 2018). Various loads that can be used in PV modules were also discussed. However, it was stated that using a fixed load resistance was discovered to be an effective and easy method to start loading PV modules located outdoors for measurement purposes (Hertzog and Swart, 2016). The system load featured five fixed high-power (100 W, 0.82 Ω, 1 Ω) resistors connected in series across a source voltage. The 1 Ω resistor was used because measuring the voltage drop across it allowed easy computation of circuit current (V = IR) using Ohms Law.

Chapter 4 discussed and analysed the empirical results of the direct-tracking system, the simulation results of the two algorithms and the fixed PV modules. The three fixed-system PV modules' instantaneous power readings for each time slot were measured. The instantaneous power readings were used to calculate the subsequent power over a period of time (Wh).

The total Wh percentage difference produced for the six-month period between the 16° and 26° fixed-type system was 3.48%, between the 16° and 36° fixed-type system was 10.69%, while between the 26° and 36° fixed-type system it was 6.97%. Similarly, the 16° (Latitude minus 10°) fixed-type system was established to be the best performer followed by the 26° fixed-type system and the 36° fixed-type system. Results suggest that a PV module installed at a tilt angle of latitude minus 10º produces more output power than those installed at other tilt angles in semi-arid regions of South Africa for the months of November through January (Hertzog and Swart, 2015). The highest yield of output power from a PV module was also found at latitude minus 10° for another study conducted during the summer season of South Africa (Hertzog and Swart, 2018).

The sunny day (cloudless day) daily power profile of the fixed system (16°), the empirical results of the direct-tracking system and the simulated fuzzy logic system were analysed in Chapter 4. The simulated fuzzy logic system marginally outperformed the empirical results of the direct-tracking system by 5.31%. The empirical direct-tracking results illustrated 32% improvement over the fixed system results. The sunny day results with a single cloud daily power profile of the fixed system (16°), the empirical results of the direct-tracking system and the simulated fuzzy logic system were also analysed. The simulated fuzzy logic system marginally outperformed the empirical results of the direct-tracking system by 3.7%. The empirical tracking results demonstrated 31% improvement over the fixed system results.

The sunny day with multiple clouds (in the afternoon) daily power profile of the fixed system (16°), the empirical results of the direct-tracking system and the simulated fuzzy logic system were also examined. It was discovered that the simulated fuzzy logic system marginally outperformed the empirical results of the direct-tracking system by 2%. The empirical tracking results showed 21.76% improvement over the fixed system results.

Analysis of the the sunny day daily power profile of the fixed system (16°), the empirical results of the direct-tracking system and the simulated linear regression algorithm was made. It was discovered that the direct-tracking system marginally outperformed the simulated linear regression algorithm by 2.24%. This was due to the fact that the direct-tracking system had the advantage of moving forward and backwards, while the linear regression algorithm only

moved forward. The simulated linear regression results showed 30.97% improvement over the fixed system results.

It was also emphasised in Chapter 4 that enabling reliability of data requires that any system be calibrated. The intention of calibrating the system was to eliminate any bias between the systems. This was done by physically measuring the output voltage across the load resistors and the current flowing through the 1 Ω resistor. The physically measured voltage and current were compared with the readings on the LabVIEW user interface. The results correlated well with a minor error percentage (0.24% for currents and the highest being 0.58% for voltage).

Chapter 5 provides the overview of the research holistically, discussing what all the chapters entail. It also provides the conclusion and recommendations on the systems (both fixed-type system and tracking-type systems) that yielded the maximum output power.

5.3 Conclusion on the system calibration

Chapter 1 listed one objective on calibration of the system as follows:

- **Clarify a simple calibration method for the systems to ensure data validity.**

Three PV modules (one fixed-type system and the two tracking-type systems, using linear regression and fuzzy logic) were set at a fixed tilt angle of 26° and orientation angle of 0° N for calibration purposes. This was only done for one day during the summer season to determine the validity between the three systems. The Rish Multi 16S True RMS multimeter was used to physically measure the systems' voltage and current on 09 February 2019. The physically measured results were compared with the readings on the LabVIEW user interface software. The readings (currents and voltages) that were measured physically and displayed by the LabVIEW interface were obtained within a 30 minutes period. A current of 8,29 A from the PV module was measured (physically) while the LabVIEW interface displayed 8,27 A. The highest error percentage for voltage occurred for the linear regression system (being 0.58%). The systems' measurements were taken on the 09 February 2019 between 12:30 noon and 1 pm when the sun was perpendicular to all the PV modules. Results indicate that the three identical PV systems produced very similar results. Systems with a variability of less than 1% are considered to be reliable with their data being considered valid (Swart and Hertzog, 2019). A consistent error percentage (0.24%) between the multimeter and LabVIEW user interface was established for the current values. The results indicated that there was no need for adjustment to the system, as all the factors were less than 1%.

5.4 Conclusion on the fixed-type systems

Chapter 1 listed one objective on the fixed-type system as follows:

- **Substantiate which tilt angle enables the highest energy yield from a fixed-type system where a singular PV module is located on the Highveld of South Africa**

The fixed-type systems consisted of three identical PV modules fixed at different tilt angles but at the same orientation angle. The optimum tilt angle for a 26° angle of latitude involves placing the PV module at an orientation angle of 0° and setting the angle of tilt to 16° , 26° or 36° , respectively. These angles are derived from the Heywood and Chinnery equations of latitude for calculating tilt angles of PV modules in South Africa. The fixed-type systems would also serve as a baseline for the tracking-type systems.

The recorded Wh for a six-month period was calculated to be 23858.22 Wh for the 16° fixed-type system, 23056.02 Wh for the 26° fixed-type system and 21554,31 Wh for the 36° fixed-type system. It is evident that 16° fixed-type system yielded more output power, followed by the 26° fixed-type system, while the 36° fixed-type system was the lowest performer for the summer months in South Africa.

5.5 Conclusion on the direct-tracking and simulated systems

Chapter 1 listed two objectives on the tracking-type systems as follows:

- **Implement a direct-tracking system where a basic Boolean algorithm is used to obtain empirical results; and**
- **Determine which algorithm (fuzzy logic or linear regression) will enable the highest output power from a proposed PV module using simulation.**

The fuzzy logic and linear regression were applied to simulate the output power of the PV module tracking systems. The direct-tracking system made use of the basic Boolean algorithm to track the movement of the sun across the sky from sunrise to sunset.

It took 41 functional blocks and four comparison calculations to execute the direct-tracking algorithm (in LabVIEW). Two comparison calculations per axis, of previous and current voltage readings, were done to detect if the PV module should move forward or backwards. The direct- tracking algorithm could move the PV module either forward or backward on both axes (X and Y axis). The sunny day daily simulated power percentage difference for both fuzzy logic and linear regression algorithms discovered that the fuzzy logic algorithm performed better than the linear regression algorithm with a percentage difference of 2.44%. Unlike the

linear regression algorithm, the fuzzy logic algorithm development involved an automatic adjustment (increases) of the lookout angle by 1.9° between 6:15 am and 9 am and by 3° between 9 am and 10 am (please refer to Annexure E and Figure 3.10). The adjustments were determined by the difference between four consecutive lookout angles at intervals of 15 minutes, then the difference was utilised to determine the hourly average change (increase). These average based adjustments result in more power harvesting for the fuzzy logic algorithm as compared to the linear regression algorithm, where the lookout angle changes were directly based on the lookout angles derived from the Keisan.com website (Annexure F).

It must be noted that the value (2.44%) might change if the linear regression values for other seasons (autumn, winter and spring) are obtained. However, the fuzzy logic algorithm would be closer because it was designed for different weather conditions, whereas the linear regression algorithms were designed to operate under all weather conditions, but using the sunny day approach.

5.6 Recommendations

The three fixed-type systems were set at 0° orientation angle and at different tilt angles of 16°, 26° and 36° respectively. The results obtained for a period of six months show the 16° fixed-type system yielding more output power as compared to the 26° and 36° fixed-typed systems. It is recommended that between November and April, for a fixed-type system, PV modules should be installed at a tilt angle of latitude minus 10° (16°) on the Highveld of South Africa. However, possible limitations of this research study include the fact that data were only collected from the Highveld region of South Africa. It is essential to obtain data for the same period from the coastal regions of South Africa.

The fuzzy logic and linear regression algorithms were applied to simulate which algorithm yielded the maximum output power for a dual-axis PV tracking-type system. It was discovered that the fuzzy logic outperformed the linear regression by producing more output power (2.44%) during a sunny day. The recommendation is to apply the fuzzy logic algorithm for a dual-axis solar tracking system on the Highveld of South Africa in the summer season. Similarly, it is also essential to obtain data for the same period from the coastal regions of South Africa.

The fuzzy logic rules for the other seasons should also be determined and then be validated using an experimental setup. The linear regression algorithm should also be applied to an experimental setup in order to determine its validity.

References

Adarsh S., Anand, A. and Singla, J. 2015. Increasing the Efficiency of a PV System Using Dual Axis Solar Tracking. 11th IRF International Conference, Bengaluru, India, February 15.

Aksoy C. and Yavuz, C. 2015. Comparison of Solar Trackers and Application of a Sensor Less Dual Axis Solar Tracker. *Journal of Energy and Power Engineering*, 9(6): pp. 556–561.

Algarín, C.R., Castro, A.O. and Naranjo, J.C. 2017. Dual-Axis Solar Tracker for Using in Photovoltaic Systems. *International Journal of Renewable Research*, 7(1): pp. 1925–1933.

Allamehzadeh, H. 2016. Solar Energy Overview and Maximizing Power Output of a Solar Array Using Sun Trackers. 4th Annual IEEE Conference on Technologies for Sustainability, Phoenix, Arizona, October 9-11.

Almorox, J. and Hontoria, C. 2004. Global Solar Radiation Estimation Using Sunshine Duration in Spain. *Energy Conversion and Management*, 45(9-10): pp. 1529–1535.

Al-najjar, H.M.T. 2013. Experimental Evaluation of the Performance of One-Axis Daily Tracking and Fixed PV Module in Baghdad, Iraq. *Journal of Engineering*, 19(9): pp. 1145–1157.

Anuraj, A. and Gandhi, R. 2014. Summary for Policymakers. *International Journal of Electronic and Electrical Engineering*, 7(6): pp. 1–30.

Asowata, O., Swart, J. and Pienaar, C. 2012. Optimum Tilt and Orientation Angles for Photovoltaic Panels in the Vaal Triangle. Asia-Pacific Power and Energy Engineering Conference, Shanghai, China, March 27-29.

Ayansola, O. D. and Yinusa, A. A. 2012. Mathematical Model of Antenna Look Angle of Geostationary Communications Satellite Using Two Models of Control Stations, *International Journal of Advanced Computer Science*, 2(9), pp: 348–351.

Bagher, A.S., Vahid, M.M.A. and Mohsen, M. 2016. Types of Solar Cells and Application. *American Journal of Optics and Photonics*, 3(5): pp. 94–113.

Bauer, P. and Lonel, R. 2013. LabVIEW Remote Panels and Web Services in Solar Energy Experiment - A comparative Evaluation. 8th IEEE International Symposium on Applied Computational Intelligence and Informatics, Timisoara, Romania, May 23–25.

Belay, Y., Amente, G. and Goro, G. 2015. Estimation of Solar Panel Orientation with Different Tilt Angles at Haramaya University. *International Journal of Sustainable Energy and Environment*, 3(2): pp. 1–23.

Birbilen, U. and Lazoglu, I. 2018. Design and Analysis of a Novel Miniature Tubular Linear Actuator. *IEEE Transection on Magnetics*, 54(4): pp. 1–6.

Bounechba, H., Bouzid, A., Nabti, K. and Benallab, H. 2014. Comparison of Perturb & Observe and Fuzzy Logic in Maximum Power Point Tracker for PV Systems. *Energy Procedia*, 50: pp. 677–684.

Campbell, D. and Campbell, S. 2008. Introduction to Regression and Data Analysis with. StatLab Workshop Series, [Online]. [Available from]: <http://statlab.stat.yale.edu/workshops/IntroRegression/StatLab-IntroRegressionFa08.pdf> [Accessed 08/02/2017].

Chai, K.K., Tay, K.M. and Abdullah, M.O. 2011. Development of a Photovoltaic System Equipped with a Sun Tracker System. *International Journal of Research and Reviews in Applied Sciences*, 7: pp. 373–379.

Chang, T. P. 2009. The Sun's Apparent Position and The Optimal Tilt Angle of a Solar Collector in the Northern Hemisphere. *Solar Energy,* 83(8): pp. 1274–1284.

Chin, C. S., Babu, A. and McBride, W. 2011. Design, Modelling and Testing of a Standalone Single Axis Active Solar Tracker Using MATLAB/Simulink. *Renewable Energy*, 36(11): pp. 1–19.

Chong, K.K., Wong, C.W., Siaw, F.L., Yew, T.K., Ng, S.S., Liang, M.S., Lim, Y.S. and Lau, S.L. 2009. Integration of an On-Axis General Sun-Tracking Formula in the Algorithm of an Open-Loop Sun-Tracking System. *Sensors*, 9(10): pp. 7849–7865.

Chow, L.S. and Abiera, M. 2013. Optimization of Solar Panel with Solar Tracking and Data Logging. IEEE Student Conference on Research and Development, Putrajaya, Malaysia, December 16-17.

Christian, D.P., Rafael, C.L., Rafael, G.G. and Ricardo, R.C. 2015. Design of a Linear Actuator Driven Solar Tracker for High Concentration Photovoltaics Technologies. *Journal of Clean Energy Technologies*, 4(3): pp. 197–201.

Clack, C.T.M. 2017. Modeling Solar Irradiance and Solar PV Power Output to Create a Resource Assessment Using Linear Multiple Multivariate Regression. *Journal of Applied*

Meteorology and Climatology, 56: pp. 109–125.

Dante, J.H., Melanie, L.S.H., Dante, R. and Myo, T. 2013. Dual-Axis Solar Tracker: Functional Model Realization and Full-Scale Simulations. A Major Qualifying Project Report Submitted to the Faculty of Worcester Polytechnic Institute in Partial Fulfilment of the Requirements for the Degree of Bachelor of Science, United States of America.

Doyle, A.C. 2009. Understanding Basic Statistics. Fifth Edition, Brooks/Cole Cengage Learning: Belmont.

Edwards, C. R. 1971. The logic of Boolean matrices. *School of Electrical Engineering, University of Bath, Claverton Down, Bath BA2 7AY*, 15(3), pp: 247–253.

Fathabadi, H. 2016. Comparative Study Between Two Novel Sensorless and Sensor Based Dual-Axis Solar Trackers. *Solar Energy*. 138: pp. 67–76.

Ferdaus, R.A., Mohammed, M.A., Rahman, S., Salehin, S. and Mannan, M.A. 2015. Energy Efficient Hybrid Dual Axis Solar Tracking System. J*ournal of Renewable Energy*, 2014: pp. 1–12.

Gabler, R., Petersen, J., Trapasso, L. and Sack, D. 2008. Earth-Sun Relationships and Solar Energy. Physical Geography. Ninth Edition. Brooks/Cole Cengage Learning: Belmont.

Garg, A., Nayak, R. and Gupta, S. 2015. Comparison of P & O and Fuzzy Logic Controller in MPPT for Photovoltaic (PV) Applications by Using MATLAB / Simulink. *IOSR Journal of Electrical and Electronics Engineering*, 10(4): pp. 53‑62.

Gogtay, N.J. and Thatte, U.M. 2017. Principles of Correlation Analysis. *Journal of Association of Physicians of India*, 65: pp. 78–81.

Gordo, E., Khalaf, N., Strangeowl, T., Dolino, R. and Bennett, N. 2015. Factors Affecting Solar Power Production Efficiency. Final Report on New Mexico Supercomputing Challenge, Miyamura High School United States.

Guo, M., Zang, H., Gao, S., Chen, T., Xiao, J. and Cheng, L. 2017. Applied Sciences Optimal Tilt Angle and Orientation of Photovoltaic Modules Using HS Algorithm in Different Climates of China. *Applied Science*, 7(1028): pp. 1−12.

Hamed, B.M. and El-Moghany, M.S. 2012. Fuzzy Controller Design Using FPGA for Sun Tracking in Solar Array System. *International Journal of Intelligent Systems and Applications*,

4(1): pp. 46–52.

Hehner, E.C.R. 2012. From Boolean Algebra. *The Mathematical Intelligencer*, 26(2): pp. 1-9.

Hertzog, P. and Swart, A. 2015. The Use of an Innovative Jig to Stimulate Awareness of Sustainable Technologies among Freshman Engineering Students. *Sustainability*, 7(7): pp. 9100–9117.

Hertzog, P.E. 2015. Validating the Optimum Tilt Angle for PV Modules in the Central Region of South Africa for the Winter Season. *Sabinet African Journal*, 4(2): pp. 207–220.

Hertzog, P.E. and Swart, A.J. 2016. The Impact of Atmospheric Conditions on the Sustainability of a PV System in a Semi-Arid Region: A Case Study from South Africa. 13th International Conference on Electrical Engineering/Electronics, Computer, Telecommunications and Information Technology, Chiang Mai, Thailand, June 28 – July 1.

Hertzog, P.E. and Swart, A.J. 2016. Validating the Optimum Tilt Angle for PV Modules in a Semi-Arid Region of South Africa for the Winter Season. *Science Publishing Corporation*, 7(4.15): pp. 1–6.

Hertzog, P.E. and Swart, A.J. 2018. Optimum Tilt Angles for PV Modules in a Semi-Arid Region of the Southern Hemisphere. *International Journal of Engineering & Technology*, 7(4.15): pp. 290–297.

Hertzog, P.E. and Swart, A.J. 2018. Validating Three Different Tilt Angles for PV Modules in a Semi-Arid Region. IEEE International Conference on Innovative Research and Development, Bangkok, Thailand, May 11-12.

Hertzog, P.E. and Swart, J. 2015. Determining the Optimum Tilt angles for PV Modules in a Semi-Arid Region of South Africa for the Summer Season. Southern Africa Telecommunication Networks and Applications Conference, Hermanus, South Africa, September 6-9.

Hichamia, N.E., Abboub, A., Rhailic, S.E. and Marhraoui, S. 2021. Maximum Power Point Tracker Method for Grid Connected Photovoltaic System Based on Hill Climbing Technique, *Turkish Journal of Computer and Mathematics Education*, 12(11): pp. 5559–5568.

Huang, C.H., Pan, H.Y. and Lin, K.C. 2016. Development of Intelligent Fuzzy Controller for a Two-Axis Solar Tracking System. *Applied Sciences*, 6(5): p. 130.

Hussein, Q. M. 2020. Principle of Logic Design. [Available from]: <https://www.researchgate.net/publication/343361413>. [Accessed 23/10/2021].

Ibrahim, S., Daut, I., Irwan, Y.M. and Irwan, M. 2012. Linear Regression Model in Estimating Solar Radiation in Perlis. *Energy Procedia*, 18: pp. 1402–1412.

Jamal, A., Bivera, S.F., Nazreen, N., George, S. and Saraswathy, K. 2016. Automatic Solar Tracking and Monitoring System Using LabVIEW. *International Journal of Advanced Research in Electrical, Electronics and Instrumentation Engineering*, 5(4): pp. 2514–2518.

Jeon, J. 2015. The Strengths and Limitations of the Statistical Modeling of Complex Social Phenomenon: Focusing on SEM, Path Analysis, or Multiple Regression Models. *International Journal of Social, Behavioral , Economic, Business and Industrial Engineering*, 9(5): pp. 1634–1642.

Jiang, Y. 2008. Prediction of Monthly Mean Daily Diffuse Solar Radiation Using Artificial Neural Networks and Comparison with Other Empirical Models. *Energy Policy*, 36(10): pp. 3833–3837.

Jovanovic, V.M., Seek, M., Ayala, O. and Marsillac, S. 2016. Single Axis Solar Tracker Actuator Location Analysis. IEEE Southeastcon, Norfolk, United States of America, March 30 - April 3.

Juang, J.N. and Radharamanan, R. 2014. Design of a Solar Tracking System for Renewable Energy. Zone 1 Conference of the American Society for Engineering Education, Bridgeport, United States of America, April 3-5.

Kacira, M., Simsek, M., Yunus Babur, Y. and Demirkol, S. 2004. Determining Optimum Tilt Angles and Orientations of Photovoltaic Panels in Sanliurfa, Turkey. *Renewable Energy*, 29(8): pp. 1265–1275.

Kaehler, S. D. 2013. Fuzzy Logic: An Introduction. [Online]. [Available from]: <http://www.123seminarsonly.com/Seminar-Reports/014/7270869-Fuzzy-Logic.pdf> [Accessed 21/04/2017].

Karafil, A., Ozbay, H., Kesler, M. and Parmaksiz, H. 2015. Calculation of Optimum Fixed Tilt Angle of PV Panels Depending on Solar Angles and Comparison of the Results with Experimental Study Conducted in Summer in Bilecik, Turkey. 9th International Conference on Electrical and Electronics Engineering, Bursa, Turkey, November 26-28.

Kaur, T., Mahajan, S., Verma, S., Priyanka, and Gambhir, J. 2016. Arduino Based Low Cost Active Dual Axis Solar Tracker. 1st IEEE International Conference on Power Electronics, Intelligent Control and Energy Systems, Delhi, India, July 4-6.

Keisan. 2019. Solar elevation angle (for a day) Calculator - High accuracy calculation. [Available from]: <https://keisan.casio.com/exec/system/1224682277>. [Accessed 20/09/2021].

Khan, A.H., Islam, M., Islam, A. and Rahman, M.S. 2015. A Systematic Approach to Find the Optimum Tilt Angle for Meeting the Maximum Energy Demand of an Isolated Area. 2nd International Conference on Electrical Engineering and Information and Communication Technology, Dhaka, Bangladesh, May 21-23.

Khatib, T., Mohamed, A. and Sopian, K. 2012. On the Monthly Optimum Tilt Angle of Solar Panel for Five Sites in Malaysia. IEEE International Power Engineering and Optimization Conference, Melaka, Malaysia, June 6-7.

Kiyak, E. and Gol, G. 2016. A Comparison of Fuzzy Logic and PID Controller for a Single-Axis Solar Tracking System. *Renewables: Wind, Water, and Solar*, 3(7): pp. 1–14.

Kumari, A. 2013. Fuzzy Logic Based Solar Tracking System by Estimation of Solar Radiation. *International Journal of Engineering Research & Technology*, 2(8): pp. 906–911.

Kuphaldt, T. 2014. 7 Voltage and Current Dividers. Air Washington Electronics – Direct Current. [Online]. [Available from]: <https://www.skillscommons.org/bitstream/ handle/taaccct/3468/DC_05_Parallel_Cks_rev02.pdf?sequence=1&isAllowed=y> [Accessed 18/02/2019].

Labview. 2012. Advantages of Using LabVIEW in Academic Research. [Online]. [Available from]: <ftp://ftp.ni.com/pub/newsimages/2009/LabVIEW2009OnlinePressKit/FeaturesOverviews/AdvantagesofNILabVIEWinAcademicResearch.pdf> [Accessed 12/03/2017].

Lai, A.C., Chong, K.K., Lim, B.H., Ho, M.C.,Yap, S.H., Heng, C.K., Lee, J.V. and King, Y.J. 2014. A Generic Sun-Tracking Algorithm for On-Axis Solar Collector in Mobile Platforms. National Physics Conference, Kuala Lumpur, Malaysia, Novemebr 18-19.

Lashkari, A. H., Mahdavi, F. and Ghomi, V. 2009. A Boolean Model in Information Retrieval for Search Engines. International Conference on Information Management and Engineering, Xian, China December 26-27

Lawless, C. and Kärrfelt, E. 2018. Sun Following Solar Panel Using Light Sensors to Implement. Bachelor's Thesis in Mechatronics, Kungliga Tekniska Högskolan, Institute of Technology, School of Industrial Engineering and Management, Stockholm, Sweden.

Le Roux, W.G. 2016. Optimum Tilt and Azimuth Angles for Fixed Solar Collectors in South Africa Using Measured Data German Society for International Cooperation. *Renewable Energy*, 96: pp. 603–612.

Lee, C.Y., Chou, P.C., Chiang, C.M. and Lin, C.F. 2009. Sun Tracking Systems. *Sensors*, 9(5): pp. 3875–3890.

Liao, H.H. 2013. Two-Axle Solar Tracking System and Device for Solar Panel. *Journal of Chemical Information and Modeling*, 53(9): pp. 1689–1699.

Linares, A., Fernández, J., Friend, M., Llarena, E., Montes, C., Moncho, G., Losada, N., González, O., Molina, D., Pio, A. and Cendagorta, M. 2012. Voltage Dips : Verification, Validation and Certification Procedure for PV Installations. 27th European Photovoltaic Solar Energy Conference and Exhibition, Frankfurt, Germany, September 24.

Liu, Y., Gong, M., Liang, L., Liu, Q. and Gao, Y. 2018. Research and Design of Low-Power Grid-Connected PV Power Generation System Based on Automatic Solar Tracking. *Systems Science and Control Engineering*, 6(3): pp. 278–288.

Mackin, B. S. 1998. A Test Engineer's Evaluation of Graphical Programming. Endgate Corporation: Sunnyvale.

Mambo, J. and Faccer, K. 2017. South Africa Risk and Vulnerability Atlas. Second Edition. Understanding the Socilal & Enviornmental Implication on Global Challenges. [Online]. [Available from]: <https://www.csir.co.za/sites/default/files/Documents/CSIR Global Change eBOOK.pdf> [Accessed 23/01/2018].

Martins, I., Esteves, J., Marques, G.D. and da Silva, P.F. 2006. Permanent-Magnets Linear Actuators Applicability in Automobile Active Suspensions. *IEEE Transactions on Vehicular Technology*, 55(1): pp. 86–94.

Millan, W., Clark, A. and Dawson, E. 2014. Boolean Function Design using Hill Climbing Methods, *Lecture Notes in Computer Science*, pp. 2–12.

Montgomery, D.C., Peck, E.A. and Vining, G.G. 1981. Introduction to Linear Regression Analysis. John Wiley & Sons, Inc., New Jersey, United States of America.

Na, W., Chen, P. and Kim, J. 2017. An Improvement of a Fuzzy Logic-Controlled Maximum Power Point Tracking Algorithm for Photovoltaic Applications, *Applied Sciences*, *7*(4): pp. 2–17.

National Instruments. 2012. National Instruments Embedded Systems Solutions. NIWeek Worldwide Graphic System Design Conference, Austin, United States of America, August 6-9.

National Instruments. 2013. Benefits of Programming Graphically in NI LabVIEW. [Online]. [Available from]: <http://www.ni.com/white-paper/14556/en/> [Accessed 09/07/2018].

National Instruments. 2015. Getting Started with LabWindows/CVI. [Online]. [Available from]: <http://www.ni.com/pdf/manuals/373552k.pdf> [Accessed 20/04/2017].

Neville, R.C. 1977. Solar Energy Collector Orientation and Tracking Mode. *Solar Energy*, 20(1): pp. 7–11.

Osterwald, C.R., Adelstein, J., del Cueto, J.A., Sekulic, W., Trudell, D., McNutt, P., Hansen, R., Rummel, S., Anderberg, A. and Moriarty, T. 2006. Resistive Loading of Photovoltaic Modules and Arrays for Long-Term ExposureTesting. *Wiley InterScience*, 14(6): pp. 567–575.

Ouali, M. and Salah, C.B. 2011. Comparison of fuzzy Logic and Neural Network in Maximum Power Point Tracker for PV Systems. *Electric Power Systems Research*, 81[1]: pp. 43–50.

Ozemoya, A., Swart, J. and Pienaar, C. 2012. Controlling the Ambient Temperature of a PV Panel to Maintain High Conversion Efficiency. Southern Africa Telecommunication Networks and Applications Conference, George, Western Cape, South Africa, September 2-5.

Pecen, R., Zora, A. and Salim, M.D. 2004. A LabView Based Instrumentation System for a Wind-Solar Hybrid Power Station a LabView Based Instrumentation System for a Wind-Solar Hybrid Power Station. *Journal of Industrial Technology*, 20(3): pp. 1–8.

Prabhakar, M., Singh, U. and Amit, K. 2019. Descriptive Statistics and Normality Tests for Statistical Data. *Annals of Cardiac Anaesthesia*, 22(1): pp. 67–72.

Pradeep, K.P.J., Reddy, K.S. P., Mouli, C.C. and Raju, K.N. 2014. Development of Dual-Axis Solar Tracking using Arduino with LabVIEW. *International Journal of Engineering Trends and Technology*, 17[7]: pp. 321-324.

Prinsloo, G. 2015. Solar Tracking - Hardware Sun Tracking Systems and Digital Sun Position Hardware Solar Tracker Controllers. First Edition, SolarBooks: Stellenbosch.

Ranabhat, K., Patrikeev, L., Revina, A.A., Andrianov, K., Lapshinsky, V. and Sofronova, E. 2016. An Introduction to Solar Cell Technology. *Journal of Applied Engineering Science*, 14(4): pp. 481–491.

Reus, N.D. 1994. Benefits and Drawbacks of Using Fuzzy Logic, Especially in Fire Control Systems. The Netherlands Organization Defence Research, pp. 2-–38.

Ristevski, B. 2013. A survey of models for inference of gene regulatory networks. *Nonlinear Analysis: Modelling and Control*, 18(4): pp. 444–465.

Robert, J., Rosario, B. and Dadios, E. 2014). Development of a Fuzzy Logic- Based PV Solar Tracking System Simulated Using QT Fuzzy Engine. 7th IEEE International Conference Humanoid, Nanotechnology, Information Technology Communication and Control, Environment and Management, Philippines,12-16 November 2014.

Rohan, A., Rabah, M., Asghar, F., Talha, M. and Kim, S.H. 2019. Advanced Drone Battery Charging System. Journal of Electrical Engineering & Technology. 14: pp. 1395–1405.

Ross, T.J. 2010. Properties of Membership Functions. Third Edition, John Wiley & Sons:Inc.: New Jersey.

Saberi, A., Lin, Z. and Teel, A.R. 1996. Control of Linear Systems with Saturating Actuators. *IEEE Transactions on Automatic Control*, 41(3): pp. 368–378.

Salas, V., Olias, E., Barrado, A. and Lazaro, A. 2006. Review of the Maximum Power Point Tracking Algorithms for Stand-Alone Photovoltaic Systems. *Solar Energy Materials and Solar Cells*, 90(11): pp. 1555–1578.

Saravanan, S., Kannan, S., Nithya, R. and Thangaraj, C. 2014. Modelling and Prediction of India's Electricity Demand Using Fuzzy Logic. International Conference on Circuit, Power and Computing Technologies, Nagercoil, India, March 20-21.

Scholtz, L., Muluadzi, K., Kritzinger, K., Mabaso, M. and Forder, S. 2017. Renewable Energy: Facts and Futures. The Energy Future We Want. *World Wildlife Fund South Africa*, 6: pp. 1–44.

Schrader, B.L. and Mex, C.N. 1958. Linear Actuator. Patented 2,860,266, November 11, 1958.

Seyed, A.M.M., Hizam, H. and Gomes, C. 2017. Estimation of Hourly, Daily and Monthly Global Solar Radiation on Inclined Surfaces: Models Re-Visited. *Energies*, 10(1): pp. 2–28.

Shariah, A. Al-Akhras, M.A. and Al-Omari, I. A. 2002. Optimizing the Tilt Angle of Solar Collectors. *Renewable Energy,* 26[4]: pp. 587–598.

Skeiker, K. 2009. Optimum Tilt Angle and Orientation for Solar Collectors in Syria. *Energy Conversion and Management*, 50(9): pp. 2439–2448.

Solargis, 2010. Download free solar resource maps . [Online]. [Available from]: <http://solargis.com/products/maps-and-gis-data/free/download/africa-and-middle-east>. [Accessed 26/02/2019].

Sotoodeh, K. 2019. Actuator Selection and Sizing for Valves. *SN Applied Sciences*, 1(1207): pp. 1–8.

Stamatescu, I., Făgărăşan, I., Stamatescu, G., Arghira, N. and Iliescu, S.S. 2014. Design and Implementation of a Solar-Tracking Algorithm. *Procedia Engineering*, 69: pp. 500–507.

Stamatescu, I., Făgărăşan, I., Stamatescu, G., Arghira, N. and Iliescu, S.S. 2014. Fuzzy Decision Support System for Solar Tracking Optimization. 12th International Conference on Development and Application Systems Suceava, Romania, May 15-17.

Sukarno, K., Hamid, A.S.A., Razali, H. and Dayou, J. 2017. Evaluation on Cooling Effect on Solar PV Power Output Using Laminar H_2O Surface Method. *International Journal of Renewable Energy Research*, 7(3): pp. 1213–1218.

Swart, A.J. and Hertzog, P.E. 2015. Validating the Acceptance Zone for PV Modules Using a Simplified Measuring Approach. 13th International Conference on Electrical Engineering/Electronics, Computer, Telecommunications and Information Technology, Chiang Mai, Thailand, June 28 - July 1.

Swart, A.J. and Hertzog, P.E. 2016. Verifying an Economic Viable Load for Experimental Purposes Relating to Small Scale PV Modules. Southern Africa Telecommunication Networks and Applications Conference, Fancourt, South Africa, September 4-7.

Swart, A.J. and Hertzog, P.E. 2019. Regularly Calibrating an Energy Monitoring System Ensures Accuracy. *WEENTECH Proceedings in Energy*, 5(1): pp. 37–45.

Ulbrich, H. 1994. Comparison of Different Actuator Concepts for Applications in Rotating

Machinery. *International Journal of Rotating Machinery*, 1(1): pp. 61–71.

United Nations. 2015. Sustainable Development Goals: Sustainable Development Knowledge Platform. [Available from]: <https://sustainabledevelopment.un.org/sdgs> [Accessed 19/10/2018].

Vermaak, H.J. 2014. Techno-Economic Analysis of Solar Tracking Systems in South Africa. *Energy Procedia*, 61: pp. 2435–2438.

Vijayalakshmi, K. 2016. Designing a Dual Axis Solar Tracking System for Maximum Power. *Journal of Electrical & Electronic Systems*, 5(3): pp. 1–3.

Vishal, A. 2018. Solar Panel Angle Considerations and Performance Implications. [Online]. [Available from]: <https://www.youtube.com/watch?v=0esRftZ3qdw> [Accessed 22/07/2019].

Wang, J. and Lu, C. 2013. Design and Implementation of a Sun Tracker with a Dual-Axis Single Motor for an Optical Sensor-Based Photovoltaic System. *Sensors*, 13(3): pp. 3157–3168.

Wang, Y. 2017. Mathematical model for solving the relationship of shadow length changing over time through solar elevation. *Advances in Engineering Research*. 118: pp. 226–229.

Wu J., Chan, C.K., Loh, J.W. and Choo, L.H. 2009. Solar Radiation Prediction Using Statistical Approaches. 7th International Conference on Information, Communications and Signal Processing, Macau, China, December 8-10.

Yao, Y., Hu, Y., Gao, S., Yang, G. and Du, J. 2014. A Multipurpose Dual-Axis Solar Tracker with Two Tracking Strategies. *Renewable Energy*, 72: pp. 88–98.

Zahoor, A. and Sharief, S. 2017. 2017. Design and Performance of Solar Tracking Photo-Voltaic System using Microcontroller. *International Journal of Advanced Research in Computer Science,* 8(4): pp. 49–55.

Zakariah, A., Jamian, J.J. and Yunus, M.A.M. 2015. Dual-axis Solar Tracking System Based on Fuzzy Logic Control and Light Dependent Resistors as Feedback Path Elements. IEEE Student Conference on Research and Development, Kuala Lumpur, Malaysia, December 13-14.

Zárate, L.E., Marques, E., Pereira, D., Paulo, J. and Silva, D. 2004. Neural Representation of a Solar Collector with Statistical Optimization of the Training Set. 17th International Conference

on Industrial and Engineering Applications of Artificial Intelligence and Expert Systems, Ottawa, Canada, May 17-20.

Zhang, Q. X., Yu, H. Y., Zhang, Q. Y., Zhang, Z. Y., Shao, C. H. and Yang, D. 2015. A solar automatic tracking system that generates power for lighting greenhouses. *Energies*, 8(7): pp.

Zohuri, B. 2017. What Is Boolean Logic and How It Works. [Online]. [Available from]: <https://link.springer.com/chapter/10.1007%2F978-3-319-53417-6_6> [Accessed 26/10/2021].

Zulfikri, A. and Ulinuha, A. 2020. Enhancement of solar photovoltaic using maximum power point tracking based on hill climbing optimization algorithm. *Journal of Physics: Conference Series*, 1517(2020): pp. 1-7.

21 December 2021

Time	Hourly Angle Difference (°)	Average M for Every 1	Average Movement Difference (≤ 0,4° Indicator)	Average Movement ≤ 0,4° Collapsed
06:15-07:00	6,1	1,5		1,9
07:00-08:00	7,5	1,9	0,3	
08:00-09:00	9,4	2,3	0,5	
09:00-10:00	12,0	3,0	0,7	3,0
10:00-11:00	15,0	3,8	0,8	3,8
11:00-12:00	17,5	4,4	0,6	4,4
12:00-13:00	17,7	4,4	0,5	4,4
13:00-14:00	15,7	3,9	0,8	3,9
14:00-15:00	12,6	3,1	0,7	3,1
15:00-16:00	9,9	2,5	0,5	2,5
16:00-17:00	7,8	1,9	0,4	1,8
17:00-18:00	6,4	1,6	1,6	

21 March 2021

Time	Hourly Angle Difference (°)	Average Movement (°) for Every 15minutes	Average Movement Difference (≤ 0,4° Indicator)	Average Movement ≤ 0,4° Collapsed
06:15-07:00	6,6	1,7		1,9
07:00-08:00	7,2	1,8	0,1	
08:00-09:00	8,8	2,2	0,4	
09:00-10:00	12,2	3,0	0,8	3,0
10:00-11:00	18,9	4,7	1,7	4,7
11:00-12:00	29,2	7,3	2,6	7,3
12:00-13:00	33,0	8,3	2,2	8,3
13:00-14:00	24,1	6,0	2,2	6,0
14:00-15:00	15,2	3,8	1,2	3,8
15:00-16:00	10,3	2,6	0,6	2,6
16:00-17:00	7,9	2,0	0,3	1,8
17:00-18:00	6,9	1,7	1,7	

21 June 2021

Time	Hourly Angle Difference (°)	Average Movement (°) for Every 15minutes	Average Movement Difference (≤ 0,4° Indicator)	Average Movement ≤ 0,4° Collapsed
06:15-07:00	5,5	1,4		1,2
07:00-08:00	4,9	1,2	-0,1	
08:00-09:00	4,8	1,2	0,0	
09:00-10:00	5,2	1,3	0,1	
10:00-11:00	7,8	1,9	0,6	
11:00-12:00	43,5	10,9	8,9	10,9
12:00-13:00	119,8	29,9	27,3	29,9
13:00-14:00	10,6	2,6	1,2	2,6
14:00-15:00	5,7	1,4	0,2	1,3
15:00-16:00	4,8	1,2	0,0	
16:00-17:00	4,8	1,2	-0,1	
17:00-18:00	5,3	1,3	1,3	

23 September 2021

Time	Hourly Angle Difference (°)	Average Movement (°) for Every 15minutes	Average Movement Difference (≤ 0,4° Indicator)	Average Movement ≤ 0,4° Collapsed
06:15-07:00	6,8	1,7		2,0
07:00-08:00	7,5	1,9	0,2	
08:00-09:00	9,5	2,4	0,5	
09:00-10:00	13,5	3,4	1,0	3,4
10:00-11:00	21,2	5,3	1,9	5,3
11:00-12:00	31,2	7,8	2,5	7,8
12:00-13:00	31,4	7,8	2,5	7,8
13:00-14:00	21,5	5,4	2,0	5,4
14:00-15:00	13,6	3,4	1,0	3,4
15:00-16:00	9,5	2,4	0,5	2,4
16:00-17:00	7,6	1,9	0,2	1,8
17:00-18:00	6,7	1,7	1,7	

Annexure B

Fuzzy Logic Lookout Angles Development

Time	Angle of the sun (°) lookout angle			Fuzzy logic lookout angles (°)	
06:00:23 AM	110,7			110,0	
06:05:35 AM	111,4			110,0	
06:10:51 AM	111,3			110,0	
06:15:08 AM	112,1	1,4		111,9	1,9
06:20:06 AM	112,9			111,9	
06:25:21 AM	112,8			111,9	
06:30:40 AM	113,6	1,5		113,8	1,9
06:35:00 AM	114,4			113,8	
06:40:00 AM	114,3			113,8	
06:45:18 AM	115,2	1,6		115,7	1,9
06:50:41 AM	116,0			115,7	
06:55:05 AM	115,9			115,7	
07:00:07 AM	116,8	1,6		117,6	1,9
07:05:29 AM	117,7			117,6	
07:10:54 AM	117,6			117,6	
07:15:21 AM	118,5	1,7		119,5	1,9
07:20:25 AM	119,4			119,5	
07:25:50 AM	119,4			119,5	
07:30:18 AM	120,4	1,8		121,4	1,9
07:35:24 AM	121,3			121,4	
07:40:54 AM	121,2			121,4	
07:45:08 AM	122,3	1,9		123,3	1,9
07:50:47 AM	123,3			123,3	
07:55:19 AM	123,2			123,3	
08:00:29 AM	124,3	2,0		125,2	1,9
08:06:04 AM	125,3			125,2	
08:10:15 AM	125,3			125,2	
08:15:47 AM	126,4	2,1		127,1	1,9
08:20:23 AM	127,5			127,1	
08:25:36 AM	127,5			127,1	
08:30:14 AM	128,7	2,3		129,0	1,9
08:35:27 AM	129,9			129,0	
08:40:03 AM	129,8			129,0	
08:45:18 AM	131,1	2,4		130,9	1,9
08:50:00 AM	132,4			130,9	
08:55:16 AM	132,3			130,9	
09:00:59 AM	133,6	2,6	1,9	133,9	3,0
09:05:16 AM	135,0			133,9	

09:10:57 AM	134,9			133,9	
09:15:16 AM	136,4	2,7		136,9	3,0
09:20:15 AM	137,8			136,9	
09:25:46 AM	137,7			136,9	
09:30:18 AM	139,3	2,9		139,9	3,0
09:35:23 AM	140,8			139,9	
09:40:58 AM	140,7			139,9	
09:45:32 AM	142,4	3,1		142,9	3,0
09:50:06 AM	144,0			142,9	
09:55:11 AM	143,9			142,9	
10:00:46 AM	145,6	3,3	3,0	146,6	3,8
10:05:23 AM	147,4			146,6	
10:10:01 AM	147,3			146,6	
10:15:11 AM	149,1	3,5		150,4	3,8
10:20:50 AM	150,9			150,4	
10:25:28 AM	150,8			150,4	
10:30:07 AM	152,8	3,7		154,2	3,8
10:35:19 AM	154,7			154,2	
10:40:58 AM	154,6			154,2	
10:45:39 AM	156,6	3,9		157,9	3,8
10:50:17 AM	158,6			157,9	
10:55:36 AM	158,6			157,9	
11:00:13 AM	160,7	4,0	3,8	162,3	4,4
11:05:43 AM	162,8			162,3	
11:10:13 AM	162,7			162,3	
11:15:15 AM	164,9	4,2		166,7	4,4
11:20:45 AM	167,0			166,7	
11:25:17 AM	166,9			166,7	
11:30:22 AM	169,2	4,3		171,0	4,4
11:35:55 AM	171,4			171,0	
11:40:28 AM	171,3			171,0	
11:45:02 AM	173,6	4,4		175,4	4,4
11:50:06 AM	175,9			175,4	
11:55:50 AM	175,8			175,4	
12:00:32 PM	178,1	4,5	4,4	179,8	4,4
12:05:20 PM	180,4			179,8	
12:10:30 PM	180,3			179,8	
12:15:40 PM	182,6	4,5		184,3	4,4
12:20:00 PM	184,9			184,3	
12:25:01 PM	184,8			184,3	
12:30:15 PM	187,1	4,5		188,7	4,4
12:35:55 PM	189,3			188,7	
12:40:35 PM	189,2			188,7	
12:45:17 PM	191,6	4,4		193,1	4,4
12:50:33 PM	193,7			193,1	
12:55:15 PM	193,6			193,1	
01:00:58 PM	195,9	4,3	4,4	197,0	3,9

01:05:41 PM	197,9			197,0	
01:10:25 PM	197,8			197,0	
01:15:10 PM	200,0	4,2		200,9	3,9
01:20:27 PM	202,0			200,9	
01:25:13 PM	201,9			200,9	
01:30:59 PM	204,0	4,0		204,9	3,9
01:35:45 PM	206,0			204,9	
01:40:32 PM	205,9			204,9	
01:45:20 PM	207,9	3,8		208,8	3,9
01:50:08 PM	209,7			208,8	
01:55:34 PM	209,6			208,8	
02:00:23 PM	211,5	3,6	3,9	211,5	2,8
02:05:25 PM	213,2			211,5	
02:10:22 PM	213,1			211,5	
02:15:21 PM	214,9	3,4		214,3	2,8
02:20:19 PM	216,3			214,3	
02:25:22 PM	216,1			214,3	
02:30:18 PM	217,6	2,6		217,1	2,8
02:35:24 PM	218,6			217,1	
02:40:24 PM	218,5			217,1	
02:45:35 PM	219,6	2,0		219,8	2,8
02:50:08 PM	221,1			219,8	
02:55:24 PM	221,0			219,8	
03:00:32 PM	222,6	3,0	2,8	222,3	2,5
03:05:41 PM	223,9			222,3	
03:10:48 PM	223,8			222,3	
03:15:57 PM	225,3	2,8		224,9	2,5
03:20:04 PM	226,6			224,9	
03:25:13 PM	226,5			224,9	
03:30:19 PM	228,0			227,4	2,5
03:35:19 PM	229,2	2,5		227,4	
03:40:22 PM	229,1			227,4	
03:45:28 PM	230,4	2,5		229,9	2,5
03:50:31 PM	231,6			229,9	
03:55:34 PM	231,4			229,9	
04:00:04 PM	232,7	2,3	2,5	231,7	1,8
04:05:15 PM	233,8			231,7	
04:10:25 PM	233,7			231,7	
04:15:37 PM	234,9	2,2		233,5	1,8
04:20:47 PM	236,1			233,5	
04:25:58 PM	236,0			233,5	
04:30:11 PM	237,3	2,4		235,3	1,8
04:35:14 PM	238,1			235,3	
04:40:35 PM	238,0			235,3	
04:45:28 PM	239,0	1,8		237,1	1,8
04:50:16 PM	239,5			237,1	
04:55:29 PM	239,4			237,1	

05:00:50 PM	240,0	0,9	1,8	238,8	1,7
05:05:13 PM	240,9			238,8	
05:10:35 PM	240,7			238,8	
05:15:07 PM	241,8	1,8		240,5	1,7
05:20:20 PM	242,6			240,5	
05:25:35 PM	242,5			240,5	
05:30:53 PM	243,5	1,7		242,2	1,7
05:35:08 PM	244,3			242,2	
05:40:24 PM	244,1			242,2	
05:45:01 PM	245,1	1,6		243,8	1,7
05:50:19 PM	245,9			243,8	
05:55:36 PM	245,7			243,8	
06:00:23 PM	246,6	1,6	1,7	245,5	1,7

Annexure C

Kesian.com website data for the Summer Solstice (21 December 2019)				Translated tilt and orientation angles		Proposed lookout angles	
Time	Elevation angle (°)	Azimuth angle (°)	Derived lookout angles (°)	Actual tilt angle (°)	Actual orientation angle (°)	Fuzzy logic lookout angles (°)	Linear regression lookout angles (°)
06:00	-11,5	110,7	110,7	90,0	100,0	110,0	103,8
06:15	-8,3	112,1	112,1	85,7	95,9	112,7	104,9
06:30	-5,2	113,6	113,6	81,4	91,8	115,4	107,0
06:45	-1,5	115,2	115,2	77,1	87,7	118,1	110,0
07:00	1,3	116,8	116,8	72,7	83,6	120,8	113,0
07:15	4,1	118,5	118,5	68,4	79,5	123,5	116,1
07:30	7,0	120,4	120,4	64,1	75,3	126,2	119,4
07:45	9,8	122,3	122,3	59,8	71,2	128,9	122,7
08:00	12,6	124,3	124,3	55,5	67,1	131,6	125,9
08:15	15,4	126,4	126,4	51,2	63,0	134,3	129,0
08:30	18,0	128,7	128,7	46,9	58,9	137,0	132,2
08:45	20,6	131,1	131,1	42,5	54,8	139,7	135,4
09:00	23,1	133,6	133,6	38,2	50,7	142,4	138,5
09:15	25,4	136,4	136,4	33,9	46,6	145,1	141,6
09:30	27,7	139,3	139,3	29,6	42,5	147,8	144,8
09:45	29,8	142,4	142,4	25,3	38,4	150,5	148,0
10:00	31,8	145,6	145,6	21,0	34,2	153,2	151,2
10:15	33,6	149,1	149,1	16,6	30,1	153,2	154,4
10:30	35,2	152,8	152,8	12,3	26,0	155,9	157,7
10:45	36,7	156,6	156,6	8,0	21,9	158,6	161,0
11:00	37,9	160,7	160,7	3,7	17,8	161,3	164,5
11:15	38,9	164,9	164,9	0,6	13,7	164,0	167,9
11:30	39,7	169,2	169,2	4,9	9,6	166,7	171,4
11:45	40,2	173,6	173,6	9,2	5,5	169,4	174,8
12:00	40,4	178,1	178,1	13,6	1,4	172,1	178,2
12:15	40,4	182,6	182,6	12,0	-2,8	174,8	181,7
12:30	40,1	187,1	187,1	7,6	-7,0	177,5	185,2
12:45	39,6	191,6	191,6	3,2	-11,3	180,2	188,8
13:00	38,8	195,9	195,9	1,3	-15,5	182,9	192,2
13:15	37,7	200,0	200,0	5,7	-19,7	185,6	195,7
13:30	36,5	204,0	204,0	10,1	-23,9	188,3	199,3
13:45	35,0	207,9	207,9	14,6	-28,2	191,0	202,8
14:00	33,3	211,5	211,5	19,0	-32,4	193,7	206,4
14:15	31,5	214,9	214,9	23,5	-36,6	196,4	209,8
14:30	29,5	218,2	217,6	27,9	-40,8	199,1	213,1
14:45	27,3	221,2	219,6	32,3	-45,1	201,8	216,3

15:00	25,0	224,1	222,6	36,8	-49,3	204,5	219,4
15:15	22,7	226,8	225,3	41,2	-53,5	207,2	222,5
15:30	20,2	229,3	228,0	45,6	-57,7	209,9	225,7
15:45	17,6	231,7	230,4	50,1	-62,0	212,6	228,7
16:00	14,9	234,0	232,7	54,5	-66,2	215,3	231,8
16:15	12,2	236,1	234,9	58,9	-70,4	218,0	234,9
16:30	9,3	238,1	237,3	63,4	-74,6	220,7	237,9
16:45	6,5	240,0	239,0	67,8	-78,9	223,4	240,7
17:00	3,6	241,8	240,0	72,3	-83,1	226,1	243,1
17:15	0,9	243,5	241,8	76,7	-87,3	228,8	245,2
17:30	-2,2	245,1	243,5	81,1	-91,5	231,5	246,9
17:45	-5,7	246,6	245,1	85,6	-95,7	234,2	248,0
18:00	-8,9	248,1	246,6	90,0	-100,0	236,9	248,6

Annexure D

Sunny day

Time	Angle of the sun (°) lookout angle	16° Tilt (°)	Angle not perpendicular to the sun (°)	Power (W) (16°)	Tracking Angle of the sun (°)	Angle not perpendicular to the sun (°)	Direct tracking power (W)	Fuzzy logic lookout angles (°)	Angle not perpendicular to the sun (°)	Simulated power (W)	Linear regression lookout angles (°)	Angle not perpendicular to the sun (°)	Simulated power (W)
06:00:23 AM	110,7	164,0	53,3	0,4	110,7	0,0	41,4	110,0	0,7	40,9	103,8	6,9	36,1
06:05:35 AM	111,4	164,0	52,6	0,5	111,4	0,0	73,1	110,0	1,4	71,2	103,8	7,6	62,7
06:10:51 AM	111,3	164,0	52,7	0,7	111,3	0,0	89,9	110,0	1,3	87,6	103,8	7,5	77,2
06:15:08 AM	112,1	164,0	51,9	1,0	112,1	0,0	120,0	112,7	0,6	118,6	104,9	7,2	103,5
06:20:06 AM	112,9	164,0	51,1	1,5	112,9	0,0	147,3	112,7	0,2	146,9	104,9	7,9	124,7
06:25:21 AM	112,8	164,0	51,2	2,3	112,8	0,0	173,3	112,7	0,1	172,9	104,9	7,9	147,0
06:30:40 AM	113,6	164,0	50,4	3,9	113,6	0,0	203,5	115,4	1,8	196,4	107,0	6,6	177,4
06:35:00 AM	114,4	164,0	49,6	6,9	114,4	0,0	233,2	115,4	1,0	228,6	107,0	7,4	199,6
06:40:00 AM	114,3	164,0	49,7	8,6	114,3	0,0	248,3	115,4	1,1	243,2	107,0	7,3	213,0
06:45:18 AM	115,2	164,0	48,8	8,6	115,2	0,0	251,6	118,1	2,9	237,1	110,0	5,2	225,6
06:50:41 AM	116,0	164,0	48,0	9,4	116,0	0,0	250,3	118,1	2,1	239,7	110,0	6,0	220,0
06:55:05 AM	115,9	164,0	48,1	11,7	115,9	0,0	251,6	118,1	2,2	240,8	110,0	6,0	221,8
07:00:07 AM	116,8	164,0	47,2	13,8	116,8	0,0	258,7	120,8	4,0	238,0	113,0	3,8	238,9
07:05:29 AM	117,7	164,0	46,3	17,1	117,7	0,0	261,8	120,8	3,1	245,3	113,0	4,7	237,1
07:10:54 AM	117,6	164,0	46,4	20,5	117,6	0,0	262,8	120,8	3,2	246,2	113,0	4,6	238,7
07:15:21 AM	118,5	164,0	45,5	24,8	118,5	0,0	263,5	123,5	5,0	237,4	116,1	2,4	250,9
07:20:25 AM	119,4	164,0	44,6	28,7	119,4	0,0	269,0	123,5	4,1	247,1	116,1	3,3	251,2
07:25:50 AM	119,4	164,0	44,6	33,7	119,4	0,0	266,9	123,5	4,1	245,4	116,1	3,2	250,0
07:30:18 AM	120,4	164,0	43,7	39,2	120,4	0,0	269,0	126,2	5,9	238,2	119,4	1,0	263,8
07:35:24 AM	121,3	164,0	42,7	44,2	121,3	0,0	273,5	126,2	4,9	247,2	119,4	1,9	263,1
07:40:54 AM	121,2	164,0	42,8	52,6	121,2	0,0	278,8	126,2	5,0	252,6	119,4	1,9	268,9
07:45:08 AM	122,3	164,0	41,7	57,5	122,3	0,0	275,7	128,9	6,6	240,9	122,7	0,4	273,5
07:50:47 AM	123,3	164,0	40,7	63,6	123,3	0,0	271,5	128,9	5,6	242,7	122,7	0,6	268,4
07:55:19 AM	123,2	164,0	40,8	68,2	123,2	0,0	262,8	128,9	5,7	235,7	122,7	0,5	260,2
08:00:29 AM	124,3	164,0	39,7	76,0	124,3	0,0	269,0	131,6	7,3	233,4	125,9	1,6	261,3
08:06:04 AM	125,3	164,0	38,7	87,3	125,3	0,0	269,0	131,6	6,3	239,6	125,9	0,5	266,5
08:10:15 AM	125,3	164,0	38,7	92,2	125,3	0,0	261,4	131,6	6,3	233,8	125,9	0,6	258,8
08:15:47 AM	126,4	164,0	37,6	97,3	126,4	0,0	260,4	134,3	7,9	226,2	129,0	2,6	249,0
08:20:23 AM	127,5	164,0	36,5	109,4	127,5	0,0	260,1	134,3	6,8	232,2	129,0	1,5	253,9
08:25:36 AM	127,5	164,0	36,5	116,0	127,5	0,0	262,1	134,3	6,8	234,8	129,0	1,6	255,9
08:30:14 AM	128,7	164,0	35,3	129,9	128,7	0,0	271,5	137,0	8,3	238,1	132,2	3,5	257,3
08:35:27 AM	129,9	164,0	34,1	136,2	129,9	0,0	268,7	137,0	7,1	241,0	132,2	2,3	259,7
08:40:03 AM	129,8	164,0	34,2	147,6	129,8	0,0	268,7	137,0	7,2	243,2	132,2	2,4	260,2
08:45:18 AM	131,1	164,0	32,9	157,1	131,1	0,0	265,6	139,7	8,6	237,2	135,4	4,3	251,3
08:50:00 AM	132,4	164,0	31,6	169,3	132,4	0,0	263,5	139,7	7,3	241,6	135,4	3,0	254,4
08:55:16 AM	132,3	164,0	31,7	177,4	132,3	0,0	258,0	139,7	7,4	239,2	135,4	3,1	250,1
09:00:59 AM	133,6	164,0	30,4	191,8	133,6	0,0	253,6	142,4	8,8	235,8	138,5	4,9	243,7
09:05:16 AM	135,0	164,0	29,0	202,3	135,0	0,0	265,4	142,4	7,4	249,3	138,5	3,5	257,8
09:10:57 AM	134,9	164,0	29,1	210,5	134,9	0,0	257,2	142,4	7,5	245,2	138,5	3,6	251,4
09:15:16 AM	136,4	164,0	27,6	218,6	136,4	0,0	252,4	145,1	8,7	241,7	141,6	5,2	246,0
09:20:15 AM	137,8	164,0	26,2	226,2	137,8	0,0	260,7	145,1	7,3	251,1	141,6	3,8	255,8
09:25:46 AM	137,7	164,0	26,3	233,3	137,7	0,0	268,0	145,1	7,4	258,3	141,6	3,9	262,9
09:30:18 AM	139,3	164,0	24,7	236,3	139,3	0,0	271,1	147,8	8,5	259,1	144,8	5,5	263,3
09:35:23 AM	140,8	164,0	23,2	241,5	140,8	0,0	276,0	147,8	7,0	265,6	144,8	4,0	270,1
09:40:58 AM	140,7	164,0	23,3	247,8	140,7	0,0	267,5	147,8	7,1	261,5	144,8	4,1	264,0
09:45:32 AM	142,4	164,0	21,7	252,2	142,4	0,0	256,3	150,5	8,2	254,8	148,0	5,6	255,3
09:50:06 AM	144,0	164,0	20,0	257,6	144,0	0,0	263,5	150,5	6,5	261,6	148,0	4,0	262,3
09:55:11 AM	143,9	164,0	20,1	260,4	143,9	0,0	265,9	150,5	6,6	264,1	148,0	4,1	264,8
10:00:46 AM	145,6	164,0	18,4	261,7	145,6	0,0	268,3	153,2	7,6	265,6	151,2	5,6	266,3
10:05:23 AM	147,4	164,0	16,6	262,4	147,4	0,0	268,7	153,2	5,8	266,5	151,2	3,8	267,2

10:10:01 AM	147,3	164,0	16,7	266,6	147,3	0,0	273,2	153,2	5,9	270,9	151,2	3,9	271,7
10:15:11 AM	149,1	164,0	14,9	270,1	149,1	0,0	275,7	153,2	4,1	274,1	154,4	5,3	273,6
10:20:50 AM	150,9	164,0	13,1	269,4	150,9	0,0	275,7	155,9	5,0	273,3	154,4	3,5	274,0
10:25:28 AM	150,8	164,0	13,2	270,1	150,8	0,0	276,7	155,9	5,1	274,2	154,4	3,6	274,9
10:30:07 AM	152,8	164,0	11,2	271,1	152,8	0,0	277,8	155,9	3,1	275,9	157,7	5,0	274,8
10:35:19 AM	154,7	164,0	9,3	270,1	154,7	0,0	275,0	158,6	3,9	272,9	157,7	3,1	273,3
10:40:58 AM	154,6	164,0	9,4	271,1	154,6	0,0	275,3	158,6	4,0	273,5	157,7	3,1	273,9
10:45:39 AM	156,6	164,0	7,4	270,8	156,6	0,0	275,0	158,6	2,0	273,8	161,0	4,4	272,4
10:50:17 AM	158,6	164,0	5,4	277,8	158,6	0,0	283,4	161,3	2,7	280,6	161,0	2,4	280,9
10:55:36 AM	158,6	164,0	5,4	284,2	158,6	0,0	289,9	161,3	2,7	287,0	161,0	2,5	287,3
11:00:13 AM	160,7	164,0	3,3	281,3	160,7	0,0	288,8	161,3	0,6	287,4	164,5	3,8	280,3
11:05:43 AM	162,8	164,0	1,2	281,7	162,8	0,0	287,0	164,0	1,2	281,7	164,5	1,7	279,6
11:10:13 AM	162,7	164,0	1,3	278,9	162,7	0,0	285,2	164,0	1,3	278,9	164,5	1,8	276,5
11:15:15 AM	164,9	164,0	0,9	279,9	164,9	0,0	285,9	164,0	-0,9	291,9	167,9	3,1	264,6
11:20:45 AM	167,0	164,0	3,0	284,6	167,0	0,0	290,6	166,7	-0,3	291,3	167,9	0,9	288,8
11:25:17 AM	166,9	164,0	2,9	288,5	166,9	0,0	295,7	166,7	-0,2	296,3	167,9	1,0	293,3
11:30:22 AM	169,2	164,0	5,2	282,4	169,2	0,0	288,1	166,7	-2,5	290,8	171,4	2,2	285,7
11:35:55 AM	171,4	164,0	7,4	281,3	171,4	0,0	287,7	169,4	-2,0	289,5	171,4	0,0	287,7
11:40:28 AM	171,3	164,0	7,3	277,4	171,3	0,0	282,7	169,4	-1,9	284,1	171,4	0,1	282,7
11:45:02 AM	173,6	164,0	9,6	284,2	173,6	0,0	290,6	169,4	-4,2	293,4	174,8	1,2	289,8
11:50:06 AM	175,9	164,0	11,9	279,6	175,9	0,0	285,2	172,1	-3,8	287,0	174,8	1,0	284,7
11:55:50 AM	175,8	164,0	11,8	267,6	175,8	0,0	271,5	172,1	-3,7	272,7	174,8	0,9	271,1
12:00:32 PM	178,1	164,0	14,1	287,4	178,1	0,0	293,5	172,1	-6,0	296,1	178,2	0,1	293,4
12:05:20 PM	180,4	164,0	16,4	278,1	180,4	0,0	281,3	174,8	-5,6	282,4	178,2	2,1	280,9
12:10:30 PM	180,3	164,0	16,3	284,9	180,3	0,0	290,2	174,8	-5,5	292,0	178,2	2,1	289,6
12:15:40 PM	182,6	164,0	18,6	290,0	182,6	0,0	295,3	174,8	-7,8	297,5	181,7	0,9	295,0
12:20:00 PM	184,9	164,0	20,9	292,9	184,9	0,0	298,6	177,5	-7,4	300,6	181,7	3,2	297,7
12:25:01 PM	184,8	164,0	20,8	288,4	184,8	0,0	299,3	177,5	-7,3	303,2	181,7	3,1	297,7
12:30:15 PM	187,1	164,0	23,1	301,7	187,1	0,0	285,2	177,5	-9,6	278,3	185,2	1,9	286,5
12:35:55 PM	189,3	164,0	25,3	290,3	189,3	0,0	300,5	180,2	-9,1	304,2	185,2	4,1	298,9
12:40:35 PM	189,2	164,0	25,2	294,3	189,2	0,0	301,6	180,2	-9,0	304,3	185,2	4,0	300,5
12:45:17 PM	191,6	164,0	27,6	298,7	191,6	0,0	292,0	180,2	-11,4	289,2	188,8	2,8	292,7
12:50:33 PM	193,7	164,0	29,7	287,8	193,7	0,0	283,9	182,9	-10,8	282,5	188,8	4,9	284,6
12:55:15 PM	193,6	164,0	29,6	277,4	193,6	0,0	291,1	182,9	-10,7	296,0	188,8	4,8	288,9
01:00:58 PM	195,9	164,0	31,9	278,9	195,9	0,0	284,1	182,9	-13,0	286,2	192,2	3,6	283,5
01:05:41 PM	197,9	164,0	33,9	275,7	197,9	0,0	291,6	185,6	-12,3	297,4	192,2	5,7	288,9
01:10:25 PM	197,8	164,0	33,8	276,4	197,8	0,0	284,6	185,6	-12,2	287,6	192,2	5,6	283,3
01:15:10 PM	200,0	164,0	36,0	282,1	200,0	0,0	287,0	185,6	-14,4	288,9	195,7	4,4	286,4
01:20:27 PM	202,0	164,0	38,0	283,1	202,0	0,0	294,2	188,3	-13,7	298,2	195,7	6,4	292,3
01:25:13 PM	201,9	164,0	37,9	285,3	201,9	0,0	303,9	188,3	-13,6	310,6	195,7	6,3	300,8
01:30:59 PM	204,0	164,0	40,0	279,2	204,0	0,0	304,3	188,3	-15,7	314,1	199,3	4,8	301,3
01:35:45 PM	206,0	164,0	42,0	276,4	206,0	0,0	303,7	191,0	-15,0	313,5	199,3	6,7	299,4
01:40:32 PM	205,9	164,0	41,9	286,4	205,9	0,0	288,5	191,0	-14,9	289,2	199,3	6,6	288,1
01:45:20 PM	207,9	164,0	43,9	282,8	207,9	0,0	301,2	191,0	-16,9	308,2	202,8	5,0	299,1
01:50:08 PM	209,7	164,0	45,7	275,7	209,7	0,0	302,6	193,7	-16,0	312,1	202,8	6,8	298,6
01:55:34 PM	209,6	164,0	45,6	277,4	209,6	0,0	292,4	193,7	-15,9	297,7	202,8	6,7	290,2
02:00:23 PM	211,5	164,0	47,5	271,8	211,5	0,0	293,9	193,7	-17,8	302,2	206,4	5,1	291,5
02:05:25 PM	213,2	164,0	49,2	281,7	213,2	0,0	294,6	196,4	-16,8	299,0	206,4	6,8	292,8
02:10:22 PM	213,1	164,0	49,1	271,5	213,1	0,0	277,4	196,4	-16,7	279,4	206,4	6,7	276,6
02:15:21 PM	214,9	164,0	50,9	264,2	214,9	0,0	270,2	196,4	-18,5	272,3	209,8	5,2	269,6
02:20:19 PM	216,3	164,0	52,3	281,3	216,3	0,0	283,4	199,1	-17,2	284,1	209,8	6,5	283,2
02:25:22 PM	216,1	164,0	52,1	273,6	216,1	0,0	280,6	199,1	-17,0	282,8	209,8	6,4	279,7
02:30:18 PM	217,6	164,0	53,6	277,1	217,6	0,0	277,1	199,1	-18,5	277,1	213,1	4,5	277,1
02:35:24 PM	218,6	164,0	54,6	273,2	218,6	0,0	272,8	201,8	-16,8	272,7	213,1	5,5	272,9
02:40:24 PM	218,5	164,0	54,5	267,3	218,5	0,0	267,6	201,8	-16,7	267,7	213,1	5,4	267,6
02:45:35 PM	219,6	164,0	55,6	263,8	219,6	0,0	262,1	201,8	-17,8	261,6	216,3	3,3	262,2
02:50:08 PM	221,1	164,0	57,1	263,5	221,1	0,0	261,8	204,5	-16,6	261,3	216,3	4,8	261,9
02:55:24 PM	221,0	164,0	57,0	258,3	221,0	0,0	257,3	204,5	-16,5	257,1	216,3	4,7	257,4
03:00:32 PM	222,6	164,0	58,6	239,0	222,6	0,0	262,8	204,5	-18,1	270,1	219,4	3,1	261,5
03:05:41 PM	223,9	164,0	59,9	235,1	223,9	0,0	264,0	207,2	-16,7	272,1	219,4	4,5	261,8
03:10:48 PM	223,8	164,0	59,8	215,5	223,8	0,0	257,8	207,2	-16,6	269,6	219,4	4,4	254,7
03:15:57 PM	225,3	164,0	61,3	210,2	225,3	0,0	252,1	207,2	-18,1	264,5	222,5	2,8	250,2
03:20:04 PM	226,6	164,0	62,6	205,0	226,6	0,0	261,4	209,9	-16,7	276,5	222,5	4,1	257,7

03:25:13 PM	226,5	164,0	62,5	207,6	226,5	0,0	264,7	209,9	-16,6	279,8	222,5	4,0	261,0
03:30:19 PM	228,0	164,0	64,0	185,4	228,0	0,0	261,8	209,9	-18,1	283,4	225,7	2,3	259,1
03:35:19 PM	229,2	164,0	65,2	175,4	229,2	0,0	260,2	212,6	-16,6	281,8	225,7	3,5	255,7
03:40:22 PM	229,1	164,0	65,1	155,6	229,1	0,0	255,9	212,6	-16,5	281,2	225,7	3,4	250,6
03:45:28 PM	230,4	164,0	66,4	157,1	230,4	0,0	253,4	212,6	-17,8	279,2	228,7	1,7	251,0
03:50:31 PM	231,6	164,0	67,6	139,1	231,6	0,0	255,5	215,3	-16,3	283,5	228,7	2,8	250,6
03:55:34 PM	231,4	164,0	67,4	140,0	231,4	0,0	257,2	215,3	-16,1	285,2	228,7	2,7	252,5
04:00:04 PM	232,7	164,0	68,7	125,2	232,7	0,0	260,5	215,3	-17,4	294,8	231,8	0,9	258,8
04:05:15 PM	233,8	164,0	69,8	128,8	233,8	0,0	260,0	218,0	-15,8	289,7	231,8	2,0	256,3
04:10:25 PM	233,7	164,0	69,7	124,2	233,7	0,0	260,0	218,0	-15,7	290,6	231,8	1,9	256,4
04:15:37 PM	234,9	164,0	70,9	120,1	234,9	0,0	258,0	218,0	-16,9	290,9	234,9	0,0	257,9
04:20:47 PM	236,1	164,0	72,1	109,7	236,1	0,0	258,8	220,7	-15,4	290,6	234,9	1,1	256,5
04:25:58 PM	236,0	164,0	72,0	97,1	236,0	0,0	239,8	220,7	-15,3	270,0	234,9	1,0	237,8
04:30:11 PM	237,3	164,0	73,3	84,8	237,3	0,0	252,0	220,7	-16,6	289,8	237,9	0,7	250,5
04:35:14 PM	238,1	164,0	74,1	73,6	238,1	0,0	246,7	223,4	-14,7	281,2	237,9	0,2	246,3
04:40:35 PM	238,0	164,0	74,0	64,3	238,0	0,0	233,4	223,4	-14,6	266,8	237,9	0,1	233,2
04:45:28 PM	239,0	164,0	75,0	64,9	239,0	0,0	217,4	223,4	-15,6	249,2	240,7	1,7	213,9
04:50:16 PM	239,5	164,0	75,5	65,8	239,5	0,0	210,1	226,1	-13,4	235,7	240,7	1,2	207,7
04:55:29 PM	239,4	164,0	75,4	44,7	239,4	0,0	196,4	226,1	-13,3	223,1	240,7	1,4	193,7
05:00:50 PM	240,0	164,0	76,0	45,1	240,0	0,0	187,7	226,1	-13,9	213,8	243,1	3,1	181,8
05:05:13 PM	240,9	164,0	76,9	32,2	240,9	0,0	187,0	228,8	-12,1	211,3	243,1	2,2	182,5
05:10:35 PM	240,7	164,0	76,7	26,8	240,7	0,0	174,2	228,8	-11,9	197,1	243,1	2,4	169,7
05:15:07 PM	241,8	164,0	77,8	19,5	241,8	0,0	167,8	228,8	-13,0	192,5	245,2	3,5	161,2
05:20:20 PM	242,6	164,0	78,6	16,0	242,6	0,0	157,3	231,5	-11,1	177,3	245,2	2,6	152,6
05:25:35 PM	242,5	164,0	78,5	16,5	242,5	0,0	136,2	231,5	-11,0	152,9	245,2	2,7	132,0
05:30:53 PM	243,5	164,0	79,5	13,5	243,5	0,0	126,3	231,5	-12,0	143,2	246,9	3,4	121,4
05:35:08 PM	244,3	164,0	80,3	10,4	244,3	0,0	115,6	234,2	-10,1	128,7	246,9	2,6	112,1
05:40:24 PM	244,1	164,0	80,1	8,0	244,1	0,0	77,3	234,2	-9,9	85,9	246,9	2,7	74,9
05:45:01 PM	245,1	164,0	81,1	4,5	245,1	0,0	88,9	234,2	-10,9	100,2	248,0	2,9	85,8
05:50:19 PM	245,9	164,0	81,9	5,7	245,9	0,0	86,5	236,9	-9,0	95,3	248,0	2,2	84,4
05:55:36 PM	245,7	164,0	81,7	3,0	245,7	0,0	15,3	236,9	-8,8	16,6	248,0	2,3	15,0
06:00:23 PM	246,6	164,0	82,6	0,4	246,6	0,0	41,4	236,9	-9,7	46,3	248,6	1,9	40,5

Central University of Technology, Free State

Annexure E

Single cloud day

Time	Angle of the sun (°)	16° Tilt (°)	Angle not perpendicular to the sun (°)	Power (W) (single cloud)	Tilt (fuzzy) (°)	Degree not perpendicular to the sun	Power (W) (direct tracking)	Tilt for new fuzzy logic system (°)	Angle not perpendicular to the sun (°)	Simulated power (W)
06:00:23 AM	110,7	164,0	53,3	0,5	110,7	0,0	41,4	110	-0,7	41,9
06:05:35 AM	111,4	164,0	52,6	0,6	111,4	0,0	73,1	110	-1,4	75,1
06:10:51 AM	111,3	164,0	52,7	4,7	111,3	0,0	89,9	110	-1,3	92,1
06:15:08 AM	112,1	164,0	51,9	1,9	112,1	0,0	120,0	111,9	-0,2	120,5
06:20:06 AM	112,9	164,0	51,1	2,1	112,9	0,0	147,3	111,9	-1,0	150,1
06:25:21 AM	112,8	164,0	51,2	4,5	112,8	0,0	173,3	111,9	-0,9	176,3
06:30:40 AM	113,6	164,0	50,4	5,2	113,6	0,0	203,5	113,8	0,2	202,8
06:35:00 AM	114,4	164,0	49,6	5,8	114,4	0,0	233,2	113,8	-0,6	235,9
06:40:00 AM	114,3	164,0	49,7	6,2	114,3	0,0	248,3	113,8	-0,5	250,9
06:45:18 AM	115,2	164,0	48,8	8,0	115,2	0,0	251,6	115,7	0,5	249,0
06:50:41 AM	116,0	164,0	48,0	8,2	116,0	0,0	250,3	115,7	-0,3	251,8
06:55:05 AM	115,9	164,0	48,1	8,1	115,9	0,0	251,6	115,7	-0,2	252,8
07:00:07 AM	116,8	164,0	47,2	10,2	116,8	0,0	264,0	117,6	0,8	259,8
07:05:29 AM	117,7	164,0	46,3	10,2	117,7	0,0	264,4	117,6	-0,1	264,8
07:10:54 AM	117,6	164,0	46,4	11,6	117,6	0,0	274,7	117,6	0,0	274,8
07:15:21 AM	118,5	164,0	45,5	12,7	118,5	0,0	276,2	119,5	1,0	270,7
07:20:25 AM	119,4	164,0	44,6	15,1	119,4	0,0	275,9	119,5	0,1	275,5
07:25:50 AM	119,4	164,0	44,6	24,6	119,4	0,0	277,6	119,5	0,1	276,9
07:30:18 AM	120,4	164,0	43,7	26,2	120,4	0,0	280,1	121,4	1,1	274,0
07:35:24 AM	121,3	164,0	42,7	26,0	121,3	0,0	287,7	121,4	0,1	287,1
07:40:54 AM	121,2	164,0	42,8	28,1	121,2	0,0	292,1	121,4	0,2	291,1
07:45:08 AM	122,3	164,0	41,7	51,2	122,3	0,0	297,4	123,3	1,0	291,2
07:50:47 AM	123,3	164,0	40,7	51,7	123,3	0,0	296,4	123,3	0,0	296,2
07:55:19 AM	123,2	164,0	40,8	57,4	123,2	0,0	293,7	123,3	0,1	293,2
08:00:29 AM	124,3	164,0	39,7	66,5	124,3	0,0	293,6	125,2	0,9	288,3
08:06:04 AM	125,3	164,0	38,7	83,2	125,3	0,0	295,9	125,2	-0,1	296,7
08:10:15 AM	125,3	164,0	38,7	92,1	125,3	0,0	293,6	125,2	-0,1	294,0
08:15:47 AM	126,4	164,0	37,6	94,7	126,4	0,0	297,1	127,1	0,7	293,3
08:20:23 AM	127,5	164,0	36,5	103,3	127,5	0,0	296,6	127,1	-0,4	299,0
08:25:36 AM	127,5	164,0	36,5	115,3	127,5	0,0	293,8	127,1	-0,4	295,7
08:30:14 AM	128,7	164,0	35,3	123,2	128,7	0,0	297,2	129	0,3	295,6
08:35:27 AM	129,9	164,0	34,1	128,2	129,9	0,0	291,8	129	-0,9	296,0
08:40:03 AM	129,8	164,0	34,2	126,5	129,8	0,0	291,6	129	-0,8	295,5
08:45:18 AM	131,1	164,0	32,9	145,0	131,1	0,0	296,5	130,9	-0,2	297,3
08:50:00 AM	132,4	164,0	31,6	156,5	132,4	0,0	291,9	130,9	-1,5	298,2

08:55:16 AM	132,3	164,0	31,7	166,0	132,3	0,0	297,4	130,9	-1,4	303,2
09:00:59 AM	133,6	164,0	30,4	173,7	133,6	0,0	294,3	132,8	-0,8	297,6
09:05:16 AM	135,0	164,0	29,0	183,4	135,0	0,0	293,1	132,8	-2,2	301,5
09:10:57 AM	134,9	164,0	29,1	190,6	134,9	0,0	291,0	132,8	-2,1	298,3
09:15:16 AM	136,4	164,0	27,6	205,6	136,4	0,0	297,9	135,8	-0,6	299,8
09:20:15 AM	137,8	164,0	26,2	219,5	137,8	0,0	296,6	135,8	-2,0	302,5
09:25:46 AM	137,7	164,0	26,3	216,6	137,7	0,0	288,1	135,8	-1,9	293,4
09:30:18 AM	139,3	164,0	24,7	227,5	139,3	0,0	295,0	138,8	-0,5	296,2
09:35:23 AM	140,8	164,0	23,2	233,7	140,8	0,0	289,9	138,8	-2,0	294,8
09:40:58 AM	140,7	164,0	23,3	264,1	140,7	0,0	297,9	138,8	-1,9	300,7
09:45:32 AM	142,4	164,0	21,7	251,8	142,4	0,0	291,8	141,8	-0,5	292,8
09:50:06 AM	144,0	164,0	20,0	251,5	144,0	0,0	289,4	141,8	-2,2	293,5
09:55:11 AM	143,9	164,0	20,1	254,2	143,9	0,0	289,7	141,8	-2,1	293,5
10:00:46 AM	145,6	164,0	18,4	264,8	145,6	0,0	291,2	144,8	-0,8	292,4
10:05:23 AM	147,4	164,0	16,6	258,3	147,4	0,0	288,4	144,8	-2,6	293,1
10:10:01 AM	147,3	164,0	16,7	299,0	147,3	0,0	309,2	144,8	-2,5	310,7
10:15:11 AM	149,1	164,0	14,9	298,5	149,1	0,0	296,8	148,6	-0,5	296,7
10:20:50 AM	150,9	164,0	13,1	296,3	150,9	0,0	295,2	148,6	-2,3	295,0
10:25:28 AM	150,8	164,0	13,2	297,0	150,8	0,0	296,2	148,6	-2,2	296,0
10:30:07 AM	152,8	164,0	11,2	293,2	152,8	0,0	294,8	152,4	-0,4	294,9
10:35:19 AM	154,7	164,0	9,3	291,6	154,7	0,0	292,3	152,4	-2,3	292,4
10:40:58 AM	154,6	164,0	9,4	295,7	154,6	0,0	295,2	152,4	-2,2	295,0
10:45:39 AM	156,6	164,0	7,4	299,5	156,6	0,0	298,1	156,2	-0,4	298,0
10:50:17 AM	158,6	164,0	5,4	295,1	158,6	0,0	294,8	156,2	-2,4	294,7
10:55:36 AM	158,6	164,0	5,4	290,0	158,6	0,0	290,8	156,2	-2,4	291,2
11:00:13 AM	160,7	164,0	3,3	289,1	160,7	0,0	291,5	160	-0,7	292,0
11:05:43 AM	162,8	164,0	1,2	297,2	162,8	0,0	297,4	160	-2,8	297,9
11:10:13 AM	162,7	164,0	1,3	296,6	162,7	0,0	295,2	160	-2,7	292,3
11:15:15 AM	164,9	164,0	0,9	291,7	164,9	0,0	290,4	164,4	-0,5	289,8
11:20:45 AM	167,0	164,0	3,0	286,2	167,0	0,0	287,2	164,4	-2,6	288,0
11:25:17 AM	166,9	164,0	2,9	293,8	166,9	0,0	295,5	164,4	-2,5	297,0
11:30:22 AM	169,2	164,0	5,2	288,8	169,2	0,0	289,4	168,8	-0,4	289,4
11:35:55 AM	171,4	164,0	7,4	297,0	171,4	0,0	296,6	168,8	-2,6	296,5
11:40:28 AM	171,3	164,0	7,3	294,1	171,3	0,0	295,5	168,8	-2,5	296,0
11:45:02 AM	173,6	164,0	9,6	293,9	173,6	0,0	292,1	173,2	-0,4	292,0
11:50:06 AM	175,9	164,0	11,9	282,5	175,9	0,0	283,2	173,2	-2,7	283,3
11:55:50 AM	175,8	164,0	11,8	293,2	175,8	0,0	294,8	173,2	-2,6	295,2
12:00:32 PM	178,1	164,0	14,1	298,1	178,1	0,0	297,0	177,6	-0,5	297,0
12:05:20 PM	180,4	164,0	16,4	289,6	180,4	0,0	290,1	177,6	-2,8	290,2
12:10:30 PM	180,3	164,0	16,3	293,7	180,3	0,0	294,4	177,6	-2,7	294,6
12:15:40 PM	182,6	164,0	18,6	299,2	182,6	0,0	300,3	181,7	-0,9	300,4
12:20:00 PM	184,9	164,0	20,9	304,2	184,9	0,0	303,3	181,7	-3,2	303,1
12:25:01 PM	184,8	164,0	20,8	296,3	184,8	0,0	298,8	181,7	-3,1	299,2
12:30:15 PM	187,1	164,0	23,1	303,1	187,1	0,0	303,3	185,8	-1,3	303,3
12:35:55 PM	189,3	164,0	25,3	304,0	189,3	0,0	306,2	185,8	-3,5	306,5
12:40:35 PM	189,2	164,0	25,2	299,7	189,2	0,0	299,6	185,8	-3,4	299,5
12:45:17 PM	191,6	164,0	27,6	296,7	191,6	0,0	296,1	189,9	-1,6	296,0

12:50:33 PM	193,7	164,0	29,7	296,7	193,7	0,0	293,9	189,9	-3,8	293,5
12:55:15 PM	193,6	164,0	29,6	299,2	193,6	0,0	297,0	189,9	-3,7	296,7
01:00:58 PM	195,9	164,0	31,9	293,4	195,9	0,0	294,6	194	-1,9	294,7
01:05:41 PM	197,9	164,0	33,9	297,3	197,9	0,0	298,1	194	-3,9	298,2
01:10:25 PM	197,8	164,0	33,8	300,1	197,8	0,0	301,9	194	-3,8	302,1
01:15:10 PM	200,0	164,0	36,0	298,8	200,0	0,0	298,8	197,9	-2,1	298,8
01:20:27 PM	202,0	164,0	38,0	287,3	202,0	0,0	295,2	197,9	-4,1	296,0
01:25:13 PM	201,9	164,0	37,9	296,9	201,9	0,0	296,7	197,9	-4,0	296,7
01:30:59 PM	204,0	164,0	40,0	295,9	204,0	0,0	295,2	201,8	-2,2	295,2
01:35:45 PM	206,0	164,0	42,0	292,7	206,0	0,0	292,1	201,8	-4,2	292,0
01:40:32 PM	205,9	164,0	41,9	291,0	205,9	0,0	292,6	201,8	-4,1	292,8
01:45:20 PM	207,9	164,0	43,9	295,4	207,9	0,0	296,5	205,7	-2,2	296,6
01:50:08 PM	209,7	164,0	45,7	298,4	209,7	0,0	298,8	205,7	-4,0	298,8
01:55:34 PM	209,6	164,0	45,6	293,9	209,6	0,0	294,0	205,7	-3,9	294,1
02:00:23 PM	211,5	164,0	47,5	290,5	211,5	0,0	289,7	209,6	-1,9	289,6
02:05:25 PM	213,2	164,0	49,2	292,4	213,2	0,0	293,3	209,6	-3,6	293,4
02:10:22 PM	213,1	164,0	49,1	295,1	213,1	0,0	296,3	209,6	-3,5	296,3
02:15:21 PM	214,9	164,0	50,9	296,7	214,9	0,0	295,4	212,7	-2,2	295,4
02:20:19 PM	216,3	164,0	52,3	289,5	216,3	0,0	290,4	212,7	-3,6	290,5
02:25:22 PM	216,1	164,0	52,1	291,0	216,1	0,0	289,3	212,7	-3,4	289,1
02:30:18 PM	217,6	164,0	53,6	290,0	217,6	0,0	294,1	215,8	-1,8	294,2
02:35:24 PM	218,6	164,0	54,6	290,7	218,6	0,0	290,8	215,8	-2,8	290,8
02:40:24 PM	218,5	164,0	54,5	267,9	218,5	0,0	284,0	215,8	-2,7	284,8
02:45:35 PM	219,6	164,0	55,6	74,7	219,6	0,0	74,7	218,9	-0,7	74,7
02:50:08 PM	221,1	164,0	57,1	66,7	221,1	0,0	66,7	218,9	-2,2	66,7
02:55:24 PM	221,0	164,0	57,0	12,9	221,0	0,0	12,9	218,9	-2,1	12,9
03:00:32 PM	222,6	164,0	58,6	239,0	222,6	0,0	296,0	222	-0,6	296,6
03:05:41 PM	223,9	164,0	59,9	285,1	223,9	0,0	295,4	222	-1,9	295,7
03:10:48 PM	223,8	164,0	59,8	285,5	223,8	0,0	293,0	222	-1,8	293,3
03:15:57 PM	225,3	164,0	61,3	270,2	225,3	0,0	289,4	224,5	-0,8	289,6
03:20:04 PM	226,6	164,0	62,6	268,0	226,6	0,0	288,2	224,5	-2,1	288,9
03:25:13 PM	226,5	164,0	62,5	263,6	226,5	0,0	283,5	224,5	-2,0	284,1
03:30:19 PM	228,0	164,0	64,0	252,4	228,0	0,0	279,7	227	-1,0	280,1
03:35:19 PM	229,2	164,0	65,2	245,4	229,2	0,0	293,8	227	-2,2	295,5
03:40:22 PM	229,1	164,0	65,1	242,6	229,1	0,0	294,6	227	-2,1	296,2
03:45:28 PM	230,4	164,0	66,4	239,1	230,4	0,0	297,4	229,5	-0,9	298,2
03:50:31 PM	231,6	164,0	67,6	237,1	231,6	0,0	297,3	229,5	-2,1	299,1
03:55:34 PM	231,4	164,0	67,4	230,0	231,4	0,0	292,5	229,5	-1,9	294,3
04:00:04 PM	232,7	164,0	68,7	225,2	232,7	0,0	291,9	232	-0,7	292,6
04:05:15 PM	233,8	164,0	69,8	218,8	233,8	0,0	296,9	232	-1,8	298,9
04:10:25 PM	233,7	164,0	69,7	212,2	233,7	0,0	296,6	232	-1,7	298,7
04:15:37 PM	234,9	164,0	70,9	206,1	234,9	0,0	295,9	233,8	-1,1	297,3
04:20:47 PM	236,1	164,0	72,1	179,7	236,1	0,0	295,0	233,8	-2,3	298,6
04:25:58 PM	236,0	164,0	72,0	172,1	236,0	0,0	293,8	233,8	-2,2	297,4
04:30:11 PM	237,3	164,0	73,3	169,8	237,3	0,0	292,0	235,6	-1,7	294,8
04:35:14 PM	238,1	164,0	74,1	157,6	238,1	0,0	290,7	235,6	-2,5	295,3
04:40:35 PM	238,0	164,0	74,0	146,3	238,0	0,0	284,4	235,6	-2,4	288,9

04:45:28 PM	239,0	164,0	75,0	138,9	239,0	0,0	284,4	237,4	-1,6	287,5
04:50:16 PM	239,5	164,0	75,5	122,8	239,5	0,0	282,1	237,4	-2,1	286,5
04:55:29 PM	239,4	164,0	75,4	108,7	239,4	0,0	270,4	237,4	-2,0	274,6
05:00:50 PM	240,0	164,0	76,0	84,1	240,0	0,0	267,7	239,2	-0,8	269,6
05:05:13 PM	240,9	164,0	76,9	82,2	240,9	0,0	267,0	239,2	-1,7	271,0
05:10:35 PM	240,7	164,0	76,7	56,8	240,7	0,0	254,2	239,2	-1,5	258,1
05:15:07 PM	241,8	164,0	77,8	49,5	241,8	0,0	237,8	241	-0,7	239,7
05:20:20 PM	242,6	164,0	78,6	46,0	242,6	0,0	247,3	241	-1,6	251,4
05:25:35 PM	242,5	164,0	78,5	36,5	242,5	0,0	236,2	241	-1,5	240,0
05:30:53 PM	243,5	164,0	79,5	33,5	243,5	0,0	226,3	242,8	-0,7	227,9
05:35:08 PM	244,3	164,0	80,3	10,4	244,3	0,0	215,6	242,8	-1,5	219,3
05:40:24 PM	244,1	164,0	80,1	8,0	244,1	0,0	197,3	242,8	-1,3	200,5
05:45:01 PM	245,1	164,0	81,1	4,5	245,1	0,0	118,9	244,6	-0,5	119,6
05:50:19 PM	245,9	164,0	81,9	5,7	245,9	0,0	86,5	244,6	-1,3	87,7
05:55:36 PM	245,7	164,0	81,7	3,0	245,7	0,0	55,3	244,6	-1,1	56,0
06:00:23 PM	246,6	164,0	82,6	0,4	246,6	0,0	41,4	246,6	0,0	41,4

Annexure F

Multiple clouds day

Time	Angle of the sun (°)	16° Tilt (°)	Angle not perpendicular to the sun (°)	Power (W) (multiple clouds)	Tilt (fuzzy) (°)	Degree not perpendicular to the sun	Power (W) (Direct tracking)	Tilt for new fuzzy logic system (°)	Angle not perpendicular to the sun (°)	Simulated power (W)
06:00:23 AM	110,7	0,2	110,5	0,2	110,7	0,0	91,2	110,7	0,0	91,2
06:05:35 AM	111,4	0,3	111,1	0,3	111,4	0,0	123,2	110,7	-0,7	124,0
06:10:51 AM	111,3	0,4	111,0	0,4	111,3	0,0	154,5	110,7	-0,7	155,4
06:15:08 AM	112,1	0,5	111,6	0,5	112,1	0,0	178,1	112,1	0,0	178,1
06:20:06 AM	112,9	0,9	112,0	0,9	112,9	0,0	205,1	112,1	-0,8	206,5
06:25:21 AM	112,8	1,4	111,4	1,4	112,8	0,0	232,8	112,1	-0,7	234,2
06:30:40 AM	113,6	2,2	111,5	2,2	113,6	0,0	250,6	113,6	0,0	250,6
06:35:00 AM	114,4	3,0	111,4	3,0	114,4	0,0	259,8	113,6	-0,8	261,6
06:40:00 AM	114,3	4,4	109,9	4,4	114,3	0,0	271,2	113,6	-0,7	273,0
06:45:18 AM	115,2	6,3	108,9	6,3	115,2	0,0	275,8	115,2	0,0	275,8
06:50:41 AM	116,0	8,1	107,9	8,1	116,0	0,0	279,0	115,2	-0,8	281,0
06:55:05 AM	115,9	10,7	105,3	10,7	115,9	0,0	281,5	115,2	-0,8	283,4
07:00:07 AM	116,8	14,1	102,7	14,1	116,8	0,0	284,2	116,8	0,0	284,2
07:05:29 AM	117,7	16,9	100,7	16,9	117,7	0,0	283,7	116,8	-0,9	286,0
07:10:54 AM	117,6	21,1	96,5	21,1	117,6	0,0	285,9	116,8	-0,8	288,1
07:15:21 AM	118,5	26,1	92,5	26,1	118,5	0,0	285,2	118,5	0,0	285,2
07:20:25 AM	119,4	29,9	89,6	29,9	119,4	0,0	286,3	118,5	-0,9	288,9
07:25:50 AM	119,4	36,1	83,3	36,1	119,4	0,0	285,0	118,5	-0,8	287,5
07:30:18 AM	120,4	41,0	79,4	41,0	120,4	0,0	286,2	120,4	0,0	286,2
07:35:24 AM	121,3	48,3	73,0	48,3	121,3	0,0	284,3	120,4	-1,0	287,4
07:40:54 AM	121,2	55,5	65,7	55,5	121,2	0,0	284,6	120,4	-0,9	287,7
07:45:08 AM	122,3	61,6	60,7	61,6	122,3	0,0	286,1	122,3	0,0	286,1
07:50:47 AM	123,3	70,0	53,3	70,0	123,3	0,0	284,5	122,3	-1,0	288,6
07:55:19 AM	123,2	76,7	46,5	76,7	123,2	0,0	285,8	122,3	-0,9	290,1
08:00:29 AM	124,3	85,3	38,9	85,3	124,3	0,0	285,1	124,3	0,0	285,1
08:06:04 AM	125,3	92,2	33,2	92,2	125,3	0,0	284,8	124,3	-1,1	291,0
08:10:15 AM	125,3	102,2	23,1	102,2	125,3	0,0	284,2	124,3	-1,0	292,1
08:15:47 AM	126,4	109,6	16,8	109,6	126,4	0,0	284,2	126,4	0,0	284,2
08:20:23 AM	127,5	120,6	7,0	120,6	127,5	0,0	285,0	126,4	-1,1	311,9
08:25:36 AM	127,5	139,6	12,1	129,6	127,5	0,0	285,8	126,4	-1,1	299,5
08:30:14 AM	128,7	141,5	12,8	141,5	128,7	0,0	281,1	128,7	0,0	281,1
08:35:27 AM	129,9	151,3	21,4	151,3	129,9	0,0	289,7	128,7	-1,2	297,4
08:40:03 AM	129,8	163,0	33,2	163,0	129,8	0,0	285,9	128,7	-1,1	290,1
08:45:18 AM	131,1	172,3	41,3	172,3	131,1	0,0	286,1	131,1	0,0	286,1
08:50:00 AM	132,4	185,1	52,8	185,1	132,4	0,0	286,5	131,1	-1,3	289,0
08:55:16 AM	132,3	192,7	60,4	192,7	132,3	0,0	284,9	131,1	-1,2	286,7
09:00:59 AM	133,6	203,8	70,2	203,8	133,6	0,0	284,6	133,6	0,0	284,6

09:05:16 AM	135,0	213,3	78,3	213,3	135,0	0,0	282,9	133,6	-1,4	284,1
09:10:57 AM	134,9	222,4	87,5	222,4	134,9	0,0	288,1	133,6	-1,3	289,0
09:15:16 AM	136,4	228,5	92,1	228,5	136,4	0,0	283,3	136,4	0,0	283,3
09:20:15 AM	137,8	237,6	99,7	237,6	137,8	0,0	289,3	136,4	-1,4	290,0
09:25:46 AM	137,7	243,8	106,1	243,8	137,7	0,0	285,6	136,4	-1,4	286,1
09:30:18 AM	139,3	245,5	106,2	245,5	139,3	0,0	282,8	139,3	0,0	282,8
09:35:23 AM	140,8	252,2	111,4	252,2	140,8	0,0	284,7	139,3	-1,5	285,2
09:40:58 AM	140,7	256,6	115,9	256,6	140,7	0,0	284,0	139,3	-1,5	284,4
09:45:32 AM	142,4	257,3	114,9	257,3	142,4	0,0	283,6	142,4	0,0	283,6
09:50:06 AM	144,0	260,4	116,4	260,4	144,0	0,0	287,3	142,4	-1,6	287,6
09:55:11 AM	143,9	266,6	122,7	266,6	143,9	0,0	288,1	142,4	-1,6	288,4
10:00:46 AM	145,6	265,9	120,3	265,9	145,6	0,0	287,9	145,6	0,0	287,9
10:05:23 AM	147,4	269,0	121,7	269,0	147,4	0,0	285,8	145,6	-1,7	286,0
10:10:01 AM	147,3	269,0	121,7	269,0	147,3	0,0	282,9	145,6	-1,7	283,1
10:15:11 AM	149,1	272,9	123,8	272,9	149,1	0,0	284,0	149,1	0,0	284,0
10:20:50 AM	150,9	276,4	125,5	276,4	150,9	0,0	285,8	149,1	-1,8	285,9
10:25:28 AM	150,8	274,6	123,8	274,6	150,8	0,0	284,0	149,1	-1,8	284,1
10:30:07 AM	152,8	278,5	125,7	278,5	152,8	0,0	286,1	152,8	0,0	286,1
10:35:19 AM	154,7	275,7	121,0	275,7	154,7	0,0	282,9	152,8	-1,9	283,0
10:40:58 AM	154,6	279,9	125,3	279,9	154,6	0,0	287,2	152,8	-1,9	287,3
10:45:39 AM	156,6	275,0	118,3	275,0	156,6	0,0	282,2	156,6	0,0	282,2
10:50:17 AM	158,6	276,4	117,7	276,4	158,6	0,0	283,2	156,6	-2,0	283,4
10:55:36 AM	158,6	280,6	122,1	280,6	158,6	0,0	286,5	156,6	-1,9	286,6
11:00:13 AM	160,7	276,7	116,1	276,7	160,7	0,0	284,7	160,7	0,0	284,7
11:05:43 AM	162,8	278,1	115,4	278,1	162,8	0,0	284,7	160,7	-2,1	284,8
11:10:13 AM	162,7	277,4	114,8	277,4	162,7	0,0	282,2	160,7	-2,0	282,3
11:15:15 AM	164,9	278,1	113,3	278,1	164,9	0,0	281,5	164,9	0,0	281,5
11:20:45 AM	167,0	284,2	117,2	284,2	167,0	0,0	287,9	164,9	-2,2	288,0
11:25:17 AM	166,9	286,4	119,4	286,4	166,9	0,0	289,7	164,9	-2,1	289,8
11:30:22 AM	169,2	288,5	119,3	288,5	169,2	0,0	291,9	169,2	0,0	291,9
11:35:55 AM	171,4	285,3	113,9	285,3	171,4	0,0	289,0	169,2	-2,2	289,1
11:40:28 AM	171,3	281,0	109,7	281,0	171,3	0,0	283,2	169,2	-2,1	283,3
11:45:02 AM	173,6	276,7	103,1	276,7	173,6	0,0	280,0	173,6	0,0	280,0
11:50:06 AM	175,9	279,2	103,3	279,2	175,9	0,0	282,2	173,6	-2,2	282,2
11:55:50 AM	175,8	285,6	109,9	285,6	175,8	0,0	289,4	173,6	-2,2	289,4
12:00:32 PM	178,1	282,8	104,7	282,8	178,1	0,0	287,9	178,1	0,0	287,9
12:05:20 PM	180,4	279,2	98,8	279,2	180,4	0,0	282,2	178,1	-2,3	282,2
12:10:30 PM	180,3	283,1	102,8	283,1	180,3	0,0	284,7	178,1	-2,2	284,7
12:15:40 PM	182,6	287,4	104,8	287,4	182,6	0,0	288,6	182,6	0,0	288,6
12:20:00 PM	184,9	279,9	95,0	279,9	184,9	0,0	282,5	182,6	-2,2	282,6
12:25:01 PM	184,8	277,8	93,0	277,8	184,8	0,0	281,1	182,6	-2,2	281,2
12:30:15 PM	187,1	282,4	95,3	282,4	187,1	0,0	284,7	187,1	0,0	284,7
12:35:55 PM	189,3	285,3	95,9	285,3	189,3	0,0	284,0	187,1	-2,2	283,9
12:40:35 PM	189,2	283,5	94,2	283,5	189,2	0,0	285,0	187,1	-2,1	285,1
12:45:17 PM	191,6	283,1	91,6	283,1	191,6	0,0	285,0	191,6	0,0	285,0
12:50:33 PM	193,7	281,3	87,6	281,3	193,7	0,0	282,2	191,6	-2,2	282,2
12:55:15 PM	193,6	277,4	83,8	277,4	193,6	0,0	279,3	191,6	-2,1	279,4

01:00:58 PM	195,9	273,6	77,7	273,6	195,9	0,0	275,8	195,9	0,0	275,8
01:05:41 PM	197,9	281,7	83,8	281,7	197,9	0,0	285,4	195,9	-2,1	285,5
01:10:25 PM	197,8	278,9	81,0	278,9	197,8	0,0	282,9	195,9	-2,0	283,0
01:15:10 PM	200,0	286,0	86,0	286,0	200,0	0,0	287,6	200,0	0,0	287,6
01:20:27 PM	202,0	284,2	82,2	284,2	202,0	0,0	286,1	200,0	-2,0	286,2
01:25:13 PM	201,9	278,5	76,6	278,5	201,9	0,0	281,1	200,0	-1,9	281,2
01:30:59 PM	204,0	284,2	80,2	284,2	204,0	0,0	285,4	204,0	0,0	285,4
01:35:45 PM	206,0	283,8	77,9	283,8	206,0	0,0	286,1	204,0	-1,9	286,2
01:40:32 PM	205,9	287,8	81,9	287,8	205,9	0,0	289,0	204,0	-1,8	289,0
01:45:20 PM	207,9	289,6	81,7	289,6	207,9	0,0	290,8	207,9	0,0	290,8
01:50:08 PM	209,7	286,7	77,0	286,7	209,7	0,0	286,1	207,9	-1,8	286,1
01:55:34 PM	209,6	282,4	72,8	282,4	209,6	0,0	280,8	207,9	-1,7	280,7
02:00:23 PM	211,5	277,4	65,9	277,4	211,5	0,0	274,4	211,5	0,0	274,4
02:05:25 PM	213,2	283,8	70,6	283,8	213,2	0,0	282,9	211,5	-1,7	282,9
02:10:22 PM	213,1	278,1	65,0	278,1	213,1	0,0	277,6	211,5	-1,6	277,5
02:15:21 PM	214,9	278,9	63,9	278,9	214,9	0,0	279,0	214,9	0,0	279,0
02:20:19 PM	216,3	278,1	61,9	278,1	216,3	0,0	276,8	214,9	-1,3	276,8
02:25:22 PM	216,1	278,4	62,2	279,6	216,1	0,0	277,9	214,9	-1,2	277,9
02:30:18 PM	217,6	279,6	62,0	283,1	217,6	0,0	279,7	217,6	0,0	279,7
02:35:24 PM	218,6	283,1	64,5	289,2	218,6	0,0	285,4	217,6	-1,0	285,3
02:40:24 PM	218,5	289,2	70,8	285,3	218,5	0,0	274,4	217,6	-0,9	274,2
02:45:35 PM	219,6	285,3	65,7	12,5	219,6	0,0	2,3	219,6	0,0	2,3
02:50:08 PM	221,1	12,5	208,6	274,3	221,1	0,0	269,5	219,6	-1,5	269,4
02:55:24 PM	221,0	274,3	53,3	252,9	221,0	0,0	244,9	219,6	-1,4	244,7
03:00:32 PM	222,6	252,9	30,3	259,7	222,6	0,0	252,0	222,6	0,0	252,0
03:05:41 PM	223,9	259,7	35,7	19,8	223,9	0,0	20,2	222,6	-1,4	20,2
03:10:48 PM	223,8	19,8	204,1	10,8	223,8	0,0	10,7	222,6	-1,3	10,7
03:15:57 PM	225,3	10,8	214,5	251,5	225,3	0,0	11,9	225,3	0,0	11,9
03:20:04 PM	226,6	251,5	24,9	8,9	226,6	0,0	2,2	225,3	-1,3	1,8
03:25:13 PM	226,5	8,9	217,7	15,5	226,5	0,0	3,0	225,3	-1,2	2,9
03:30:19 PM	228,0	15,5	212,5	20,2	228,0	0,0	3,3	228,0	0,0	3,3
03:35:19 PM	229,2	20,2	208,9	232,0	229,2	0,0	11,8	228,0	-1,2	10,5
03:40:22 PM	229,1	232,0	3,0	129,6	229,1	0,0	8,1	228,0	-1,1	-37,5
03:45:28 PM	230,4	129,6	100,8	7,4	230,4	0,0	6,9	230,4	0,0	6,9
03:50:31 PM	231,6	7,4	224,2	189,5	231,6	0,0	221,9	230,4	-1,2	222,0
03:55:34 PM	231,4	189,5	41,9	174,6	231,4	0,0	11,8	230,4	-1,0	7,8
04:00:04 PM	232,7	174,6	58,1	164,9	232,7	0,0	147,2	232,7	0,0	147,2
04:05:15 PM	233,8	164,9	68,9	6,5	233,8	0,0	6,2	232,7	-1,1	6,1
04:10:25 PM	233,7	6,5	227,2	27,3	233,7	0,0	32,3	232,7	-1,0	32,3
04:15:37 PM	234,9	27,3	207,6	122,9	234,9	0,0	11,4	234,9	0,0	11,4
04:20:47 PM	236,1	122,9	113,1	115,7	236,1	0,0	11,6	234,9	-1,2	10,5
04:25:58 PM	236,0	115,7	120,2	112,1	236,0	0,0	11,0	234,9	-1,1	10,1
04:30:11 PM	237,3	112,1	125,1	8,6	237,3	0,0	2,3	237,3	0,0	2,3
04:35:14 PM	238,1	90,4	147,7	101,8	238,1	0,0	8,3	237,3	-0,9	7,8
04:40:35 PM	238,0	8,6	229,5	85,2	238,0	0,0	7,1	237,3	-0,8	6,8
04:45:28 PM	239,0	20,8	218,3	69,8	239,0	0,0	6,3	239,0	0,0	6,3
04:50:16 PM	239,5	101,8	137,7	58,1	239,5	0,0	5,8	239,0	-0,5	5,7

04:55:29 PM	239,4	85,2	154,2	2,8	239,4	0,0	1,0	239,0	-0,4	1,0
05:00:50 PM	240,0	69,8	170,1	44,7	240,0	0,0	5,3	240,0	0,0	5,3
05:05:13 PM	240,9	58,1	182,7	11,9	240,9	0,0	9,7	240,0	-0,9	9,7
05:10:35 PM	240,7	2,8	238,0	30,6	240,7	0,0	55,7	240,0	-0,8	55,8
05:15:07 PM	241,8	44,7	197,0	24,3	241,8	0,0	42,0	241,8	0,0	42,0
05:20:20 PM	242,6	11,9	230,7	19,3	242,6	0,0	34,6	241,8	-0,9	34,7
05:25:35 PM	242,5	30,6	211,9	16,5	242,5	0,0	31,5	241,8	-0,7	31,6
05:30:53 PM	243,5	24,3	219,1	14,9	243,5	0,0	29,4	243,5	0,0	29,4
05:35:08 PM	244,3	19,3	225,0	11,7	244,3	0,0	24,5	243,5	-0,8	24,5
05:40:24 PM	244,1	16,5	227,6	8,6	244,1	0,0	18,9	243,5	-0,7	19,0
05:45:01 PM	245,1	14,9	230,2	6,1	245,1	0,0	14,3	245,1	0,0	14,3
05:50:19 PM	245,9	11,7	234,1	1,6	245,9	0,0	2,3	245,1	-0,8	2,3
05:55:36 PM	245,7	8,6	237,1	2,0	245,7	0,0	1,9	245,1	-0,7	1,9
06:00:23 PM	246,6	6,1	240,5	0,4	246,6	0,0	1,3	246,6	0,0	1,3